INVESTIGATION OF EXCITED STATE PROTON TRANSFER KINETICS, SOLUTE-SOLVENT INTERACTIONS AND TRIPLET STATE PROPERTIES OF SOME ORGANIC MOLECULES

A Thesis
Submitted for the Degree of

DOCTOR OF PHILOSOPHY

by

Sanghamitra Banerjee

School of Chemistry
University of Hyderabad
Hyderabad – 500 046
INDIA

December 2013

To

My Family
And
Friends

“The highest education is that which does not merely give us information but makes our life in harmony with all existence.”

Rabindranath Tagore

CONTENTS

STATEMENT

I hereby declare that the matter embodied in the thesis entitled **"*Investigation of Excited State Proton Transfer Kinetics, Solute-Solvent Interactions and Triplet State Properties of Some Organic Molecules*"** is the result of investigations carried out by me in the School of Chemistry, University of Hyderabad, India under the supervision of **Prof. Anunay Samanta**.

In keeping with the general practice of reporting scientific investigations, the acknowledgements have been made wherever the work described is based on the findings of other investigators. Any omission or error that might have crept in is regretted.

December 2013 **Sanghamitra Banerjeee**

SCHOOL OF CHEMISTRY

UNIVERSITY OF HYDERABAD

HYDERABAD-500 046, INDIA

Phone: +91-40-2313 4813 (O)
+91-40-2313 0715 (R)
Fax: +91-40-2301 1594
Email: anunay@uohyd.ac.in
anunay.samanta@gmail.com

Prof. Anunay Samanta

CERTIFICATE

Certified that the work embodied in the thesis entitled **"*Investigation of Excited State Proton Transfer Kinetics, Solute-Solvent Interactions and Triplet State Properties of Some Organic Molecules*"** has been carried out by **Ms. Sanghamitra Banerjee** under my supervision and the same has not been submitted elsewhere for any degree.

Anunay Samanta
(Thesis Supervisor)

Dean
School of Chemistry
University of Hyderabad

Acknowledgement

I express my sincere gratitude to Prof. Anunay Samanta, my research supervisor, for his constant cooperation, encouragement and kind guidance. He has been quite helpful to me in both academic and personal fronts.

I would like to acknowledge Prof. M. Durga Prasad for providing much needed theoretical insights. I also thank Dr. R. Nagarajan for his help and cooperation.

I would like to thank the former and present Dean(s), School of Chemistry, for their constant support, inspiration and for the available facilities. I am extremely appreciative individually to all the faculty members of the school for their help, cooperation and encouragement at various stages.

I am grateful to all my former teachers for their help. I express my sincere gratitude to Syamaprasad da, Monojanjan da (khoka), Abhik da, Partha da, Tamal da for helping me in many ways during my school life in Patha-Bhavana, Santiniketan.

I value the association with my former lab-mates Aniruddha, Bhaswati, Ravi, Dinesh and Santhosh from whom I have learned many valuable aspects of research. I am extremely thankful to Santhosh for giving me useful advices. I acknowledge my junior friends Satyajit, Soumya, Ashok, Chandu, Praveen, Navendu for maintaining the friendly and cooperative atmosphere in the lab. I also value my association with Tanmay da. I am extremely thankful to Shalini di for not only helping me academically but also otherwise.

I also thank all other non-teaching staff for their timely help, Mr. Shetty in particular.

I am thankful to all my colleagues in the school of chemistry for helping me with various things. I would like to specially thank Raja, Nayan, Sanatan and Koushik for their help with the glove box.

I have some wonderful memories with Vasudhara di, Rumpa di and Tulika di and they are the people who made my stay possible in Hyderabad during those initial years. We were like a family ans shared a feeling of a home away from home. I never felt alone in the hostel due to the lovely company

of Promiti, Paromita, Debparna and Arpita. I will cherish each and every moment I spent with them throughout my life. I would also like express my gratitude to all my big brothers Tapta da, Tanmoy da, Subrata da, Arindam da and Sandip da. I am really lucky to associate myself with some of my batch mates and juniors Tanmoy, Sugata, Rudro, Suman (Ghosh), Raju, Suman, Mona, Dibya and Kaijar.

I must not forget my childhood buddies. I sincerely thank God for the precious friendship of Supratik (Chotu), Arnab, Subha, Sharmin, Padma and Riten. I am really lucky to have them in my life.

I express my sincere gratitude to my uncle (chotomama), Mamima and my wonderful cousins Tubba and Rimpa. Uncle's support and suggestions for my higher studies are always memorable and valuable.

This thesis would have not been possible without the selfless love and support of Ma, Baba, Jethu, Didi, Suddha, Mamoni, Bapi, Moni and Dadabhai. I am blessed with two very special people in my life Jia (my niece) and Pogo, without them life would have been color-less.

Satwik is beyond any sense of gratitude as he is a friend, philosopher and guide to me since my college days.

Financial assistance from UGC-RFSMS, New Delhi is greatly acknowledged.

Sanghamitra

List of Publications

1. "Fluorescence Response of 4-(N,N′-Dimethylamino)benzonitrile in Room Temperature Ionic Liquids: Observation of Photobleaching under Mild Excitation Condition and Multiphoton Confocal Microscopic Study of the Fluorescence Recovery Dynamics" K. Santhosh, **S. Banerjee,** N. Rangaraj and A. Samanta, ***J. Phys. Chem. B***, 114 (**2010)** 1967-1974.

2. "Laser Flash Photolysis Study on 9-Phenylxanthenium tetrafluoroborate: Identification of New Features due to the Triplet State" **S. Banerjee** and A. Samanta, ***J. Chem. Sci.,*** 123 **(2011)** 15-20. **(Chapter 6)**

3. "Dual Fluorescence of Ellipticine: Excited State Proton Transfer from Solvent versus Solvent Mediated Intramolecular Proton Transfer" **S. Banerjee,** A. Pabbathi, M. Chandra Sekhar and A. Samanta, ***J. Phys. Chem. A,*** 115 **(2011)** 9217-9225. **(Chapter 3)**

4. "Does Excited State Proton Transfer Reaction Contribute to the Emission Behavior of 4-Aminophthalimide in Aqueous Media?" D. C. Khara, **S. Banerjee** and A. Samanta ***(Manuscript under preparation)*** **(Chapter 5)**

Conference Presentations

1. "Excited State Proton Transfer Reaction of 5,11-dimethyl-6H-pyrido[4,3-b]carbazole in Conventional Solvents", **National Symposium on Radiation and Photochemistry (NSRP)**, Jay Narain Vyas (JNV) University, Jodhpur, Rajasthan, March 10^{th} - 12^{th}, 2011. (Poster Presentation) [Best poster award]

2. "Protonation Equilibria of Ellipticine in the Lowest Excited Singlet State: A Steady State and Time-resolved Fluorescence Study", **Chemfest-2012**, 9^{th} Annual In-House Symposium of the School of Chemistry, University of Hyderabad, February 24^{th} - 25^{th}, 2012. (Poster Presentation)

3. "Characterization of Triplet State of Ellipticine and Solvent Dependent Triplet Energy Transfer Process Monitored by Laser Flash Photolysis", **Chemfest-2013**, 10^{th} Annual In-House Symposium of the School of Chemistry, University of Hyderabad, February 15^{th} - 16^{th}, 2013. (Oral + Poster Presentation)

4. "Characterization of Triplet State of Ellipticine and Solvent Dependent Triplet Energy Transfer Process Monitored by Laser Flash Photolysis", **26th**

International Conference on Photochemistry (ICP 2013), KU Leuven, Belgium, 21st – 26th, 2013. (Poster Presentation)

Thesis Layout

The thesis has been divided into eight chapters. **Chapter 1** provides a brief introduction on various processes that follow photoexcitation of a molecule. Different photophysical processes, like fluorescence, phosphorescence, excited state proton transfer and energy transfer, are then discussed in this context. This is followed by a discussion on the excited state acidity/basicity constant and its estimation using different methods. The superiority of determination of excited state prototropic equilibrium constant (pK^*) by the kinetic method over the other two methods is highlighted. This chapter also presents a discussion on what motivates us to study the photophysical properties of the chosen molecules. **Chapter 2** provides the details of the materials, methods of synthesis, methods of purification of the solvents, various methodologies for the sample preparation for different experiments, instrumentation and methods of data analysis. **Chapter 3** deals with solvent mediated excited state intramolecular proton transfer of ellipticine. **Chapter 4** delineates excited state proton transfer kinetics and excited state acidity constant of ellipticine in aqueous media. **Chapter 5** deals with the fluorescence behavior of 4-aminophthalimide using steady state and time-resolved technique. **Chapter 6** presents laser flash photolysis study on 9-phenylxanthenium tetrafluoroborate. **Chapter 7** deals with Triplet State parameters of Ellipticine in different solvents. **Chapter 8** summarizes the findings of the present investigations by touching upon the scope of further studies based on the present work.

Chapter 1

Introduction

This chapter provides a brief introduction on various processes that follow photoexcitation of a molecule. Different photophysical processes, like fluorescence, phosphorescence, excited state proton transfer and energy transfer, are then discussed in this context. This is followed by a discussion on the excited state acidity/basicity constant and its estimation using different methods such as, Förster cycle, Weller method and kinetic method. The superiority of determination of excited state prototropic equilibrium constant (pK^*) by the kinetic method over the other two methods is highlighted. This chapter also includes a brief discussion on the molecules of interest, their importance and different unknown properties, which motivate to study the photophysical properties of those molecules.

1.1. Photoexcitation and fate of the excited molecule

A molecule has several electronic energy levels referred to as 'states' and such state is associated with vibrational and rotational energy levels. On photoexcitation by UV-visible light, a molecule originally residing in the ground state absorbs a photon and gets elevated to the excited state. Once in an excited state, the properties of the molecule will be quite different from those in the ground state. An excited state molecule will often have different geometry, reactivity and dipole moment compared to the ground state. A molecule in the excited state is very short-lived. An excited molecule will ultimately decay to the

more stable ground state unless it is involved in some photochemical process in the short-lived excited state thereby losing its identity. An excited molecule deactivating to the ground state can do so via several either radiative or non-radiative dissipation processes. The possible fate of a molecule excited to the lowest excited singlet state (S_1) from the ground state (S_0) is discussed below.

Following the $S_0 \rightarrow S_1$ transition, the molecule return to the S_0 state either by radiative process (fluorescence and/or phosphorescence) or non-radiative pathway (internal conversion and/or intersystem crossing).[1-3] Deactivation from S_1 to S_0 state by radiative process yield fluorescence while non-radiative deactivation is known as internal conversion. Molecule residing in S_1 state can undergo intersystem crossing to populate the neighbouring T_1 state. In the T_1 state, the molecule can undergo a whole host of excited state processes including radiative and non-radiative decays to the ground state. If it decays radiatively to the ground S_0 state, phosphorescence is observed whereas non-radiative decay can yield an intersystem crossing.

After photoexcitation, molecule in the lowest excited state can undergo absorptive transition to the higher excited state by using a second 'monitoring' light source. This kind of excited state absorption is called as transient absorption. The transient absorption is possible from both lowest singlet and triplet excited state leading to $S_1 \rightarrow S_n$ and $T_1 \rightarrow T_n$ transition (where $n>1$) respectively. To monitor $T_1 \rightarrow T_n$ transition, the lowest excited triplet state should be sufficiently populated. High intense laser sources are therefore popularly used to achieve the triplet excited state population. Excitation by a high intense laser light source may lead to photolysis of the molecule producing radical, radical anion or radical

cation. These kinds of transient species and the processes that they undergo can be studied by using pump-probe techniques, like laser flash photolysis.

Within the lifetime of the excited state, an excited molecule might also undergo several photophysical processes that would yield entirely different excited state species. These processes mainly include excited state proton transfer (ESPT), excited state electron transfer, excited state energy transfer, photoisomerisation etc. These reactions occur by non-radiative pathways and may lead to generation of a new species affecting the several photophysical parameters, such as fluorescence quantum yield, lifetime etc. of the molecule. Studies on photoinduced processes have attracted a great deal of attention, primarily because of their applications in different fields of chemistry and biology. For instance, the concept of FRET (Förster resonance energy transfer)[2] is widely used for understanding biological processes at microscopic level[4] and the electron transfer process is the basis of design and development of luminescent systems for sensing environment,[5] devices for solar energy conversion,[6-9] nanometer scaled wires,[10-12] logic gates[13,14] etc. ESPT phenomenon is used in chromosensors,[15] imaging[16] and white light emitting materials.[17] While the concept of photoisomerisation is involved in polymer vesicles and liquid crystals,[18-21] photoswitching[22,23] etc. The work in this thesis is primarily based on some of the processes described above and shall now be elaborately discussed in the following sections.

1.1.1. Fluorescence

Fluorescence is emission of a photon by photoexcited (S_1) molecule on its return to ground state (S_0). The fluorescence spectrum appears on the red side of

the absorption spectrum indicating that the energy of the photon emitted through fluorescence is less than that of the photon absorbed. The change in energy is termed as Stokes shift. The extent of this shift depends on several relaxation and photophysical processes involved in the excited state. Solvent relaxation is the one which commonly affects the extent of Stokes shift particularly in electron donor acceptor molecule. With the change of solvent polarity, the extent of solvent stabilization of excited state dipolar molecule changes which in turn alters the energy of excited singlet state and the resultant Stokes shift varies.

The most common generalization in solution phase photochemistry is that the photoreaction and luminescence occur from vibrationally relaxed molecule in their lowest excited singlet state (Kasha's rule). This implies that irrespective of the excitation energy, polyatomic molecules should emit from the lowest excited singlet state and hence, display a single fluorescence emission. The most photochemical and luminescent events in solution occur from the lowest vibrational level of the lowest excited electronic state, which implies that the nonradiative decay rate is ordinarily faster than competing radiative deacy or photoreaction from higher excited states.

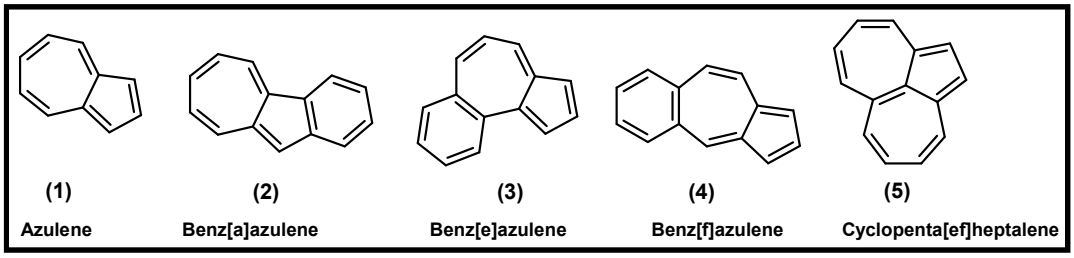

Chart 1.1.

However, this conclusion is not absolute as one expects that photochemistry and luminescence from higher excited states might be most easily observable when radiationless deactivation rates are unusually slow or when radiative or photochemical deactivation rates are unusually fast. Indeed, the best documented example is the dual fluorescence of azulene (**1** in Chart 1.1.).[24] This system emits from both S_1 and S_2 states, as the energy gap between S_2 and S_1 is large making the nonradiative $S_2 \rightsquigarrow S_1$ transition slower or comparable to the $S_2 \rightarrow S_0$ fluorescence. Likewise, some benzene annulated azulene derivatives (**2-4** in Chart 1.1.)[25-27] and the derivatives of Hafner's hydrocarbon (**5** in Chart 1.1.)[28] exhibit dual fluorescence. S_2 emission from many other systems which include acenaphthylene,[29] ketocyanine dye[30] are also reported.

Multiple fluorescence emissions can also arise due to ground and excited state processes. Ground and excited state complexation of a fluorescent system with other species like DNA,[31] cyclodextrin,[32] solvent[33] etc. may give rise to dual fluorescence. Excited state processes, such as energy transfer,[34-37] exciplex formation[38-40] and proton transfer[41-43] also lead to dual emission. In this context, excited state proton transfer phenomenon (ESPT) is one of the most extensively studied processes. In a widely studied molecule 3-hydroxyflavone[44,45] (Chart 1.2.), the proton moves from the hydroxy group to an adjacent carbonyl group on photoexcitation producing dual emission. While in the case of 7-hydroxyquinoline (7-HQ)[46-52] (Chart 1.2.), which contains both acidic (-OH group) and basic (-N=) groups, it requires participation of protic solvent molecules in the ESPT process to exhibit dual emission. Twisted intramolecular charge transfer (TICT)[53-55]process also leads to dual emission in electron donor-acceptor molecules.

Grabowski and his coworkers explained the dual emission of 4-(N,N-dimethylamino)benzonitrile (DMABN)[56,57] (Chart 1.2.) by TICT mechanism. According to this concept, the short-wavelength fluorescence of DMABN originates from the locally excited (LE) state and the long-wavelength band from the TICT state.

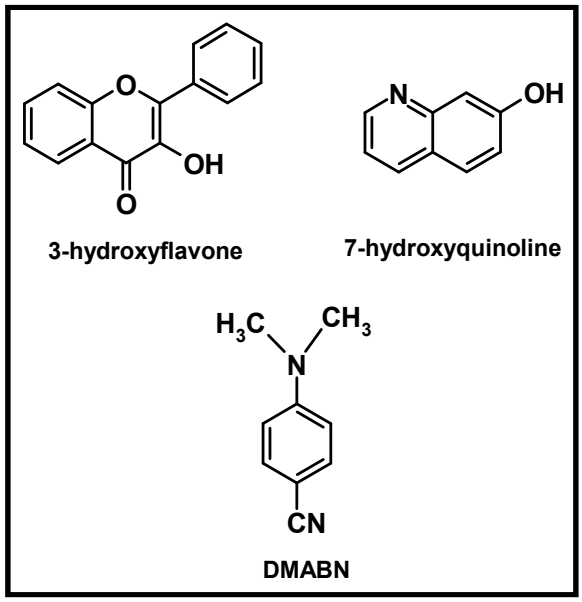

Chart 1.2.

1.1.2. Phosphorescence

The radiative deactivation from lowest excited triplet state (T_1) to the ground state (S_0) is referred to as phosphorescence. The forbidden $T_1 \rightarrow S_0$ transition is observed due to spin-orbit coupling. However, at room temperature numerous collisions with solvent lead to radiationless deactivation via vibrational relaxation to the ground state (S_0). Several methods have been used to restrict this

collisional deactivation and enable the observation of phosphorescence. One of the most common techniques is to supercool solutions to a rigid glass state usually at the temperature of liquid nitrogen (77 K).[3,58] At these very low temperatures, molecular collisions are greatly reduced and strong phosphorescence signals are observed. Phosphorescence signals in solution can also be quenched by dissolved oxygen. For this reason, sample solutions have to be degassed prior to recording the phosphorescence spectra. Various other methods have also been developed to reduce the effect of dissolved oxygen on phosphorescence.[59]

Phosphorescence spectrum is located at wavelengths higher than the fluorescence spectrum because the energy of the lowest vibrational level of the excited triplet state (T_1) is lower than that of the singlet state (S_1). Since triplet to singlet transition is forbidden by the prohibition against spin selection rule, the spontaneous process occurs with low probability and continues relatively over a longer period of time compared to fluorescence.

Generally phosphorescence refers to transitions between $T_1 \rightarrow S_0$ states. However, in some cases like fluoranthene and ferrocene (Chart 1.3.), $T_n \rightarrow S_0$ ($n>1$) transitions have been reported.[60,61] Phosphorescence can also be observed by inserting the molecule of interest into a rigid polymer matrix. The phosphorescence of coronene, triphenylene and fluorene (Chart 1.3.) embedded in a poly(methylmethacrylate) matrix can be observed but only after the removal of the oxygen molecules, which may have diffused into the matrix.[62] However, phosphorescence of benzil (Chart 1.3.) is observed in non-degassed imidazolium ionic liquids due to low solubility of oxygen in these highly viscous ionic liquids.[63] Recently, phosphorescence is being used as a technique to detect singlet

oxygen in various molecular sensors and photodynamic therapeutic drugs.[64-67] In this thesis phosphorescence has been employed to calculate triplet state energy of the molecule of interest.

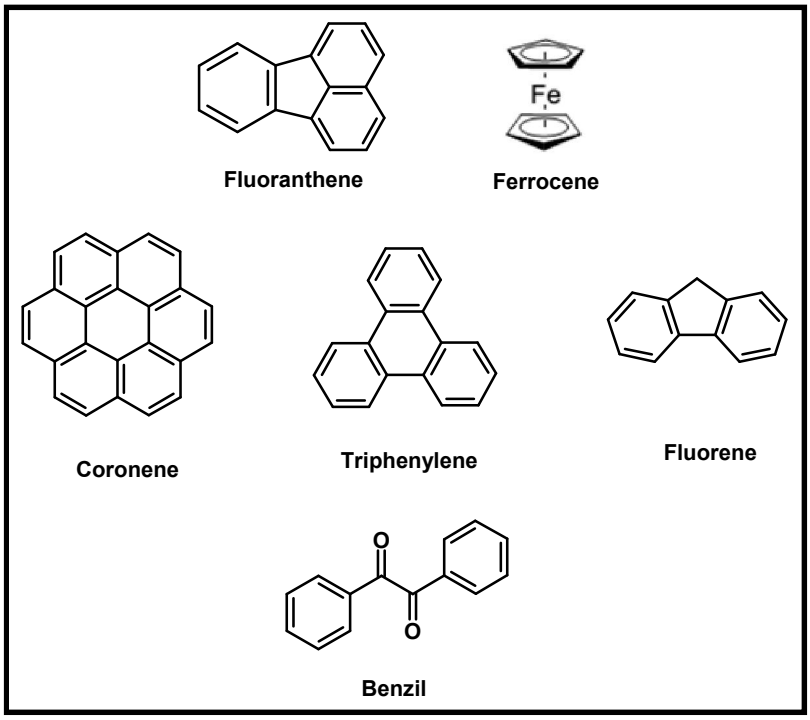

Chart 1.3.

1.1.3. Excited state proton transfer

Ground state intramolecular H-bonded structures can be formed by the molecules having both hydrogen bond donor and acceptor moiety in close proximity. A redistribution of electronic charge in the intramolecular H-bonded structure takes place on photoexcitation and as a consequence the proton gets translocated from the hydrogen bond donor group to the hydrogen bond acceptor group. This phenomenon is known as excited state intramolecular proton transfer

(ESIPT). Excitation of an intramolecular H-bonded system usually leads to dual fluorescence which is attributed to the normal form and the tautomer of the molecule. This process has received a great deal of attention both experimentally and theoretically and considered as one of the most important photoreactions in chemical and biological systems.[41,68-81] ESIPT phenomenon is most commonly monitored using fluorescence technique.[16,77,82,83] To understand the mechanism of ESIPT, one has to focus on the interplay between the molecular structure and potential energy surface.[74] The tautomer fluorescence gets highly Stokes-shifted (6000-10000 cm^{-1}) due to enormous change of the electronic distribution in the excited state.[41] Consideration of a double-well potential energy surface depicted in the Scheme 1.1 can give a better understanding of this phenomenon.

As can be seen from the Scheme 1.1, due to photoexcitation, there occurs huge electronic change and consequently the proton moves on a double-well potential surface as shown in the scheme. In the ground state there exists significant energy barrier for proton transfer, whereas, in the excited state as the barrier becomes smaller the proton is much easily transferred to generate the excited tautomer species. The $S'_1 \rightarrow S'_0$ energy gap of the tautomer is much lower than that of the normal form, which accounts for the large Stokes shift of the fluorescence originating from the tautomer.

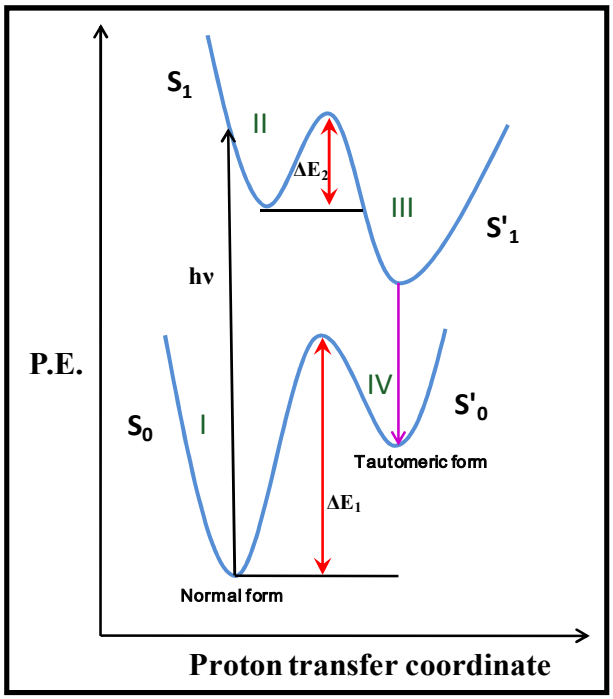

Scheme 1.1.

ESIPT requires hydrogen bond formation between the proton donor (generally, a moiety containing –OH or –NH group) and the acceptor (generally, a moiety containing =N– or =O group). The dynamics of this ESIPT phenomenon, on a symmetrical double-well potential, has been well reviewed in literature.[74,84] The presence of an unsymmetrical double-well potential is often visualized as a representation of nearly barrierless proton transfer.[71] Quantum mechanical calculations have shown the impact of tunneling effect and vibration dynamics of the bonds involved in hydrogen bonded network on the proton transfer dynamics; thus the potential energy surfaces have shown to be dependent on the nature of the molecules.[52,72,74]

In aprotic solvents, where solvent perturbation is negligible, ESIPT phenomenon normally takes place through the pre-existing strong intramolecular hydrogen bonded structure. However, in protic solvents the solvent perturbation is expected to become significant, particularly when the intramolecular hydrogen-bonding between the donor and acceptor moieties is weak. In the latter case, the intermolecular hydrogen bonded network inhibits to some extent the ESIPT phenomenon. The most striking feature of the ESIPT dynamics in aprotic solvents is its ultrafast nature, occurring in sub-picosecond to few femtoseconds time scale.

The ESIPT phenomenon has vast utility. Classical examples of these include four-level dye lasers, energy or data storage devices and optical switching,[85-94] Raman filters,[95] scintillation counters,[96] polymer stabilizers.[97] Moreover, ESIPT molecules have also been used in metal ion chelates.[98] These ESIPT molecules are known to possess photochemical stability, and are resistant to thermal degradation. Low self-absorption of the tautomer fluorescence has been utilised in electroluminescence.[99]

From the mechanistic point of view, the ESPT phenomenon can be classified into three groups,[41] (i) intrinsic intramolecular proton transfer, (ii) excited state double proton transfer, and (iii) proton transfer through relay. Each group is discussed separately as follows.

1.1.3.1. Intrinsic intramolecular proton transfer

This is considered as the simplest type of proton transfer, occurring in systems in which five/six-membered intramolecularly hydrogen bonded structure

is already present. Enormously studied, molecules like methyl salicylate,[100-102] 2-hydroxybenzophenone,[103] salicylidenaniline,[104] 3-hydroxyflavone,[44,85] salicylamide,[105] 2-(2′-hydroxyphenyl)benzimidazole,[106-108] 2-(2′-hydroxyphenyl)benzoxazole[107,109,110] and 2-(2′-hydroxyphenyl)benzothiazole[104,111] (Chart 1.4.) serve as good examples for this kind of proton transfer. In each case, specific molecular structure and conformation lead to specific behavior. Environmental and/or solvent-cage perturbations are found to be quite significant in the ESIPT studies of these molecules. Effect of media,[112] substituted moiety[113] etc. on ESIPT reaction is topic of interest till date.

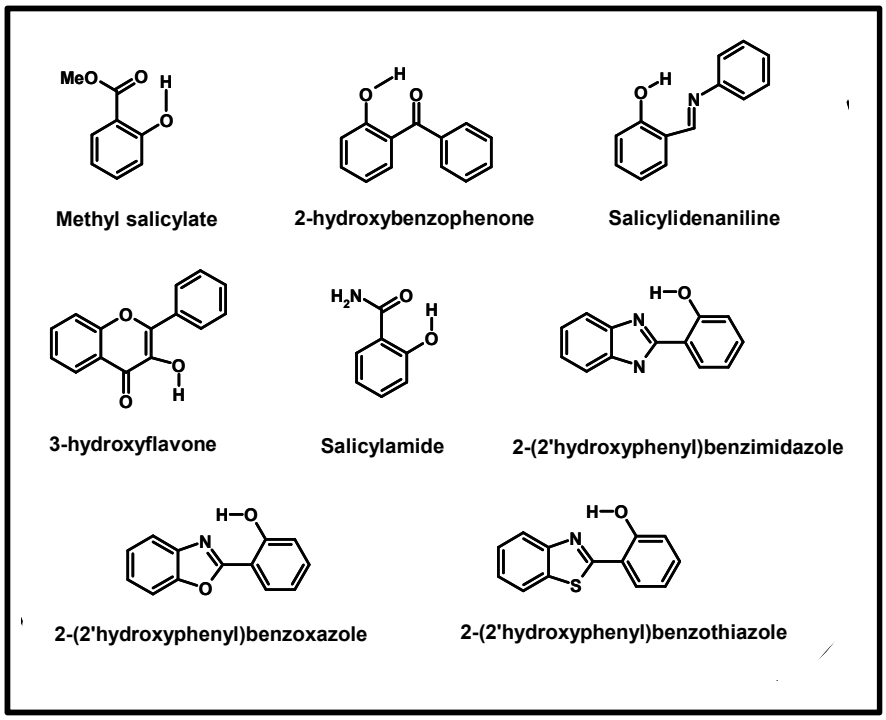

Chart 1.4.

1.1.3.2 Excited state double proton transfer

Excited state double proton transfer (ESDPT) reaction is a very important reaction in biology which involves the transfer of two protons across the two pre-existing H-bonds in the system. The first reported example of this kind is 7-azaindole (homodimer)[114-117] (Chart 1.5.). At high probe concentration, in addition to the violet emission from the 'normal form' of the molecule, another green fluorescence is observed which is attributed to the double proton transferred tautomer. Excited state double proton transfer is also observed in heterodimer like 7-azaindole-2-pyridone (Chart 1.5.).[118] The ESDPT study involving heterodimer is very important because it is relevant to DNA base pairs. It is reported that

ESDPT plays a crucial role in DNA replication and hence in determining the structure and properties of DNA bases.[119] Other molecule, which shows similar biprotonic transfer is benzanilide (Chart 1.5.).[120]

Although there is large number of experimental and theoretical work to find out the mechanistic details of ESDPT, like (i) whether the process is concerted or stepwise and (ii) whether the process is reversible, there are still some ambiguities in the literature regarding the mechanism of ESDPT reaction.[121-124]

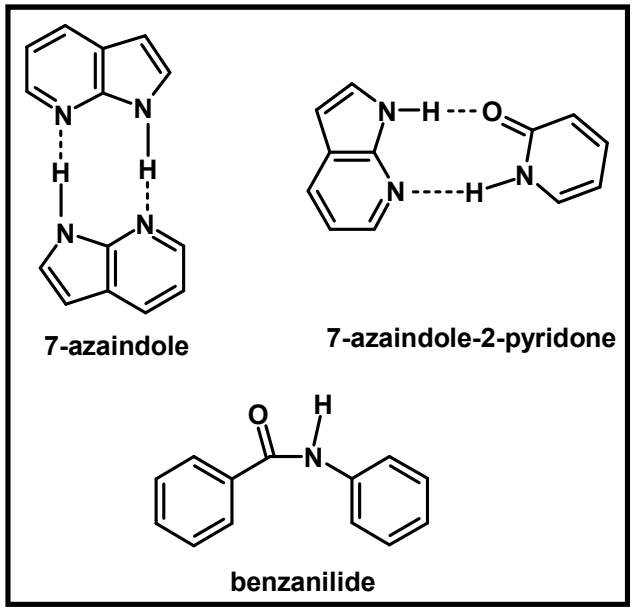

Chart 1.5.

1.1.3.3. Proton transfer through relay

This is another type of proton transfer, where the proton donor group is at a distance from the proton acceptor. A 'molecular companion', (say acetic acid,

water or alcohol) must be involved in the form of a cyclic H-bonded complex, where protons are transferred in a relay mechanism during the excited state lifetime of the fluorophore.[125-131] This is observed in case of lumichrome,[132,133] adenine and guanine[41] where acetic acid is involved in the cyclic hydrogen bonded complex (Chart 1.6.). ESPT of 7-hydroxyquinoline[46,47,49,52](7-HQ) (Chart 1.2.) is used as a model system for understanding the mechanism of long distance proton translocation mediated by a hydrogen bonded network due to the close resemblance of this excited state process with proton relay over large distance. The extensive studies on the ESPT dynamics of 7-HQ suggested the formation of 1:1 or 1:2 solute-solvent complex depending upon the solvent molecule.[134] The rate constant of ESPT in the complex is found to be dependent on the H-bond donating ability of the alcohols, as measured by the Kamlet-Taft acidity (α) of the alcohols.[135]

In Chapter 3, the ESPT process of ellipticine (Chart 1.7.) is studied where involvement of polar protic solvents leads to the formation of tautomeric form in the excited state.[83] Various types of cyclic and noncyclic solute-solvent complexes are also observed in ground and excited state in presence of 'molecular companion' such as methanol.

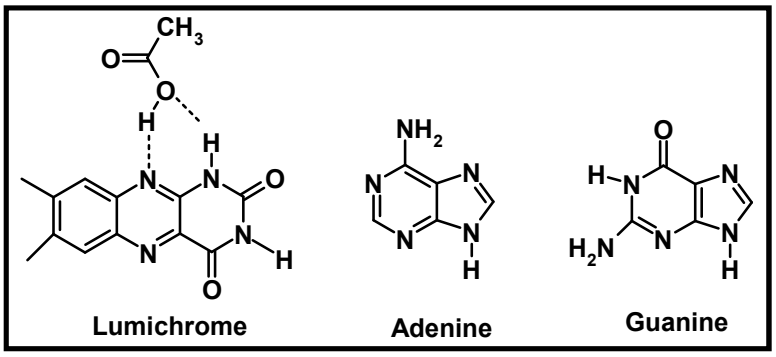

Chart 1.6.

1.1.4. Excited state energy transfer

Excited state energy transfer process is a well studied concept in photophysics to comprehend various biological processes both at macroscopic and microscopic level.[1] For instance, Förster resonance energy transfer (FRET)[2] is widely explored to study molecular/protein dynamics[136] and to estimate the intermolecular distances in biomolecules,[137] supramolecular associations[138] and assemblies. Excited state energy transfer mechanism between a donor and acceptor molecule is based on Coulombic interaction and intermolecular orbital overlap.[1] The Coulombic interactions consist of long range dipole–dipole interactions (Förster's mechanism) and short-range multi-polar interactions. The interactions due to intermolecular orbital overlap, which include electron exchange (Dexter's mechanism) and charge resonance interactions, are short range interactions. Generally Coulombic mechanism is effective at long distances (up to 80–100 Å) whereas electron exchange is operative only at short distances (<10 Å) because of its orbital overlapping requirement. The motion of electrons for the donor (D) and acceptor (A) involved in energy transfer process via

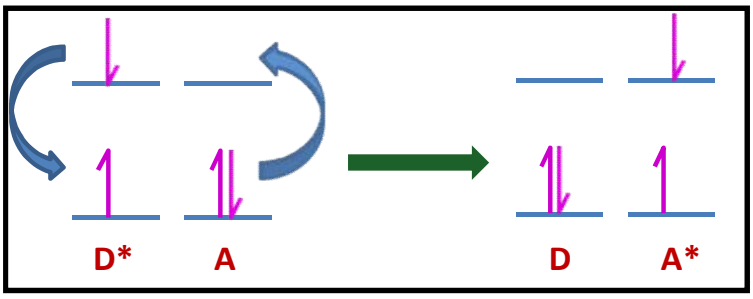

Scheme 1.2.

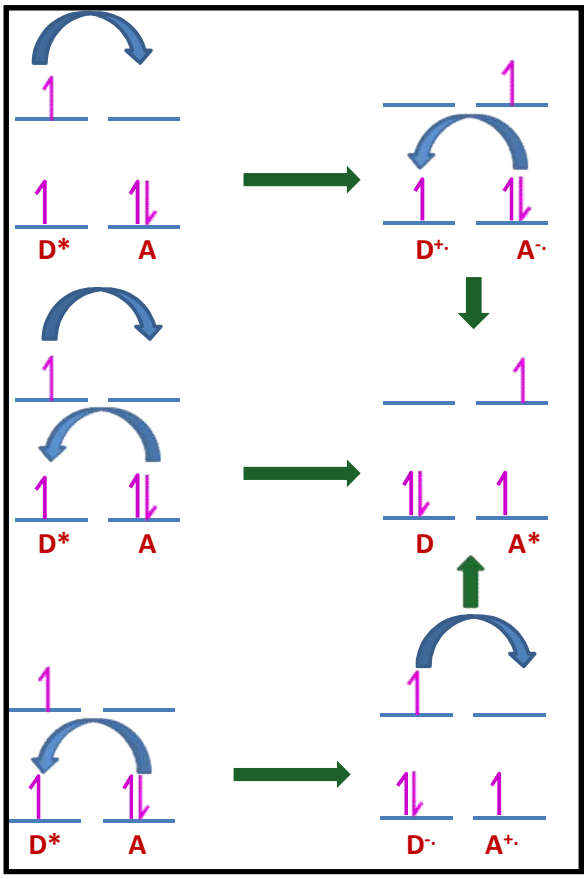

Scheme 1.3.

Coulombic interactions and electron exchange mechanism are presented in Schemes 1.2 and 1.3 respectively.

All types of interactions are possible in the case of singlet-singlet energy transfer ($^1D^* + {}^1A \rightarrow {}^1D + {}^1A^*$), whereas triplet-triplet energy transfer occur ($^3D^* + {}^1A \rightarrow {}^1D + {}^3A^*$) only due to molecular orbital overlap.

1.1.4.1. Singlet-singlet energy transfer

Though interactions of different kinds are possible in singlet-singlet energy transfer, the Coulombic interactions through dipole-dipole interaction is the topic of discussion in this section. In the case of dipole-induced dipole mechanism, transfer of excitation energy requires dipole-dipole interactions between donor and acceptor along with the spectral overlap criterion, where the donor emission matches with acceptor absorption spectrum. The efficiency of this energy transfer depends on the distance between the donor-acceptor partner molecules and their overlap integral. Such transitions are coupled, i.e. they are in resonance and known as Förster resonance energy transfer (FRET). The Förster resonance energy transfer can be used as a spectroscopic ruler in the range of 10–100 Å. The distance between the donor and acceptor molecules should be constant during the donor lifetime and greater than about 10 Å in order to avoid the effect of short-range interactions. The validity of such a spectroscopic ruler has been confirmed by studies on model systems in which the donor and acceptor are separated by well-defined rigid spacers. For example, Oligomers of poly(L-proline) are used as spacers of defined length to separate an energy donor and acceptor by distances ranging from 12 to 46 Å. The energy donor was an α-naphthyl group at the carboxyl end of the polypeptide, while the energy acceptor

is a dansyl group at the imino end.[139] Single molecular FRET study by Winkler et al. along poly(L-proline) proves that longer proline oligomers are distinctly more flexible.[140]

1.1.4.2. Triplet-triplet energy transfer

As already mentioned, triplet-triplet energy transfer (TET) occurs ($^3D^* + {}^1A \rightarrow {}^1D + {}^3A^*$) only due to electron exchange mechanism through molecular orbital overlap (Scheme 1.3.). The theory of energy transfer by electron exchange was given by Dexter. The mechanism of populating the triplet state of an acceptor by the triplet state of a donor is called as photosensitization. For example, the triplet state of thymine in frozen solutions was populated by energy transfer from acetophenone.[16] Scheme 1.4. illustrates the triplet-triplet energy transfer process between a triplet donor and acceptor pair.

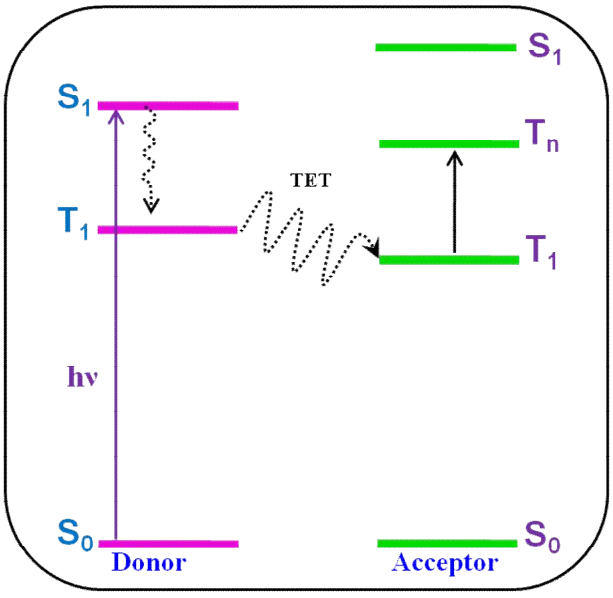

Scheme 1.4.

The triplet state energy of the donor must be greater than that of the acceptor for the energy transfer to occur. To avoid direct excitation, the ground state absorption of the donor must be higher than the acceptor at the excitation wavelength. The excited state triplet-triplet energy transfer is used as a tool to populate the triplet excited state of an acceptor molecule where intersystem crossing rate is very low due to high singlet-triplet energy gap (Scheme 1.4.). For example, triplet state of acenaphthylene[141] was populated by this photosensitization method.

Triplet state of the molecule needs to be characterized for many real life applications such as photodynamic therapy,[142-144] which is widely used for cancer treatment and to characterize molecule as an anticancer agent. These studies are possible only when the triplet states of the drug molecules are well characterized. However, in many cases poor triplet state quantum yield of the molecules hinders these studies. Triplet-triplet energy transfer process made these studies possible where different donor molecules, having high triplet quantum yield, are used to transfer the triplet state energy to the acceptor drug molecule.

1.2. Excited state acidity/basicity constant (pK^*)

In this section, acid-base properties of excited state aromatic compounds are discussed in aqueous media. The occurrence of the excited state proton transfer during the fluorescence lifetime of the molecule depends on competitive radiative and non-radiative deactivation pathways of the molecule to its ground and triplet states. The acidic or basic properties of a molecule change from the ground to the excited state mainly due to change in the electronic structure. Hence the excited state acidity/basicy constant (pK^*) of a molecule completely differs

from its ground state pK value and the difference will decide whether the fluorophore gains or loses the proton in its excited state. Fluorophore loses a proton in the excited state when pK^* < pK value and gains a proton in the opposite case. For instance, 2-naphthol[2] undergoes excited state deprotonation (Scheme 1.5) reaction, resulting in a decrease in pK from 9.2 to pK^* = 2.0, whereas acridine undergoes excited state protonation reaction with an increase in the pK value from 5.45 to 10.7 (pK^*) in the excited state.[145,146] In general, due to the presence of lone pair of electrons, electron donor groups such as –OH, –SH,–NH_2 strongly conjugate to the aromatic ring systems to make pK^* < pK and the molecules undergo excited state deprotonation reaction. On the other hand, electron withdrawing groups such as $–CO_2^-$ and –COOH, having vacant π–orbitals increase the electron density of the molecule in the excited state and weaken the excited state deprotonation reaction (pK^* > pK).

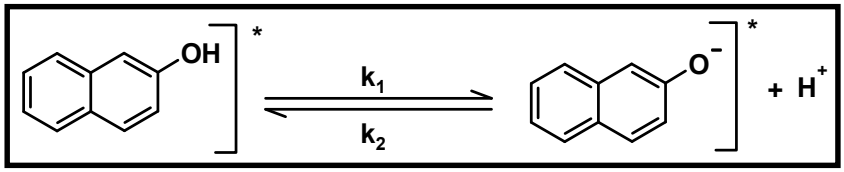

Scheme 1.5.

Acidity or basicity of a molecule in the excited singlet or triplet state (pK^*) can be determined by different methods. Concentrating on the work outlined in the present thesis, methods of calculating excited singlet state pK are discussed in the following sections along with their advantages and limitations.

1.2.1. Förster cycle

The value of pK^* can be theoretically predicted by popular Förster cycle[1] (Scheme 1.6) in conjunction with spectroscopic measurements.

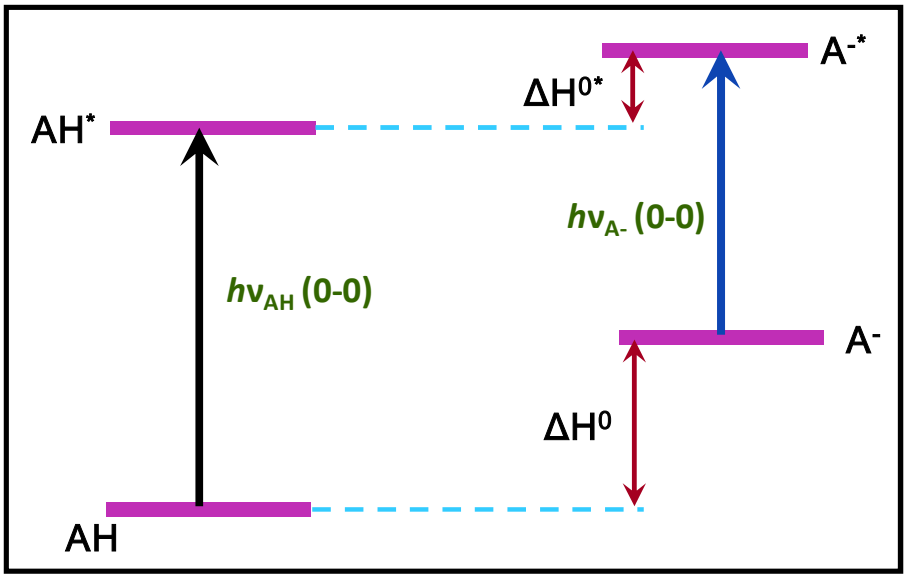

Scheme 1.6.

According to this cycle,

$$N_a h\nu_{AH} + \Delta H^{0*} = N_a h\nu_{A^-} + \Delta H^0 \quad (1)$$

Where ΔH^0 and ΔH^{0*} are the standard ionization enthalpies of AH and AH^*, respectively, $h\nu_{AH}$ and $h\nu_{A^-}$ are the energy difference (corresponding to the 0-0 transitions) between the excited state and the ground state of AH and A^-, respectively, and N_a is Avogadro's number. The equation is rearranged as,

$$\Delta H^{0*} - \Delta H^0 = N_a (h\nu_{A^-} - h\nu_{AH}) \quad (2)$$

Taking an assumption that the ionization entropies ΔS^0 and ΔS^{0*} of AH and AH^*, respectively, are equal to the enthalpies ΔH^0 and ΔH^{0*}, respectively, the difference in standard free energies $\Delta G^{0*} - \Delta G^0$ can be represented as,

$$\Delta G^0 - \Delta G^{0*} = \Delta H^0 - \Delta H^{0*} = RT \ln (K^*/K) \quad (3)$$

Where R is the gas constant and T is the absolute temperature. Rearranging equation 3,

$$pK^* - pK = \frac{N_a hc}{2.303RT} (\bar{\nu}_{A^-} - \bar{\nu}_{AH}) \quad (4)$$

Generally the wavenumbers $\bar{\nu}_{AH}$ and $\bar{\nu}_{A^-}$ correspond to the 0–0 transitions of AH and A^- respectively.

Förster cycle is a simple method, which explains why it has been extensively used. One of the important features of this cycle is that it can be used even in cases where the equilibrium is not established within the excited-state lifetime. However, use of the Förster cycle is questionable when (i) the 0–0 transition energies for AH and A^- are not accurately measured; (ii) the electronic levels invert during the excited-state lifetime (usually in a solvent-assisted relaxation process); (iii) the excited acidic and basic forms are of different orbital origins (electronic configuration or state symmetry); and (iv) the changes in dipole moment upon excitation are different for the acidic and basic forms.

For calculation of pK_a^* by Förster cycle it is necessary to calculate accurately the 0–0 transition energies. But because of the fact that at room temperature absorption and emission spectra of most of the molecules are

characterized by broad bands, it is often very difficult to determine accurately the 0–0 transition energies from either absorption or emission spectra. However, the best approximation is found by using the intersection point of the mutually normalized absorption and emission spectra. Another important problem while calculating pK_a^* by Förster cycle is the solvation which is often noticed by large Stokes shift of the fluorescence band. Finding the 0–0 transition from intersection point of the mutually normalized absorption and emission spectra is not possible in those cases. The averaging of absorption and emission maxima, however, eliminates such solvation effect if the energy of solvent relaxation in the two states is same.

Förster cycle thus suffers from many disadvantages and it can be concluded that pK_a^* calculated using Förster cycle is mostly not reliable.

1.2.2. Weller method

The value of the excited state pK_a can be determined by Weller method[100,146] based on the pH dependence of the fluorescence intensities.

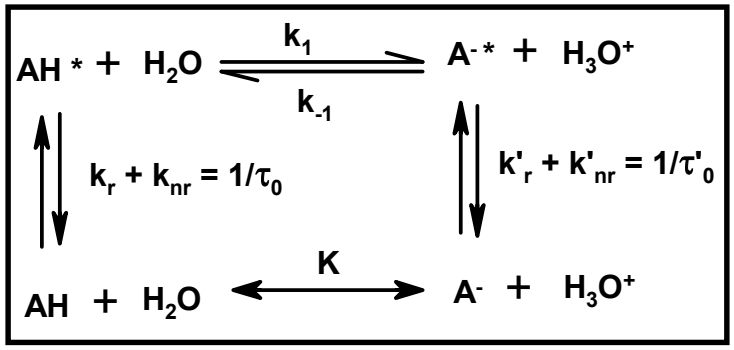

Scheme 1.7.

In a schematic representation of excited state deprotonation of an acid (AH), various processes involved in the dynamics are shown in Scheme 1.7. The excited state lifetimes of the acidic (AH^*) and basic (A^{-*}) forms are represented by τ_0 and τ_0' (which are the inverse of radiative and non-radiative rate constants), and k_1 and k_{-1} are the rate constants for deprotonation and reprotonation, respectively. k_1 is a pseudo-first order rate constant, whereas k_{-1} is a second-order rate constant.

On the basis of simple steady state method, Weller[147] has shown that the ratio of steady state fluorescence intensities at a given pH is given by

$$\frac{I_{AH^*}}{(I_{AH^*})_0} = \frac{\Phi}{\Phi_0} = \frac{1+k_{-1}\,\tau_0'\,[H_3O^+]}{1+\,k_1\tau_0+k_{-1}\,\tau_0'\,[H_3O^+]} \qquad (5)$$

$$\frac{I_{A^{-*}}}{(I_{A^{-*}})_0} = \frac{\Phi'}{\Phi'_0} = \frac{k_1\,\tau_0}{1+\,k_1\tau_0+k_{-1}\,\tau_0'\,[H_3O^+]} \qquad (6)$$

Where Φ_0 and Φ_0' are the fluorescence quantum yields of AH and A^-, respectively, in the absence of the excited state reaction and Φ and Φ' are in presence of excited state reaction. Eqn 5 and 6, the ratio of the quantum yields is divided by $(1 + k_{-1}\,\tau_0')$ and rearranged to get

$$(\Phi/\Phi_0)/(\Phi'/\Phi'_0) = 1/\,(1+ R \times 10^{pH}) \qquad (7)$$

Where, $R = k_1\tau_0\, K_w / (1 + k_{-1}\,\tau_0')$

Now steady state fluorescence intensity versus pH plot for both acid and its conjugate base gives sigmoidal curves and the point of inflection corresponds to the pK^* value.

Weller method can be used to calculate pK_a^* value accurately only if (i) equilibrium is established within the lifetime of the excited state species and (ii) fluorescence lifetime of two species are equal and (iii) both the species are fluorescent. Again, the pH at the point of inflection of fluorescence titration curve cannot always be taken to be equal to pK_a^* even if both the species are fluorescent. The pH at the inflection point will correspond to pK_a^* only when excited state species is not quenchd by the added acid/base.

So in conclusion, steady state fluorescence method also suffers from some serious limitations.

1.2.3. Kinetic method

It is already discussed in the previous sections that determination of pK_a^* either by the Förster cycle or Weller method suffers from several limitations arising from drastic assumptions made in those methods. The most reliable way to find out the actual pK_a^* value is to look directly into the reaction process by measuring the fluorescence decays involved in the reaction. Measuring the rate constants involved in the reaction is the only way to know whether the excited state equilibrium is attended or not. The determination of individual excited state rate constants, such as k_1 and k_{-1} (Scheme 1.7.) will yield the actual value of pK_a^* where the excited-state equilibrium constant is represented as

$$K^* = k_{-1}/k_1 \quad (8)$$

The time evolution of the fluorescence intensity of the acidic form AH^* and the conjugate basic form A^{-*} following photoexcitation (Scheme 1.7.) is obtained from the following differential equations:

$$\frac{d[AH^*]}{dt} = -\left(k_1 + {}^{1}/_{\tau_0}\right)[AH^*] + k_{-1}[A^{-*}][H_3O^+] \quad (9)$$

$$\frac{d[A^{-*}]}{dt} = k_1[AH^*] - \left(k_{-1}[H_3O^+] + {}^{1}/_{\tau_0'}\right)[A^{-*}] \quad (10)$$

After selective excitation of AH, the time responses of the fluorescence intensities, under the initial conditions $[AH^*] = [AH^*]_0$ and $[A^{-*}] = 0$ (at t = 0) are

$$i_{AH^*}(t) = k_r[AH^*] = \frac{k_r[AH^*]_0}{\beta_1 - \beta_2}\left[(X-\beta_2)e^{-\beta_1 t} + (\beta_1 - X)e^{-\beta_2 t}\right] \quad (11)$$

$$i_{A^{-*}}(t) = k_r'[A^{-*}] = \frac{k_r' k_1[AH^*]_0}{\beta_1 - \beta_2}\left[e^{-\beta_2 t} - e^{-\beta_1 t}\right] \quad (12)$$

Where k_r and k_r' are the radiative rate constants of AH^* and A^{-*} respectively, and β_1 and β_2 are given by

$$\beta_{2,1} = \frac{1}{2}\left\{(X+Y) \pm [(Y-X)^2 + 4k_1k_{-1}[H_3O^+]]^{\frac{1}{2}}\right\} \quad (13)$$

Where, $X = k_1 + {}^{1}/_{\tau_0}$, $Y = k_{-1}[H_3O^+] + {}^{1}/_{\tau_0'}$

Measurements of the lifetime of AH^* and A^{-*} and pre-exponential factors from the decay profiles recorded by time-resolved single photon counting technique enable us to determine individual rate constants (Scheme 1.7.) and thereby pK^* value.

Excited state deprotonation of carbazole was studied by Samanta et al.[82] All the rate constants involved with this system were calculated and it was proved that the equilibrium is not attained at the pK^* value when it was calculated by steady state fluorescence intensity measurements. It is also reported that in excited state protonation/deprotonation reaction of norharman involving three ground and

four excited state species, the back reaction plays a significant role in its acid-base chemistry.[148,149] The excited state behavior of few green fluorescent proteins (GFP), having different chromophores, is explained by using its excited state pK value calculated accurately by the kinetic method.[150,151] In Chapter 4 excited state protonation of ellipticine, producing ellipticinium cation, is studied in a particular pH range and all the rate constants involved with the excited state process are measured to calculate the accurate pK^* value.

1.3. Motivation behind the thesis

The work embodied in this thesis deals with synthesis and exploration of the photophysical properties of some important molecules in different media. The molecules selected for this investigation (Chart 1.7.) are those whose ground and excited state properties are sensitive to solvent polarity, pH and specific solute-solvent interactions. The present thesis mainly comprises three different studies; (i) effect of hydrogen bond donating and accepting ability of a solvent on the proton transfer kinetics and hydrogen bonding interactions, (ii) effect of pH on the proton transfer kinetics and (iii) characterization of new triplet states, triplet-triplet energy transfer and relative actinometry studies. Photophysical studies have been carried out using UV-visible absorption, steady state and time-resolved fluorescence and phosphorescence and laser flash photolysis techniques. Theoretical calculations based on density functional methods have also been carried out in some cases for a better understanding of the experimental results.

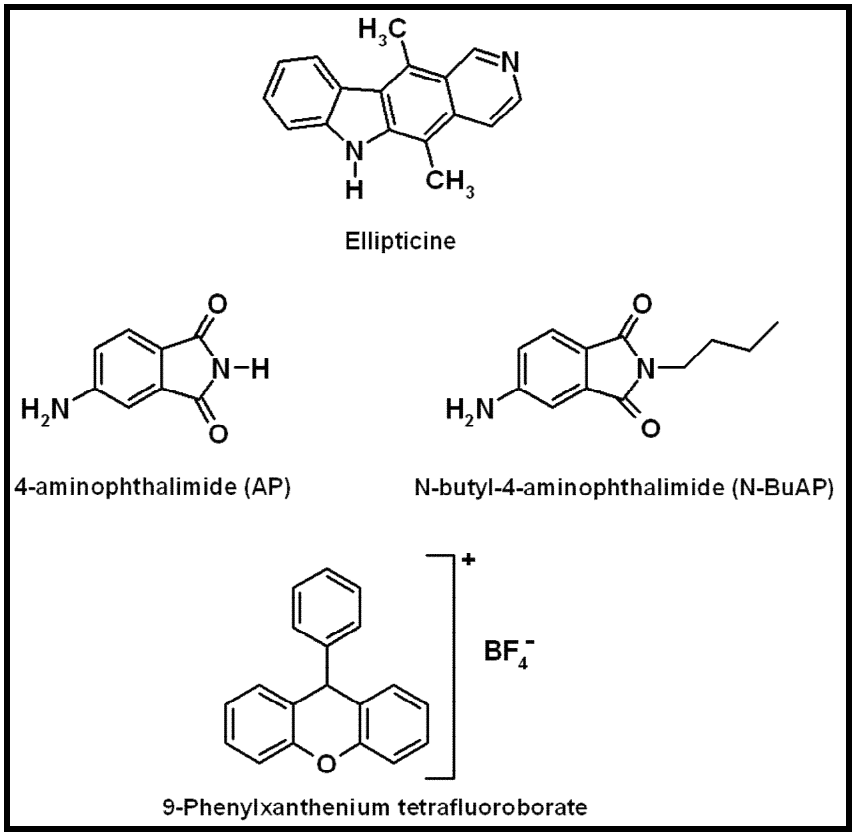

Chart 1.7.

Photophysical properties of ellipticine (5,11-dimethyl-6H-pyrido[4,3-b]carbazole), comprising of both proton donating and accepting sites, have been studied in different solvents using steady state and time-resolved fluorescence techniques primarily to understand the origin of dual fluorescence that the molecule exhibits in some specific alcoholic solvents like methanol and ethylene glycol. Ground and excited state calculations based on density functional theory have also been carried out to help in interpretation of the experimental data. It is shown that the long-wavelength emission of this molecule is dependent on the

hydrogen bond donating ability of the solvent, and in methanol, this emission band arises solely from an excited state reaction. However, in ethylene glycol, both ground and excited state reactions contribute to the long wavelength emission. The time-resolved fluorescence data of the molecule in methanol and ethylene glycol indicates the presence of two different hydrogen bonded species of ellipticine of which only one participates in the excited state reaction. The rate constant of the excited state reaction in these solvents is also estimated. It appears that the present results are better understood in terms of solvent mediated excited state intramolecular proton transfer reaction from the pyrrole nitrogen to the pyridine nitrogen leading to the formation of the tautomeric form of the molecule rather than excited state proton transfer from the solvents leading to the formation of the protonated form of ellipticine.

Steady state absorption, emission and time-resolved fluorescence behavior of ellipticine have been studied in aqueous media over a wide pH range. Time-resolved fluorescence measurements have been carried out in aqueous alkaline media to monitor the excited state protonation kinetics of ellipticine which is possible by increased basicity of the pyridine nitrogen in the excited state. The individual rate constants are evaluated from the excited state kinetics based on which, for the first time, excited state protonation equilibrium constant of ellipticine is calculated which provide the pK_a^* value of 12.7. The pK_a^* value calculated from relatively simpler and popularly used Förster cycle showed considerable deviation from the accurate pK_a^* value calculated from the kinetic method. Weller method, based on steady state fluorescence intensity measurements, could not be used to calculate pK_a^* value due to faster rate of

excited state backward reaction than the radiative and non-radiative deactivation of excited ellipticinium cation, as found by the time-resolved fluorescence measurements.

Fluorescence behavior of 4-aminopthalimide (AP) and its imide-H protected derivative (N-BuAP) has been reinvestigated in aqueous media to address some of the points raised in a recent paper by Durantini et al.[152] The results show that solvent assisted keto-enol transformation does not contribute to the observed steady state and time-resolved emission behavior of AP in aqueous media. Instead, the results reveal that the fluorescence of AP in aqueous media arises from two distinct hydrogen bonded species. The deuterium isotope effect on the fluorescence quantum yield and lifetime of AP, earlier thought to be a reflection of the excited state proton transfer process,[152,153] is now explained by considering the difference between the influence of deuterated and undeuterated solvents on the rate of non-radiative processes and also the ground state exchange of the proton with the solvent.

Laser flash photolysis studies on a highly fluorescent and stable salt of 9-phenylxanthenium cation in neutral environment has been carried out for the first time. A new transient absorption band of this extensively studied system that most probably remained buried under the fluorescence envelope and hitherto undetected has been identified and attributed to the triplet state of the system. The newly identified triplet–triplet absorption band of 9-phenylxanthenium cation, which is insensitive to oxygen and appears in the visible region, is well-separated from the absorption bands of 9-phenylxanthenyl radical or 9-phenylxanthenol triplet and hence, interference from these species has been avoided.

Triplet excited state of ellipticine in different solvents has been characterized by using laser flash photolysis technique. The various triplet state parameters (extinction coefficient and quantum yield) of the molecule are estimated by triplet-triplet energy transfer and relative actinometry technique. Interestingly, even though in polar aprotic solvent acetonitrile, the triplet-triplet energy transfer from thioxanthone to ellipticine is observed, the process is found to be inefficient in nonpolar methylcyclohexane. This observation is attributed to the dependence of triplet state energy on the solvent polarity, which is confirmed by low-temperature phosphorescence studies. In methylcyclohexane, the triplet-triplet energy transfer process is observed from xanthone, having higher triplet state energy, to acceptor ellipticine. Nearly 4-fold decrease in the triplet extinction coefficient and a noticeable increment in the triplet quantum yield of ellipticine are found on changing the solvent from polar acetonitrile to nonpolar methylcyclohexane. Studies in 1,1,1,3,3,3-hexafluoro-2-propanol reveal complete ground state protonation of ellipticine thereby producing transient of ellipticinium cation. However, in 2,2,2-trifluoroethanol, where both neutral and cationic forms are present the ground state, sensitized triplet absorption spectrum resembles that of neutral ellipticine only.

Reference

(1) Valeur, B. *In Molecular Fluorescence Principles and Applications*; WILEY-VCH: Weinheim, **2002**.

(2) Lakowicz, J. R. *In Principles of Fluorescence Spectroscopy, 3rd edition*; Springer: New York, **2006**.

(3) Hurtubise, R. J. *In Phosphorimetry: Theory, Instrumentation and Applications*; VCH Publishers: New York, **1990**.

(4) Demchenko, A. P. *Lab Chip* **2005**, *5*, 1210.

(5) deSilva, A. P.; Sandanayake, K. R. A. S. *Angew. Chem. Int. Ed.* **1990**, *29*, 1173.

(6) Julliard, M.; Chanon, M. *Chem. Rev.* **1983**, *83*, 425.

(7) Whitten, D. G. *Acc. Chem. Res.* **1980**, *84*, 981.

(8) Bi, D.; Wu, F.; Qu, Q.; Yue, W.; Cui, Q.; Shen, W.; Chen, R.; Liu, C.; Qiu, Z.; Wang, M. *J. Phys. Chem. C* **2011**, *115*, 3745.

(9) Kawatsu, T.; Coropceanu, V.; Ye, A.; Bredas, J.-L. *J. Phys. Chem.* **2008**, *112*, 3429.

(10) Yang, L. X.; Zhu, Y. J.; Wang, W. W.; Tong, H.; Ruan, M. L. *J. Phys. Chem. B* **2006**, *110*, 6609.

(11) Okazaki, K.-I.; Kiyama, T.; Hirahara, K.; Tanaka, N.; Kuwabata, S.; Torimoto, T. *Chem. Commun.* **2008**, 691.

(12) deSilva, A. P.; Leydet, Y.; Lincheneau, C.; McClenagham, N. D. *J. Physics: Condensed Matter* **2006**, *18*, S1847.

(13) deSilva, A. P.; Gunaratne, H. Q. N.; McCoy, C. P. *Nature* **1993**, *364*, 42.

(14) deSilva, A. P.; McClenaghan, N. D. *J. Am. Chem. Soc.* **2000**, *122*, 3965.

(15) Chen, J.-S.; Zhou, P.-W.; Yang, S.-Q.; Fu, A.-P.; Chu, T.-S. *Phys. Chem. Chem. Phys.* **2013**, *15*, 16183.

(16) Zhao, J.; Ji, S.; Chen, Y.; Guo, H.; Yang, P. *Phys. Chem. Chem. Phys.* **2012**, *14*, 8803.

(17) Park, S. Y.; Park, S. H.; Kwon, J. E., **2011**; Vol. WO2010123266 A3.

(18) Sun, K.; Chen, K.; Xue, G.; Cai, J.; Zou, G.; Li, Y.; Zhang, Q. *R. Soc. Chem. Adv.* **2013**, *3*, 23997.

(19) Blasco, E.; Serrano, J. L.; Pinol, M.; Oriol, L. *Macromol.* **2013**, *46*, 5951.

(20) Miao, Z.-C.; Zhang, Y.-M.; Zhao, Y.-Z.; Wang, D. *Mol. Cryst. Liq. Cryst.* **2013**, *582*, 98.
(21) Bogdanov, A. V.; Vorobiev, A. K. *J. Phys. Chem. B* **2013**, *117*, 12328.
(22) Siewertsen, R.; Schoenborn, J. B.; Hartke, B.; Renth, F.; Temps, F. *Phys. Chem. Chem. Phys.* **2011**, *13*, 1054.
(23) Yildiz, I.; Impellizzeri, S.; Deniz, E.; McCaughan, B.; Callan, J. F.; Raymo, F. M. *J. Am. Chem. Soc.* **2011**, *133*, 871.
(24) Birks, J. B. *Chem. Phys. Lett.* **1972**, *17*, 370.
(25) Binsch, G.; Heilbronner, E.; Kankow, R.; Schmidt, D. *Chem. Phys. Lett.* **1967**, *1*, 135.
(26) Eaton, P. F.; Evans, T. R.; Lennakers, P. A. *Mol. Photochem.* **1969**, *1*, 347.
(27) Turro, N. J.; Ramamurthy, V.; Cherry, W.; Farneth, W. *Chem. Rev.* **1978**, *78*, 125.
(28) Dhingra, R.; Poole, J. A. *Chem. Phys. Lett.* **1968**, *2*, 108.
(29) Samanta, A.; Devadoss, C.; Fessenden, R. W. *J. Phys. Chem.* **1990**, *94*, 7106.
(30) Mondal, J. A.; Ghosh, H. N.; Mukherjee, T.; Palit, D. K. *J. Phys. Chem.* **2005**, *109*, 6836.
(31) BÎrlâ, L.; Bertorelle, F.; Rodrigues, F.; Badré, S.; Pansu, R.; Fery-Forgues, S. *Langmuir* **2006**, *22*, 6256.
(32) Agbaria, R. A.; Butterfield, T.; Warner, I. M. *J. Phys. Chem.* **1996**, *100*, 17133.
(33) Valentium, R.; Gehlen, M. W. *J. Phys. Chem. A* **2006**, *110*, 7539.
(34) Tsourkas, A.; Bhelke, M. A.; Xu, Y.; Bao, G. *Anal. Chem.* **2003**, *75*, 3697.
(35) Getz, D.; Ron, A.; Rubin, M. B.; Speiser, S. *J. Phys. Chem.* **1980**, *84*, 768.
(36) Wilson, G. J.; Launikonis, A.; Sasse, W. H. F.; Mau, A. O. H. *J. Phys. Chem. A* **1997**, *101*, 4860.
(37) Liu, J.; Lu, Y. *J. Am. Chem. Soc.* **2002**, *124*, 15208.
(38) Bhattacharya, K.; Chowdhury, M. *Chem. Rev.* **1993**, *93*, 507.
(39) Weigel, W.; Wagner, P. J. *J. Am. Chem. Soc.* **1996**, *118*, 12858.
(40) Yip, W. T.; Levy, D. H. *J. Phys. Chem.* **1996**, *100*, 11539.
(41) Kasha, M. *J. Chem. Soc., Faraday, Trans. 2* **1986**, *82*, 2379.

(42) Ormson, S. M.; Brown, R. G.; Vollmer, F.; Rettig, W. *J. Photochem. Photobiol. A: Chem.* **1994**, *81*, 65.

(43) Das, K.; Sarkar, N.; Mazumder, D.; Bhattacharya, K. *Chem. Phys. Lett.* **1992**, *198*, 443.

(44) Sengupta, P. K.; Kasha, M. *Chem. Phys. Lett.* **1979**, *68*, 382.

(45) MaMorrow, D.; Kasha, M. *J. Phys. Chem.* **1984**, *88*, 2235.

(46) Mason, S. F.; Philip, J.; Smith, B. E. *J. Chem. Soc.* **1968**, 3051.

(47) Thistlethwaite, P. J.; Corkill, P. *J. Chem. Phys. Lett.* **1982**, *85*, 317.

(48) Thistlethwaite, P. J. *J. Chem. Phys. Lett.* **1983**, *96*, 509.

(49) Itoh, M.; Adachi, T.; Tokumara, K. *J. Am. Chem. Soc.* **1983**, *105*, 4828.

(50) Tokumara, K.; Itoh, M. *J. Phys. Chem.* **1984**, *88*, 3921.

(51) Itoh, M.; Adachi, T.; Tokumara, K. *J. Am. Chem. Soc.* **1984**, *106*, 850.

(52) Kwon, O.-H.; Lee, Y.-S.; Yoo, B. K.; Jang, D.-J. *Angew. Chem. Int. Ed.* **2006**, *45*, 415.

(53) Rettig, W. *Angew. Chem. Int. Ed. Engl.* **1986**, *25*, 971.

(54) Grabowski, Z. R.; Dobkowski, J. *Pure. Appl. Chem.* **1983**, *55*, 245.

(55) Grabowski, Z. R.; Rotkiewicz, K.; Rettig, W. *Chem. Rev.* **2003**, *103*, 3899.

(56) Rotkiewicz, K.; Grellmann, K. H.; Grabowski, Z. R. *Chem. Phys. Lett.* **1973**, *19*, 315.

(57) Rotkiewicz, K.; Grabowski, Z. R.; Krowczynski, A.; Kühnle, W. *J. Lumin* **1976**, *12*, 877.

(58) McGlynn, S. P.; Azumi, T.; Kinoshita, M. *In Molecular Spectroscopy of the Triplet State*; Prentice-Hall: New Jersey, **1969**.

(59) Englander, S. W.; Calhoun, D. B.; Englander, J. J. *Anal. Biochem.* **1987**, *161*, 300.

(60) Scott, D. R.; Becker, R. S. *J. Chem. Phys.* **1961**, *35*, 516.

(61) Scott, D. R.; Becker, R. S. *J. Chem. Phys.* **1961**, *35*, 2246.

(62) El-Sayed, F. E.; MacCallum, J. R.; Pomery, P. J.; Shepherd, T. M. *J. Chem. Soc., Faraday Trans. 2* **1979**, *75*, 79.

(63) Khara, D. C.; Samanta, A. *Aust. J. Chem.* **2012**, *65*, 1291.

(64) Kim, S.; Fujitsuka, M.; Majima, T. *J. Phys. Chem. B* **2013**, *10.1021/jp406638g*.

(65) Ogilby, P. R. *Chem. Soc. Rev.* **2010**, *39*, 3181.

(66) daSilva, E. F. F.; Pedersen, B. W.; Breitenbach, T.; Toftegaard, R.; Kuimova, M. K.; Arnaut, L. G.; Ogilby, P. R. *J. Phys. Chem. B* **2011**, *116*, 445.

(67) Kuimova, M.; Botchway, S.; Parker, A.; Balaz, M.; Collins, H.; Anderson, H.; Suhling, K.; Ogilby, P. R. *Nat. Chem.* **2009**, *1*, 69.

(68) Klopffer, W. *Adv. Photochem.* **1977**, *10*, 311.

(69) Huppert, D.; Gutman, M.; Kaufmann, M. *J. Adv. Chem. Phys.* **1981**, *47*, 643.

(70) Barbara, P. F.; Walsh, P. K.; Brus, L. E. *J. Phys. Chem.* **1989**, *93*, 29.

(71) Chou, P. T. *J. Chin. Chem. Soc.* **2001**, *48*, 651.

(72) Scheiner, S. *J. Phys. Chem.* **2000**, *104*, 5898.

(73) Arnaut, L. G.; Formosinho, S. J. *J. Photochem. Photobiol. A: Chem.* **1993**, *75*, 1.

(74) Douhal, A.; Lahmani, F.; Zewali, A. *Chem. Phys.* **1996**, *207*, 477.

(75) Aquino, A. J. A.; Lischka, H.; Christof, H. *J. Phys. Chem. A* **2005**, *109*, 3201.

(76) Agmon, N. *J. Phys. Chem. A* **2005**, *109*, 13.

(77) Kennis, J. T. M.; vanStokkum, I. H. M.; Peterson, D. S.; Pandit, A.; Wachter, R. M. *J. Phys. Chem. B* **2013**, *117*, 11134.

(78) vanThor, J. J.; Lincoln, C. N.; Kellner, B.; Bourdakos, K. N.; Thompson, L. M.; Bearpark, M. J.; Champion, P. M.; Sage, J. T. *Vib. Spectrosc.* **2012**, *62*, 1.

(79) Liu, K.; Huo, J.; Zhu, B.; Huo, R. *J. Fluorec.* **2012**, *22*, 1231.

(80) Erez, Y.; Gepshtein, R.; Presiado, I.; Trujillo, K.; Kallio, K.; Remington, J. S.; Huppert, D. *J. Phys. Chem. B* **2011**, *115*, 11776.

(81) Piatkevich, K. D.; Malashkevich, V. N.; Almo, S. C.; Verkhusha, V. V. *J. Am. Chem. Soc.* **2010**, *132*, 10762.

(82) Samanta, A.; Chattopadhyay, N.; Nath, D.; Kundu, T.; Chowdhury, M. *Chem. Phys. Lett.* **1985**, *121*, 507.

(83) Banerjee, S.; Pabbathi, A.; Sekhar, M. C.; Samanta, A. *J. Phys. Chem. A* **2011**, *115*, 9217.

(84) Shida, N.; Almlof, J.; Barbara, P. F. *J. Phys. Chem.* **1991**, *95*, 10457.

(85) Chou, P. T.; McMorrow, D.; Aartsma, T. J.; Kasha, M. *J. Phys. Chem.* **1984**, *88*, 4596.

(86) Nishiya, T.; Yamauchi, S.; Hirota, N.; Baba, M.; Hanazaki, I. *J. Phys. Chem.* **1986**, *90*, 5730.

(87) Nagaoka, S.; Fujita, M.; Takemura, T.; Baba, M. *Chem. Phys. Lett.* **1986**, *123*, 489.

(88) Ernsting, N. P.; Nikolaus, B. *Appl. Phys. B* **1986**, *39*, 155.

(89) Kasha, M. *In Molecular Electronic Devices*; Elsevier Science: New York, **1988**.

(90) Ferrer, M. L.; Acuna, A. U.; Amat-Guerri, F.; Costela, A.; Figuera, J. M.; Florido, F.; Sastre, R. *Appl. Oct.* **1994**, *33*, 2266.

(91) Jones, G.; Rahman, M. A. *J. Phys. Chem.* **1994**, *98*, 13028.

(92) Liphardt, M.; Gooneskera, A.; Jones, B. E.; Ducharme, S.; Takacs, J. M.; Zhang, L. *Science* **1994**, *263*, 367.

(93) Douhal, A.; Sastre, R. *Chem. Phys. Lett.* **1994**, *219*, 91.

(94) Kuldova, K.; Corval, A.; Lehn, J. M.; Trommsdorff, H. P. *J. Phys. Chem. A* **1997**, *101*, 6850.

(95) Chou, P. T.; Studer, S.; Martinez, M. L. *Appl. Spectr.* **1991**, *45*, 513.

(96) Renschler, C. L.; Harrah, L. A. *In Nucl. Inst. Methods Phys. Res.*U.S., **1985**; Vol. A235.

(97) Williams, D. L.; Heller, A. *J. Phys. Chem.* **1970**, *74*, 4473.

(98) Roshal, A. D.; Grigorovich, A. V.; Doroshenko, A. O.; Pivovarenko, V. G.; Demchenko, A. P. *J. Phys. Chem.* **1998**, *102*, 5907.

(99) Tarkka, R. M.; Zhang, X.; Jenekhe, S. A. *J. Am. Chem. Soc.* **1996**, *118*, 9438.

(100) Weller, A. *Z. Elektrochem.* **1956**, *60*, 1144.

(101) Smith, K. K.; Kauffman, J. K. *J. Phys. Chem.* **1978**, *82*, 2286.

(102) Helmbrook, L.; Kenny, J. E.; Kohler, B. E.; G. W, S. *J. Phys. Chem.* **1983**, *87*, 280.

(103) Lamla, A. A.; Sharp, J. L. *J. Phys. Chem.* **1966**, *70*, 2634.

(104) Barbara, P. F.; Rentzepis, P. M.; Brus, L. E. *J. Am. Chem. Soc.* **1980**, *102*, 2786.

(105) Woolfe, G. J.; Thistlethwaite, P. J. *J. Am. Chem. Soc.* **1980**, *102*, 6917.

(106) Sinha, H.; Dogra, S. K. *Chem. Phys.* **1986**, 337.

(107) Das, K.; Sarkar, N.; Ghosh, A. K.; Mazumdar, D.; Nath, D. N.; Bhattacharyya, K. *J. Phys. Chem.* **1994**, *98*, 9126.

(108) Mosquera, M.; Penedo, J. C.; Rodriguez, M. C. R.; Prieto, F. R. *J. Phys. Chem.* **1996**, *100*, 5398.

(109) Woolfe, G. J.; Melzig, M.; Schneider, S.; Dorr, F. *Chem. Phys. Lett.* **1983**, *77*, 213.

(110) Itoh, H.; Fujiwara, Y. *J. Am. Chem. Soc.* **1985**, *107*, 1561.

(111) Potter, C. A. S.; Brown, R. G. *Chem. Phys. Lett.* **1988**, *153*, 7.

(112) Suda, K.; Terazima, M.; Sato, H.; Kimura, Y. *J. Phys. Chem. B* **2013**, *117*, 12567.

(113) Jana, S.; Dalapati, S.; Guchhait, N. *Photochem. Photobiol. Sci.* **2013**, *12*, 1636.

(114) Taylor, C. A.; El-Bayoumi, M. A.; Kasha, M. *Proc. Natl. Acad. Sci. U.S.A.* **1969**, *63*, 253.

(115) Ingham, K. C.; Abu-Elgheit, M.; El-Bayoumi, M. A. *J. Am. Chem. Soc.* **1971**, *93*, 5023.

(116) Hetherington, W. H.; Micheels, R. H.; Eisenthal, K. B. *Chem. Phys. Lett.* **1979**, *66*, 230.

(117) Catalan, J.; Perez, P.; delValle, J. C.; dePaz, J. L. G.; Kasha, M. *Proc. Natl. Acad. Sci. U.S.A.* **2004**, *101*, 419.

(118) Hazra, M. K.; Samanta, A. K.; Chakraborty, T. *J. Phys. Chem. A* **2007**, *111*, 7813.

(119) Muller, A.; Talbot, F.; Leutwyler, S. *J. Am. Chem. Soc.* **2002**, *124*, 14486.

(120) Tang, G. Q.; Macinnis, J.; Kasha, M. *J. Am. Chem. Soc.* **1987**, *109*, 2531.

(121) Douhal, A.; Kim, S. K.; Zewali, A. H. *Nature* **1995**, *378*, 260.

(122) Takeuchi, S.; Tahara, T. *J. Phys. Chem. A* **1998**, *102*, 7740.

(123) Chang, C.-P.; Wen-Chi, H.; Meng-Shin, K.; Chou, P.-T.; Clements, J. H. *J. Phys. Chem.* **1994**, *98*, 8801.

(124) Kwon, O.-H.; Jang, D.-J. *J. Phys. Chem. B* **2005**, *109*, 20479.

(125) Yamabe, S.; Tsuchida, N.; Hayashida, Y. *J. Phys. Chem. A* **2005**, *109*, 7216.

(126) Tortonda, F. R.; Pascul-Ahuir, J. L.; Silica, E.; Tunon, I. *Chem. Phys. Lett.* **1996**, *260*, 21.

(127) Markova, N.; Enchev, V.; Timtchera, I. *J. Phys. Chem. A* **2005**, *109*, 1981.

(128) Dkhissi, A.; Adamowick, L.; Maes, G. *Chem. Phys. Lett.* **2000**, *324*, 127.

(129) Kim, Y.; Lim, S.; Kim, H.-J.; Kim, Y. *J. Phys. Chem.* **1999**, *103*, 617.

(130) Tsuchida, N.; Yambe, S. *J. Phys. Chem.* **1999**, *109*, 1974.

(131) Li, Q.-S.; Fang, W.-H. *Chem. Phys. Lett.* **2003**, *367*, 637.

(132) Song, P. S.; Sun, M.; Koziolawa, A.; Koziol, J. *J. Am. Chem. Soc.* **1974**, *96*, 4319.

(133) Choi, J. D.; Fugate, R. D.; Song, P. S. *J. Am. Chem. Soc.* **1980**, *102*, 5293.

(134) Nakagawa, T.; Kohtani, S.; Itoh, M. *J. Am. Chem. Soc.* **1995**, *117*, 7952.

(135) Reichardt, C. In *Solvents and Solvent Effects in Organic Chemistry*; WILEY-VCH **2004**.

(136) Kuzmenkina, E. V.; Heyes, C. D.; Nienhaus, G. U. *Proc. Natl. Acad. Sci. U.S.A.* **2005**, *102*, 15471.

(137) Zhong, D.; Pal, S. K.; Zhang, D.; Chan, S. I.; Zewail, A. *Proc. Natl. Acad. Sci. U.S.A.* **2002**, *99*, 13.

(138) Dang, Y.; Li, H.; Wu, Y. *Appl. Mater. Interfaces* **2012**, *4*, 1267.

(139) Stryer, L.; Haugland, R. P. *Proc. Natl. Acad. Sci. U. S. A.* **1967**, *58*, 719.

(140) Winkler, J. R. *Science* **2013**, *339*, 1530.

(141) Samanta, A.; Fessenden, R. W. *J. Phys. Chem.* **1989**, *93*, 5823.

(142) Meunier, B.; Paillous, N. *J. Chem. Soc. Chem. Commun.* **1990**, *16*, 1131.

(143) Wiessler, M.; Frei, E. *Cancer Research* **2004**, *64*, 8374.

(144) Bae, S. I.; Zhao, R.; Snapka, R. M. *Biochem. Pharmacol.* **2008**, *76*, 1653.

(145) Gafni, A.; Brand, L. *Chem. Phys. Lett.* **1978**, *58*, 346.

(146) Weller, A. *Prog. React. Kinetics* **1961**, *1*, 189.

(147) Weller, A. *Z. Elektrochem.* **1952**, *56*, 662.

(148) Draxler, S.; Lippitsch, M. E. *J. Phys. Chem.* **1993**, *97*, 11493.

(149) Dias, A.; Varela, A. P.; Miguel, M. G.; Macanita, A. L.; Becker, R. S. *J. Phys. Chem.* **1992**, *96*, 10296.

(150) Baranov, M. S.; Lukyanov, K. A.; Borissova, A. O.; Shamir, J.; Kosenkov, D.; Slipchenko, L. V.; Tolbert, L. M.; Yampolsky, I. V.; Solntsev, K. M. *J. Am. Chem. Soc.* **2012**, *134*, 6025.

(151) Scharnagl, C.; Raupp-Kossmann, R. A. *J. Phys. Chem. B* **2004**, *108*, 477.

(152) Durantini, A. M.; Falcone, R. D.; Anunziata, J. D.; Silber, J. J.; Abuin, E. B.; Lissi, E. A.; Correa, N. M. *J. Phys. Chem. B* **2013**, *117*, 2160−2168.

(153) Datta, A.; Das, S.; Mandal, D.; Pal, S. K.; Bhattacharyya, K. *Langmuir* **1997**, *13*, 6922.

Chapter 2

Materials, Methods and Instrumentation

This chapter provides a brief description of different materials used in this study including the synthesis and purification of 9-phenylxanthenium tetrafluoroborate and N-butyl-4-aminophthalimide employed in this work. Methods of purification of various solvents and reagents used in this study are discussed. The sample preparation procedure for the spectral measurements is discussed briefly in this context. Different instrumental setups used in this work are also discussed. Various methodologies like measurements of molar extinction coefficient of a transient species by triplet-triplet energy transfer, determination of triplet quantum yield by relative actinometry, data analysis and construction of time-resolved emission spectra, theoretical calculations etc. have been explained in detail.

2.1. Materials

Ellipticine was purchased from Fluka (for fluorescence, ≥ 98% HPLC) and Enzo Life Sciences (98%) and used without further purification. Ellipticine was stored in a glovebox below – 20 °C and prepared solutions were kept inside refrigerator. 4-aminophthalimide was obtained from TCI (Japan) and was recrystallised from ethanol prior to use. 9-phenylxanthen-9-ol (Aldrich) was recrystallized twice from cyclohexane prior to photophysical experiments. Propionic anhydride (≥ 99 %, Aldrich), tetrafluoroboric acid 48 wt. % solution in water (Aldrich), anhydrous diethyl ether (Merck), N-butyl amine (Merck) were

used as received for synthesis. Thioxanthone (98 %, Aldrich), xanthone (98 %, Aldrich) and benzophenone (Nice Chemicals, India) were recrystallized twice from ethanol. Phosphate buffer tablets (pH = 7.0) were obtained from Fisher Scientific, whereas buffer tablets of pH = 4 and 9.2 were purchased from Qualigens. Aqueous solutions of different pH were prepared by adding sodium hydroxide (NaOH) or hydrochloric acid (HCl). The purity of the compounds was confirmed by thin layer chromatography (TLC), nuclear magnetic resonance spectroscopy (NMR), Infrared (IR) spectroscopy and also by matching the absorption and emission spectra with the literature.

The various drying agents and chemicals such as phosphorous pentoxide (P_2O_5), sodium metal, magnesium turnings and iodine used at different stages of the purification procedure, were purchased from local companies. Calcium hydride (CaH_2) was obtained from Spectrochem (India). GR and spectroscopic grade solvents were obtained from Merck (India) for synthetic and spectroscopic purposes and their purification procedures are outlined in the following section. Deuterated solvents, chloroform-d, methanol-d_4 and acetone-d_6 used for NMR spectral measurements were obtained either from Aldrich or from Merck (India).

2.2. Synthesis of 9-phenylxanthenium tetrafluoroborate

Tetrafluoroborate salt of 9-phenylxanthen-9-ol was prepared by following the method of Dauben et al.[1,2] A brief description of synthesis of 9-phenylxanthenium tetrafluoroborate used in this study is provided here. 9-phenylxanthen-9-ol (1.7 mmol) was dissolved in propionic anhydride (4.5 mL) at 50 °C. The temperature was maintained while addition of fluoroboric acid (0.33 g, 3.8 mmol), which immediately gave an yellow solution. The xanthylium

tetrafluoroborate salt precipitated and collected by suction filtration. Finally the salts were purified by repeated washing with cold, anhydrous diethyl ether to yield bright yellow solid.

9-Phenylxanthenium tetrafluoroborate. ^{1}H NMR data ($CDCl_3$): δ 7.75-7.95(m, 7H), 8.15(d, 2H), 8.4-8.54(m, 4H); ^{13}C NMR: δ 155.5, 143.7, 132.5, 131.7, 130.5, 130.2, 129.1, 124.1, 123.5, 120.2, 116.5.

MP: 227 ^{0}C.

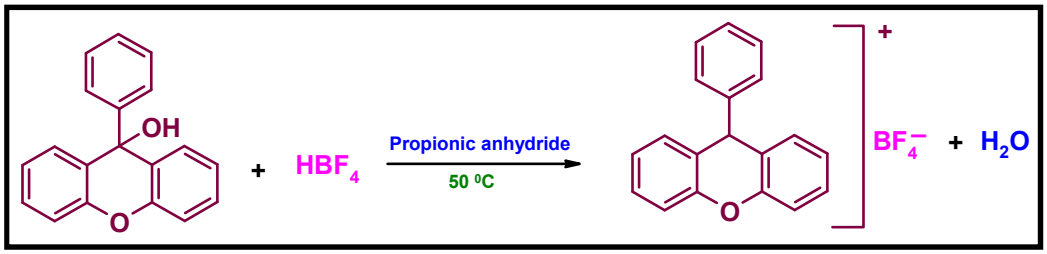

Scheme 2.1. Synthetic procedure of 9-phenylxanthenium tetrafluoroborate.

2.3. Synthesis of n-butyl-4-aminophthalimide

N-butyl-4-aminophthalimide (N-BuAP) was synthesized following a standard procedure[3] which is briefly described below. Equimolar mixtures of 4-aminophthalimide and n-butylamine in dimethylformamide (DMF) were heated at 80 °C for 10 hours. Water was added to the cooled reaction mixture and the product was extracted with ethyl acetate. Removal of the solvent followed by purification by column chromatography (silica gel column, hexane-ethyl acetate mixture as eluent) yielded yellowish crystalline solids.

N-butyl-4-aminophthalimide. ^{1}H NMR data ($CDCl_3$): δ 0.9 (t, 3H), 1.4 (m, 2H), 1.6 (t, 2H), 3.7 (t, 2H), 6.8 (dd, 1H), 7.0 (d, 1H), 7.6 (d, 1H), 4.4 (s, 2H).

MP: 120 ^{0}C.

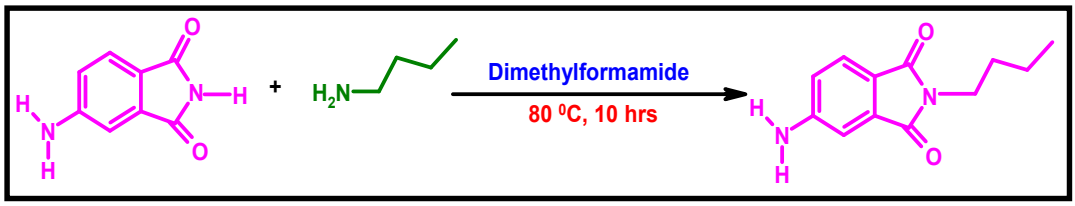

Scheme 2.2. Synthetic procedure of n-butyl-4-aminophthalimide.

2.4. Purification of the solvents

The solvents used at various stages of the study were purified using standard procedures.[4,5] Specifically, we adopted the following procedures for the purification of various solvents.

Hexane and methylcyclohexane: The solvents were refluxed over metallic sodium for 3-4 hrs and then benzophenone was added after cooling. The dark blue solution was refluxed for another hour and distilled under dry condition. The purified solvents were optically transparent in the spectral region of the compounds of interest.

Acetonitrile (ACN): The solvent was stirred with CaH_2 overnight or refluxed with P_2O_5 for 3-4 hrs and then distilled. The distilled solvent was collected over molecular sieves and stored in desiccator.

Dimethylformamide (DMF): The solvent was stirred with calcium hydride for 5-6 h and distilled under vacuum at 80°C. The solvent was collected under dry conditions.

Ethyl acetate: After stirring with P_2O_5 for 3-4 hours, the solvent was distilled out under dry atmosphere

Ethanol, 2-propanol, 1-butanol and methanol: The protic polar solvents were refluxed with stirring over anhydrous calcium oxide for 6 hours. The solution was left at room temperature overnight. This was then distilled and dried over magnesium and iodine and collected under dry atmosphere with molecular sieves.

Ethylene glycol (EG): This solvent was dried over freshly dehydrated sodium sulfate. Then it was collected by fractional distillation under high vacuum conditions.

2,2,2-Trifluoroethanol (TFE): The solvent was stirred with anhydrous potassium carbonate overnight. This was then fractionally distilled at atmospheric pressure.

Water: Milli-Q water produced from Millipore, Synergy Pack was used for all the experiments.

2.5. Sample preparation for spectral measurements

For measurements in conventional solvents, the solutions were prepared such that the absorbance of the solution (1 cm pathlength) at the excitation wavelength was around 0.1-0.2. The concentration of the probe molecules corresponding to an absorbance value of 0.2 was found to be between 10^{-6} and 10^{-4} M.

For laser flash photolysis experiments, quartz cuvettes with pathlength of 0.3 cm and 1 cm were used and the probe concentrations were maintained such that the absorbance was around 0.4-0.5 at the excitation wavelength (355 nm or

266 nm). The solutions were deaerated by purging argon gas into the sealed cuvettes for about 20 minutes prior to the experiments.

The pH calibration was done using the phosphate buffer tablets (pH = 4.01, 7.0 and 9.18) by dissolving in 100 mL milli-Q water. Sodium hydroxide (NaOH) and hydrochloric acid (HCl) were added to the buffer solution to achieve solutions of specific basic and acidic pH respectively. Aqueous solution of ellipticine at a given pH was prepared by adding concentrated ethanolic solution of ellipticine to the respective aqueous pH solutions. It is to be noted that addition of ethanol improved the solubility of ellipticine in aqueous media and that a variation of the amount of added ethanol did influence the spectral characteristics and lifetime values.

2.6. Instrumentations

The IR spectra were measured using Jasco FT/IR-5300 spectrophotometer and all ^{1}H and ^{13}C NMR spectra were recorded on a Bruker AVANCE 400 MHz NMR spectrometer operating at 400 and 100 MHz, respectively. Steady state absorption and fluorescence spectra were recorded on a UV-visible spectrophotometer (Cary100, Varian) and a spectrofluorimeter (FluoroLog-3, Horiba Jobin Yvon), respectively. Phosphorescence spectra were recorded in the same instrument employing a pulsed xenon lamp (FWHM = 3 μs). The low temperature (77 K) studies were performed by directly immersing the solution taken in quartz tube into a dewar flask containing liquid nitrogen. Both phosphorescence and fluorescence emission spectra were corrected for the instrumental response.

2.6.1. Picosecond time-correlated single-photon counting setup

Time-resolved fluorescence measurements were carried out using a time correlated single-photon counting (TCSPC) spectrometer (Horiba Jobin Yvon IBH).[6] The block diagram of the setup is shown in Scheme 2.3. While nano LEDs and PicoBrite diode lasers were used as excitation sources, micro-channel plate (MCP) photomultiplier tube (Hamamatsu R3809U-50, 160-850 nm range) was used as the detector. Two nano LEDs having output at 281 nm (FWHM = 960 ps), 439 nm (FWHM = 150 ps) and two PicoBrite lasers with output at 375 nm (FWHM = 55 ps), 405 nm (FWHM = 50 ps) were employed in the present study. While nano LEDs were operated at a maximum pulse repetition rate of 1 MHz, PicoBrite laser sources were operated at 10 MHz repetition rate. Whenever it was needed, neutral density (ND) filters were used to reduce the excitation intensity. The experiment starts with simultaneous excitation of the sample and sending a signal to the electronics (Scheme 2.3).[7] Constant fraction discriminator (CFD) receives the excitation signal and accurately measures the arrival time of the photon and then diverts the signal towards the time to amplitude convertor (TAC) to start the voltage ramp. The second channel (CFD) which accurately measures the arrival time of the emitted photon makes TAC to stop the voltage ramp. The voltage ramp developed by TAC is proportional to the delay time between the excitation and emission signals. Programmable gain amplifier (PGA) amplifies the resultant voltage, which later is converted to a numerical value by analog-to-digital convertor (ADC). The numerical value with the measured time delay is stored as a single event and by repeating the process several times with a pulsed

excitation source, histogram of the fluorescence intensity decay with time is constructed.

The lamp profile was recorded by placing a scatterer (dilute solution of Ludox in water) in place of the sample. The analysis of the decay curves and construction of time-resolved emission spectra are discussed in a later section.

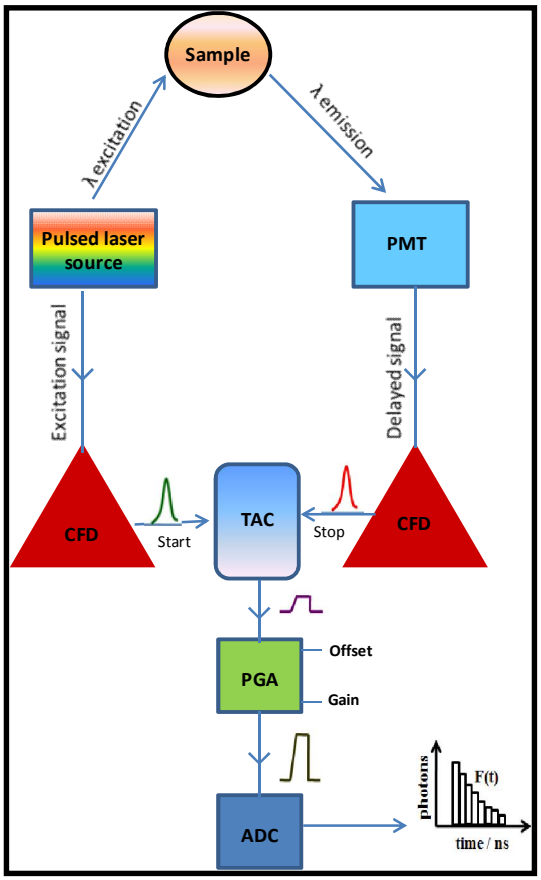

Scheme 2.3. Schematic block diagram of a TCSPC setup.

2.6.2. Nanosecond laser flash photolysis setup

The transient absorption measurements were performed by a laser flash photolysis (LFP) setup (Scheme 2.4.) which was equipped with a laser system (Q-switched Nd:YAG, pulse width ~ 8 ns) from Spectra Physics (Quanta-Ray INDI series) and a spectrometer from Applied Photophysics (model LKS.60). The spectrometer consisted of a 150 W pulsed xenon lamp, a programmable f/3.4 grating monochromator, a digitized oscilloscope (Agilent, 600 MHz), and an R-928 photomultiplier tube. The solutions were excited by the third (355 nm) and fourth harmonic (266 nm) of the laser. A perpendicular configuration was chosen for the excitation of the sample. Applied Photophysics LKS.60 Kinetic Spectrometer workstation software was used for the collection and analysis of the data.

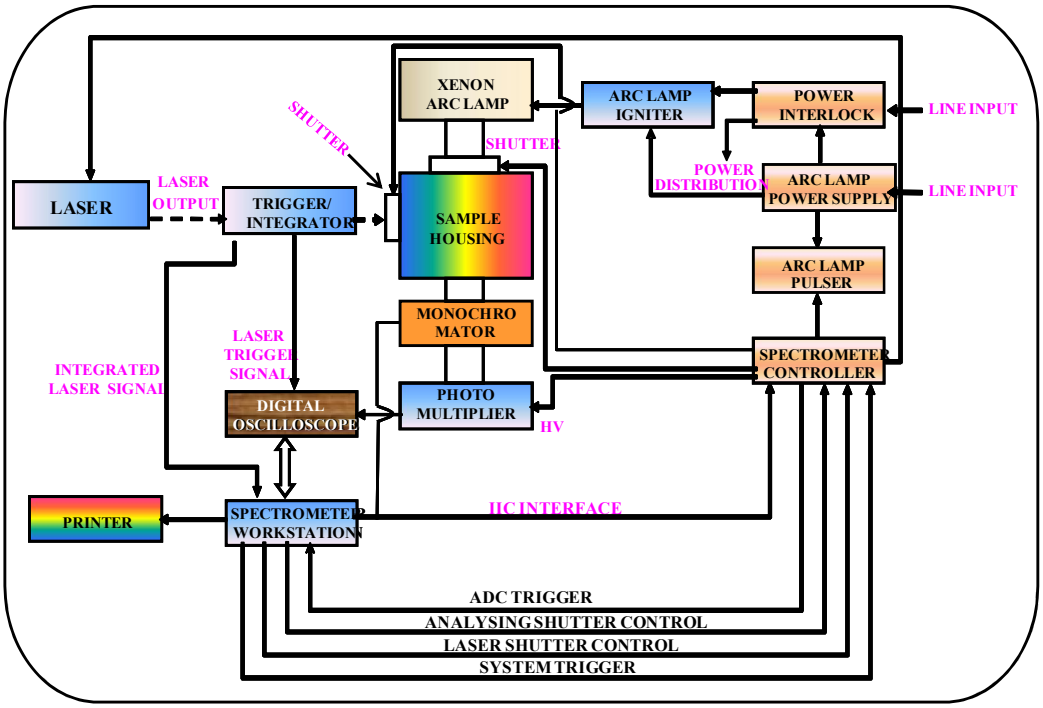

Scheme 2.4. Schematic diagram of the LFP setup

2.6.3. pH meter

All pH measurements were performed by pH meter (Hanna Instruments) which was equipped with a double-junction pH electrode with gelled electrolyte (HI 1230B) and a temperature probe. Two point calibrations were performed for the pH electrode prior to the pH measurements. Along with the pH 7 buffer, pH 4.01 was used to calibrate the instrument when measuring the pH of acidic solutions and pH 9.18 was used while measuring the pH of basic solutions. The instrument was calibrated to the pH value corresponding to the measured temperature by using the temperature probe. High concentrations of sodium ions interfere in accurate measurements of pH in alkaline solutions. This kind of interference is called alkaline error and affects the actual pH measurements. The

pH value was corrected for the alkaline error by Hanna's glass formulations given with the instrument.

2.7. Measurement of photophysical parameters

2.7.1. Molar extinction coefficient of triplet-triplet absorption

This quantity was determined by energy transfer technique using a reference molecule as the triplet energy donor. The quenching of the reference molecule was assumed to be entirely dominated by exothermic triplet energy transfer process. Experiments were carried out (355 nm and 266 nm excitation) in different solvents containing both reference and the sample. The end of pulse absorbance change $(\Delta OD)_o^R$ caused by the reference at its triplet-triplet absorption maxima (λ^{T}_{max}) was compared with the absorbance change $(\Delta OD)_\infty$ of the sample at its corresponding λ^{T}_{max}. The ε_T value was calculated from the following equation.[8]

$$\varepsilon_T - \varepsilon_S = \frac{\varepsilon_T^R (\Delta OD)_\infty k_{obs}}{(\Delta OD)_0^R (k_{obs} - k_0)} \quad (1)$$

Where, ε_T^R is the extinction coefficient of the reference triplet–triplet absorption, ε_S is the ground state extinction coefficient of sample and k_{obs} and k_0 are the rate constants for the triplet decay of the reference in the presence and absence of sample, respectively.

2.7.2. Triplet quantum yield

The triplet quantum yield (Φ_T) was determined by comparative actinometry method using benzophenone as a standard. The end of pulse

absorbance change $(\Delta OD)_0$ due to the triplet of the sample at λ_{max}^{T} was compared with the absorbance change $(\Delta OD)_0^R$ due to the triplet of the standard at its λ_{max}^{T}, the latter being observed in a optically matched solution with that of the sample at the excitation wavelength. As the triplet-triplet extinction coefficient (ε_T) was dependent on solvent polarity, the triplet quantum yield (Φ_T) calculated using it was also found different for solvents of different polarities.

$$\Phi_T = \frac{\Phi_T^R (\Delta OD)_0 \varepsilon_T^R}{(\Delta OD)_0^R \varepsilon_T} \quad (2)$$

2.8. Data analysis of fluorescence lifetime

The fluorescence lifetimes of the samples were estimated from the measured fluorescence decay curves and the instrumental profiles using a nonlinear least-squares iterative fitting procedure (using decay analysis software IBH DAS6, Version 2.2). This program uses a reconvolution method for the analysis of the experimental data.[9] When the decay time is long compared to the pulse width of the excitation pulse, the excitation may be described as a δ-function. However, when the lifetime is short, distortion of the experimental data occurs by the finite decay time of the lamp pulse and response time of the photomultiplier and associated electronics. Since the measured decay function is convolution of the true fluorescence decay and the instrumental pulse, it is necessary to analyze the data by deconvolution in order to get the actual

fluorescence lifetime. The mathematical statement of the problem is given by the following equation:

$$D(t) = \int_0^t P(t')G(t - t')dt' \quad (3)$$

Where, D(t) is the fluorescence intensity at any given time t, P(t') is the intensity of the exciting light at time t' and G(t–t') is the response function of the experimental system. The experimental data D(t) and P(t') from the MCA were fed into a personal computer (PC) to determine the lifetime. We used the IBH program to analyze the multi-exponential decays. An excitation pulse profile was recorded and then deconvolution started with mixing of the excitation pulse and a projected decay to form a new reconvoluted set. The data was compared with the experimental set and the difference between the data points was added, generating χ^2 function for fitting. The deconvolution proceeded through a series of such iterations until an insignificant change of χ^2 occurred between iterations. The inspection of reduced χ^2, a plot of weighted residuals and autocorrelation function of the residuals allowed assessment of the quality of the fit.

2.9. Construction of time-resolved emission spectra

The time-resolved emission spectra (TRES) were constructed following a standard procedure.[7] The time-resolved emission decay profiles were collected at 5/10 nm intervals across the steady state emission spectrum. The wavelength selection was made by a monochromator with a band-pass of 1/4 nm. Depending upon the fluorophore, the total number of measurements was between 30 and 46. Each decay curve was then fitted to a biexponential decay function with an

iterative reconvolution program provided by the IBH, to achieve best fits with χ^2 around 1.0 – 1.3. This fitting procedure deconvolutes the measured decay from the instrumental response to achieve effective time resolution of the experiments to ~ 50 ps. For the construction of TRES, the impulse response function, I(λ,t) was then calculated from the best fitted curve at each monitoring emission wavelength. To equate time-integrated intensity at each wavelength to the steady state intensity at the same wavelength, a normalization factor, H(λ), of the following form[7]

$$H(\lambda) = \frac{I_{SS}(\lambda)}{\sum_i \alpha_i(\lambda)\tau_i(\lambda)} \quad (4)$$

was constructed, where, $I_{ss}(\lambda)$ is the steady-state fluorescence intensity, $\alpha_i(\lambda)$ and $\tau_i(\lambda)$ are the preexponential factor and fluorescence lifetime respectively, at a particular wavelength with $\sum \alpha_i(\lambda) = 1$. The TRES were constructed from the normalized intensity decay functions, I′(λ,t) for the given set of wavelengths and different times, where I′(λ,t) = H(λ) x I(λ,t). Nonlinear least squares fitting was used to obtain the best fitted curves until successive iterations gave identical χ^2 value.

2.10. Theoretical calculations based on density functional theory

Structural parameters and ground state dipole moments were calculated by using density functional theory (DFT),[10-12] which is a more improved method of calculations than the Hartree-Fock theory in the sense that it includes terms for both exchange energy and the electron correlation. Instead of a pure DFT method, a hybrid method in which the exchange functional is a linear combination of the

Hartree-Fock exchange and a functional integral was employed in the calculations. The structural parameters and energies of the various systems were determined using the hybrid DFT functional B3LYP[13,14] at the B3LYP/6-31G* level. Charge density analysis was performed using the natural bond orbital (NBO) approach based on the B3LYP/6-31G* wave function.[15]

Excited state calculations were performed within the time-dependent (TD-DFT) framework[16,17] in both vacuo and in presence of solvents. The excited state calculations incorporating the solvents were carried out by self-consistent reaction field (SCRF) method[18] and using polarized continuum (PCM) model.[19] All these calculations were performed using the Gaussian 03 program package.

2.11. Standard error limits

Standard error limits involved in the measurements are:

λ_{max} (abs./fluo.)	± 2 nm
pH	± 0.01 unit
τ_f (> 1 ns)	± 5%
τ_f (< 1 ns)	± 5-8% (depending on the excitation source used)

Reference

(1) Dauben, H.; Harmon, K. *J. Org. Chem.* **1960**, *25*, 1442.
(2) Valentino, M. R.; Boyd, M. K. *J. Org. Chem.* **1993**, *58*, 5826.
(3) Saroja, G.; Samanta, A. *J. Chem. Soc., Faraday Trans.* **1998**, *94*, 3141.
(4) Perrin, D. D.; Armarego, W. L. F.; Perrin, D. R. *Purification of Laboratory Chemicals*; Pergamon Press: New York, **1980**.
(5) Marcus, Y. *Pure & Appl. Chem.* **1990**, *62*, 139.
(6) O'Connor, D. V.; Philips, D. *Time-Correlated Single Photon Counting*; Academic Press: New York, **1984**.
(7) Lakowicz, J. R. *In Principles of Fluorescence Spectroscopy, 3rd edition*; Springer: New York, **2006**.
(8) Carmichael, I.; Hug, G. L. *J. Phys. Chem. Ref. Data* **1986**, *15*, 1.
(9) Bevington, P. R. *Data Reduction and Analysis for the Physical Sciences*; McGraw-Hill: New York, **1969**.
(10) Hohenberg, P.; Kohn, W. *Phys. Rev.* **1964**, *B864*, 136.
(11) Kohn, W.; Sham, L. J. *Phys. Rev.* **1965**, *140*, A1133.
(12) Parr, R. G.; Yang, W. *Density-functional theory of atoms and molecules*; Oxford Univ. Press: Oxford, **1989**.
(13) Becke, D. A. *J. Chem. Phys* **1993**, *98*, 5648.
(14) Lee, C.; Yang, W.; Parr, R. G. *Phys. Rev. B* **1988**, *37*, 785.
(15) Reed, A. E.; Curtiss, L. A.; Weinhold, F. *Chem. Rev.* **1988**, *88*, 899.
(16) Bauernschmitt, R.; Ahlrichs, R. *Chem. Phys. Lett.* **1996**, *256*, 454.
(17) Casida, M. E.; Jamorski, C.; Casida, K. C.; Salahub, D. R. *J. Chem. Phys* **1998**, *108*, 4439.
(18) Wong, M. W.; Frish, M. J.; Weiberg, K. B. *J. Am. Chem. Soc.* **1991**, *113*, 4776.
(19) Cossi, M.; Barone, V. *J. Chem. Phys.* **2000**, *112*, 2427.

Chapter 3

Dual Fluorescence of Ellipticine: Excited State Proton Transfer from Solvent versus Solvent Mediated Intramolecular Proton Transfer

Photophysical properties of ellipticine (5,11-dimethyl-6H-pyrido[4,3-b]carbazole), comprising both proton donating and accepting sites, have been studied in different solvents using steady state and time-resolved fluorescence techniques primarily to understand the origin of dual fluorescence that this molecule exhibits in some specific alcoholic solvents like methanol and ethylene glycol. Ground and excited state calculations based on density functional theory have also been carried out to help in interpretation of the experimental data. It is shown that the long wavelength emission of this molecule is dependent on the hydrogen bond donating ability of the solvent, and in methanol, this emission band arises solely from an excited state reaction. However, in ethylene glycol, both ground and excited state reactions contribute to the long wavelength emission. The time-resolved fluorescence data of the system in methanol and ethylene glycol indicates the presence of two different hydrogen bonded species of ellipticine of which only one participates in the excited state reaction. The rate constant of the excited state reaction in these solvents is estimated to be around 4.2 – 8.0 X 10^8 s^{-1}. It appears that the present results are better understood in terms of solvent mediated excited state intramolecular proton transfer reaction from the pyrrole nitrogen to the pyridine nitrogen leading to the

formation of the tautomeric form of the molecule rather than excited state proton transfer from the solvents leading to the formation of the protonated form of ellipticine.

3.1. Introduction

Ellipticine (5,11-dimethyl-6H-pyrido[4,3-b]carbazole, Chart 3.1.), a natural plant alkaloid, is long been known for its anti-cancer activity with brain tumor specificity.[1-5] In recent years, ellipticine and structurally related compounds have found use in the treatment of obesity and tested for human pre-AIDS treatment in association with other drugs.[6,7] Although the potential of ellipticine as an anti-tumor drug was discovered in early sixties, its use is limited for its low solubility in aqueous media and in many organic solvents.[8-11] This problem, however, is circumvented in recent years using modern drug delivery technologies by attaching them with polymers, peptides or micelles.[12-17]

Ellipticine and its derivatives, which belong to the family of azacarbazoles, comprise both proton donating and accepting sites, and can exist in different prototropic forms. Studies in living cells have revealed that ellipticine exists both in neutral and protonated forms in aqueous cytoplasm, but only in its protonated form in the nucleus.[18,19]

Much of research work on ellipticine is focused on its biological activity, sequence selectivity, and metabolism.[20-30] Very few photophysical studies have so far been performed on this system.[2,18,31-33] As ellipticine and its derivatives can exist in different prototropic forms, understanding the influence of environment on the prototropic equilibria is extremely important from the point of view of understanding the photophysical behavior of the system, which, in turn, can help

monitoring the transport of ellipticine to its target and its uptake and release by/from the carrier.

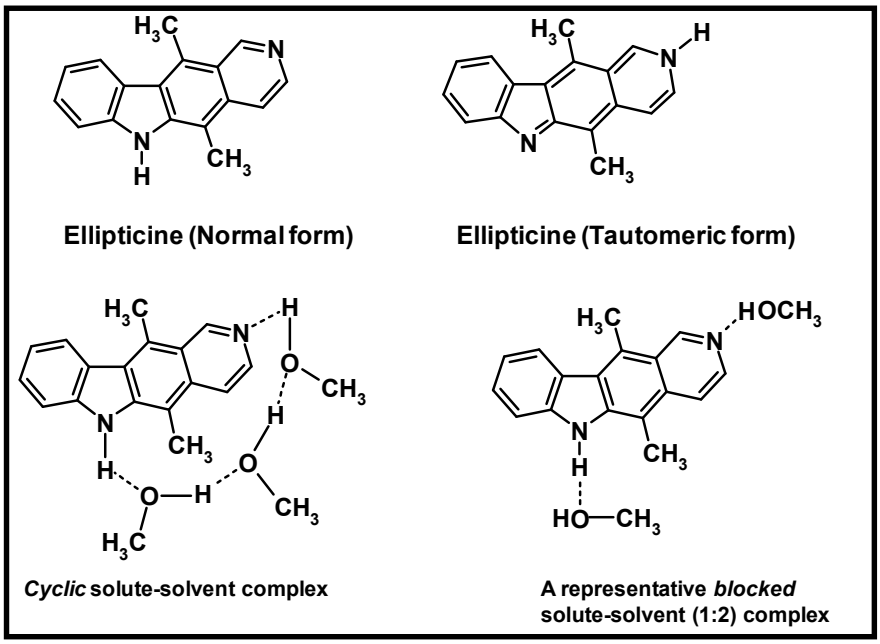

Chart 3.1.

Chen and coworkers recently studied the solvent effect on the photophysical properties of ellipticine.[31] In this work, which involved several media of a wide polarity range, solvent dependence of the absorption and fluorescence spectral shift were studied for the estimation of change of dipole moment on electronic excitation of the molecule. In addition to establishing the polar nature of the emitting state of the molecule, it was found that specific hydrogen bonding interaction between ellipticine and protic solvents led to a more pronounced shift of the emission maxima in these media and contributed to a longer fluorescence lifetime compared to nonalcoholic solvents. It was also found

that ellipticine exhibits a second fluorescence band in methanol. Even though the dual fluorescence was attributed to two different forms of ellipticine, the identity of the two forms was not determined or speculated and no attempt was made to find out whether the two forms arose from a ground or excited state reaction. The issue of why methanol behaved differently from the other alcohols was also not explored. Earlier Cabo et al. studied the photophysical properties of olivacine (1,5-dimethyl-6H-pyrido[4,3-b]carbazole), a molecule differing from ellipticine only in the position of a methyl group, and observed dual emission of this system as well in methanol.[34] The second emission was attributed to the tautomeric form of the molecule (Chart 3.1.), with the latter formed via solvent-assisted excited state intramolecular proton transfer reaction from the pyrrole to the pyridine nitrogen. Miskolczy et al., who later studied the photophysical behavior of ellipticine and 6-methylellipticine, observed dual emission for both the systems in methanol.[32] They argued against the long distance, solvent-assisted excited state proton transfer reaction proposed by Cabo et al. for structurally related molecule, olivacine, and instead, based on the observation of dual emission in 6-methylellipticine, which lacks the transferable hydrogen atom, attributed the dual fluorescence of ellipticine and its 6-methyl derivative to excited-state protonation of the pyridine moiety of the molecule by the solvent.[34] The spectral behavior of ellipticine in different solvents was correlated with the pK_a values of the respective solvents in dimethyl sulfoxide (DMSO).[32] Even though this work proposed a new mechanism for dual fluorescence of ellipticine observed only in some selected alcoholic solvents, a number of important issues concerning the excited state reaction were not addressed in this work, which necessitates further

investigations. For example, neither the spectral data, nor the temporal data presented in this work provides evidence of the excited state reaction in neat alcoholic solvents. The dual fluorescence of ellipticine in methanol can very well be due to excitation of the normal form and a second species (assigned as the protonated form of ellipticine produced by reaction with the solvent), both of which are present in the ground state.[35] The time-resolved fluorescence data of the system also does not provide unambiguous evidence for the excited state reaction as no lifetime component with a negative pre-exponential factor (rise component) is reported. Secondly, the kinetics of the excited state reaction, which is so crucial for understanding the mechanism of dual fluorescence in methanol, was not investigated in neutral solvents using time-resolved fluorescence technique. As the rate parameters were estimated in the presence of external acid and base, they do not represent the reaction rates in neutral solvents. There are additional issues discussed at later stages of the chapter, which require further investigation. The objective of this chapter is to obtain a deeper insight and provide a more comprehensive picture of the origin of dual fluorescence of ellipticine in methanol taking into consideration additional experimental results and theoretical findings. In this chapter, we have studied in detail the fluorescence decay behavior of the molecule in several carefully chosen solvents, which include some mixed solvents as well. It appears that solvent-assisted excited state intramolecular proton transfer (from the pyrrole nitrogen to the pyridine nitrogen), which is similar to that observed in other systems such as 7-hydroxyquinoline, where the proton donor and acceptor sites are separated from each other by a large distance,[36-38] better explains the dual fluorescence of ellipticine.

3.2. Spectral studies in neat solvents

The spectral behavior of ellipticine has been studied in nonpolar (hexane), polar aprotic (acetonitrile) and polar protic solvents (2-propanol, 1-butanol, ethanol, methanol, ethylene glycol (EG) and 2,2,2-trifluoroethanol (TFE)). The polarity of these solvents, as indicated by their microscopic solvent polarity parameter, E_T^N values[39,40] and the hydrogen bond donating ability of the solvents, as characterized by the Kamlet-Taft's hydrogen bond acidity parameter (α),[39,40] are collected in Table 3.1. Representative absorption and fluorescence spectra of ellipticine in these solvents are shown in Fig. 3.1. and Fig. 3.2. As can be seen, the first absorption maximum of ellipticine appears at ~ 382 nm in n-hexane and the band shows small bathochromic shift with increase in polarity of the medium. In protic solvents such as 2-propanol, 1-butanol, ethanol and methanol, the spectral shift is more pronounced compared to polar aprotic solvent such as acetonitrile. This behavior is consistent with the literature and in accordance with specific hydrogen bonding interaction with the protic solvents.[31] It is interesting to note the appearance of a new absorption band above 420 nm in EG (and also in TFE), which has resulted from the interaction of ellipticine with the solvent in the ground state. Miskolczy et al. attributed the new absorption band to the protonated form of ellipticine as a similar absorption band was observed in more acidic solvent, 1,1,1,3,3,3-hexafluoro-2-propanol (HFP).[32] We are however not so sure about this assignment as methanol and EG may not be acidic enough to protonate ellipticine in the ground state. The 420 nm species can very well be due to the hydrogen bonded complex of ellipticine, as hydrogen bonding also leads to the formation of long wavelength absorption band.[41,42] It should be noted in this

context, contrary to the findings of Miskolczy et al., who observed a similar absorption band in methanol as well,[32] we did not observe this new absorption band in methanol.

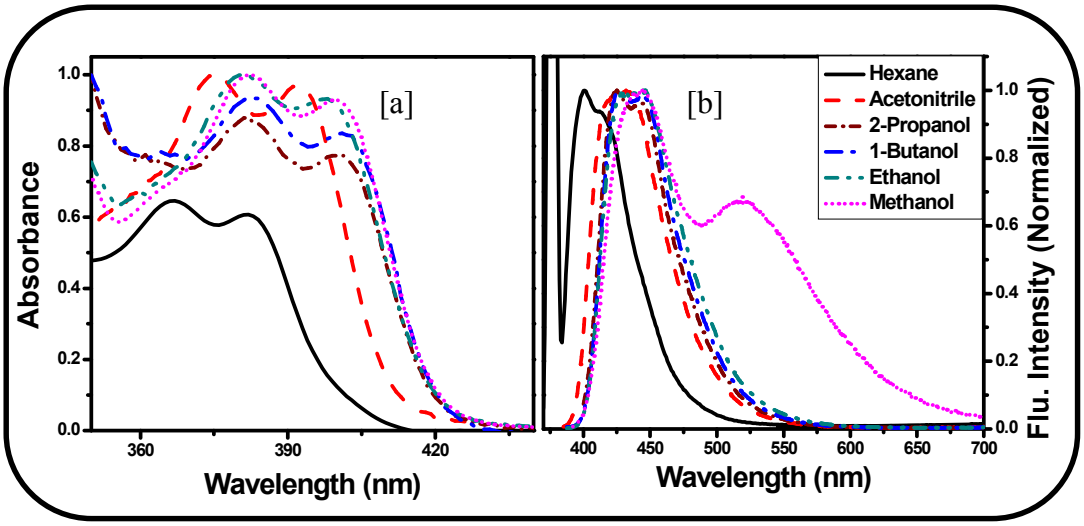

Figure 3.1. Absorption [a] and fluorescence spectra [b] (λ_{exc} = 375 nm) of ellipticine in hexane (solid line), acetonitrile (dash), 2-propanol (short dash dot), 1-butanol (dash dot), ethanol (dash dot dots) and methanol (short dot). All spectra normalized at their peak maximum.

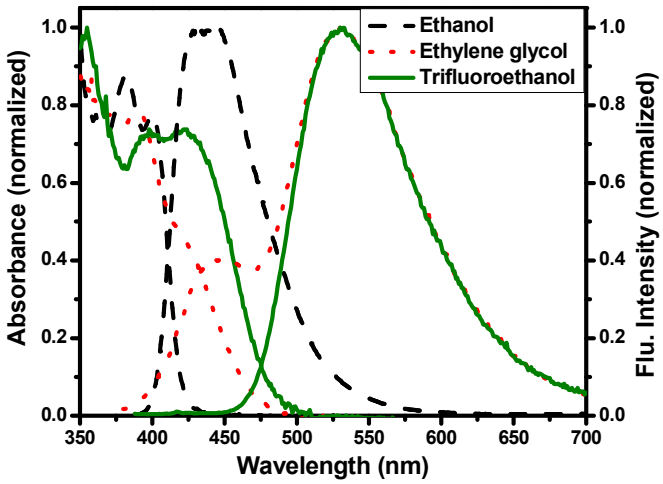

Figure 3.2. Absorption and fluorescence emission spectra (λ_{exc} = 405 nm) of ellipticine in ethanol (dash), ethylene glycol (dot) and trifluoroethanol (solid line). All spectra normalized at their peak maximum.

The steady state fluorescence spectrum of ellipticine is characterized by a broad band in all the solvents. The fluorescence displays a more pronounced red shift compared to the absorption spectrum with increase in polarity of the medium. This is due to the more polar nature of the emitting state of ellipticine compared to the ground state.[31] In n-hexane, the emission maximum is observed at 401 nm and it shifts to 432 nm in acetonitrile. A further red shift due to hydrogen bonding interaction is observed in alcoholic solvents (Table 3.1.). The most interesting aspect of the fluorescence behavior of ellipticine is that the molecule exhibits a second emission band at a longer wavelength ($\lambda \geq 520$ nm) in methanol and EG. However, in 2-propanol, 1-butanol and ethanol, this long wavelength emission band could not be observed. In TFE, the molecule exhibits only the long wavelength emission band (Fig. 3.2). Miskolczy et al., who found that in highly acidic HFP, ellipticine shows only the long wavelength fluorescence

band similar to that observed in TFE, suggested that this emission band arises from the protonated form of ellipticine.[32]

Table 3.1. Spectral and temporal parameters of ellipticine in selected solvents of different polarity (measured in E_T^N scale) and hydrogen bond donor acidity (measured in α scale).

Solvents	E_T^N[a]	α[b]	λ_{max}^{abs} /nm	λ_{max}^{flu} /nm	Decay parameters[c] τ_i (ns) [a_i]
Hexane	0.009	0.00	382	401	15.3
Acetonitrile	0.46	0.19	392	432	11.2
2-Propanol	0.546	0.76	399	442	29.8
1-Butanol	0.586	0.79	399	444	28.2
Ethanol	0.654	0.83	400	444	29.5
Methanol	0.762	0.98	398	443, 521	[d]
Ethylene glycol	0.79	0.9	402,424	444, 529	[d]
Trifluoroethanol	0.89	1.51	424	530	3.6 [0.009], 7.6 [0.99]
HFP	1.068	1.96	428[e]	525[e]	6.4[e]

[a] from ref.39, [b] from ref.40, [c] monitored at 435 nm, [d] see Table 4.2, [e] from ref.32.

We find the fluorescence excitation spectra of ellipticine corresponding to the long wavelength emission in methanol and EG (Fig. 3.3.), which is such an important experimental data, but was not recorded earlier, to be quite instructive. These spectra clearly indicate that in methanol, the species responsible for the second emission band is formed only in the excited state. This finding is contrary to the earlier report.[32] In EG, the species is, however, formed in the ground state.

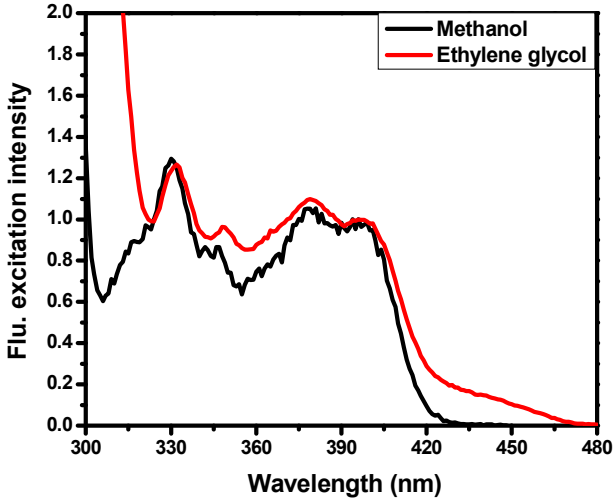

Figure 3.3. Fluorescence excitation spectra of ellipticine in methanol and ethylene glycol. The monitoring wavelength was 575 nm (normalized at 396 nm).

3.3. Time-resolved fluorescence studies in neat solvents

In hexane, acetonitrile, 2-propanol, 1-butanol and ethanol, where only one emission band is observed, the fluorescence decay behavior is found to be single exponential with lifetime ranging from 11 ns to 30 ns (Table 3.1.). However, in methanol and EG, where dual fluorescence is observed, the fluorescence decay profiles corresponding to both the short and long wavelength emission are best described by a sum of two exponentials. As can be seen from the decay parameters collected in Table 3.2, the two measured lifetime components in methanol in the short wavelength region (420-470 nm) are 2.2 (~ 20%) and 3.5 ns (~ 80%).

Table 3.2. Fluorescence decay parameters of ellipticine (λ_{exc} = 405 nm) in methanol and ethylene glycol (EG).

Monitoring Wavelength (nm)	Decay parameters τ_i (ns) [a_i] in Methanol	in EG	χ^2 MeOH	EG
420	2.2 [0.185], 3.55 [0.815]	1.1 [0.632], 3.4 [0.367]	1.05	1.1
430	2.17 [0.184], 3.57 [0.815]	1.2 [0.605], 3.4 [0.394]	1.08	0.9
440	2.21 [0.205], 3.58 [0.794]	1.1 [0.594], 3.4 [0.405]	1.01	1.1
520	2.0 [-0.302], 8.1 [0.070]	1.1 [-0.051], 8.2[0.949]	1.12	1.01
530	2.2 [-0.36], 8.2 [0.638]	1.2 [-0.126], 8.2[0.873]	1.1	1.05
540	2.2 [-0.39], 8.2 [0.601]	1.3 [-0.157], 8.2[0.843]	1.13	1.07
550	2.2 [-0.421], 8.2 [0.578]	1.2 [-0.184], 8.3[0.815]	1.18	1.04

On the other hand, the fluorescence time profiles of the long wavelength emission are characterized by a rise component (which is associated with a negative pre-exponential factor) of 2.2 ns, along with a decay component of 8.2 ns. Representative decay profiles for the two emission bands along with the biexponenial fits to the decay profiles are shown in Fig. 3.4.

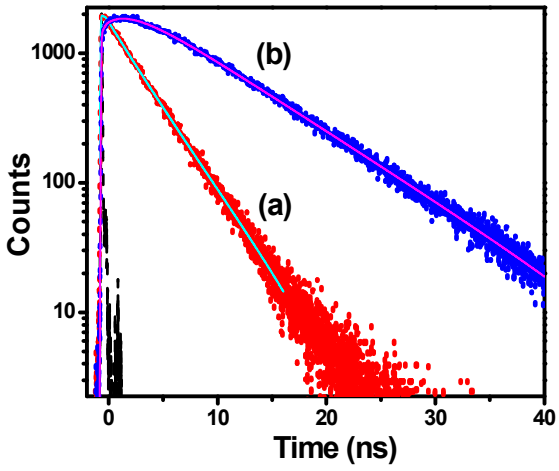

Figure 3.4. Fluorescence decay profiles (λ_{exc} = 405 nm) of ellipticine in methanol at 435 (a) and 535 nm (b). The experimental decay profiles are indicated by the dots and the instrument profile as dash. The solid lines represent the best-fit to the decay curves.

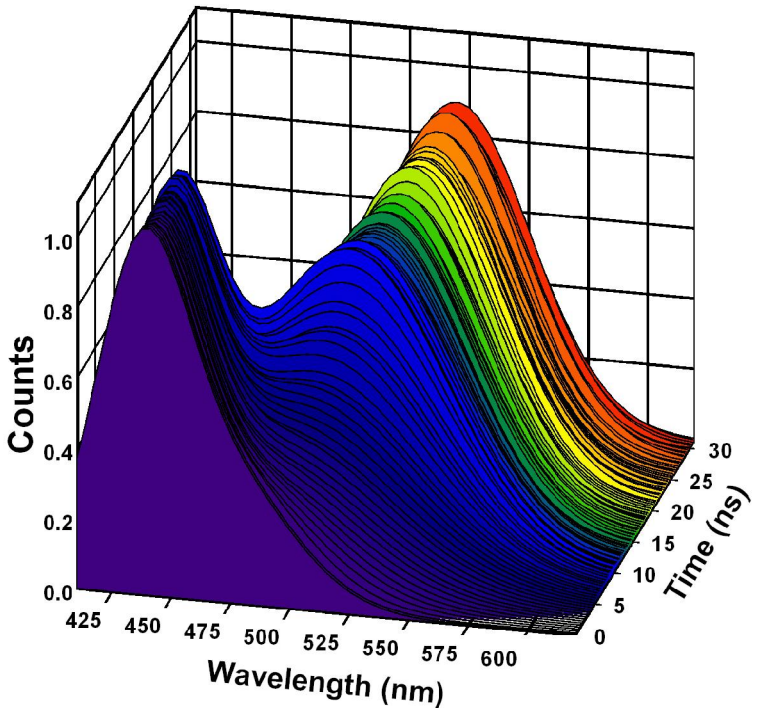

Figure 3.5. Time-resolved fluorescence emission spectra of ellipticine in methanol (λ_{exc} = 405 nm).

The time-resolved emission spectra (TRES) show time-evolution of the two different components of ellipticine in methanol (Fig. 3.5.), in particular, it clearly captures the evolution of the long wavelength component, thus providing the first direct evidence of the formation of this species as a result of an excited state reaction. In EG, where dual emission is also observed, the fluorescence decay parameters (λ_{exc} = 405 nm) shown in Table 3.2. suggest that the time-dependence of the two emission bands is very similar to that in methanol. However, when EG solution of ellipticine is excited at 439 nm, which

corresponds to the long wavelength absorption band arising from ground state interaction, no rise component is observed (Fig. 3.6.)

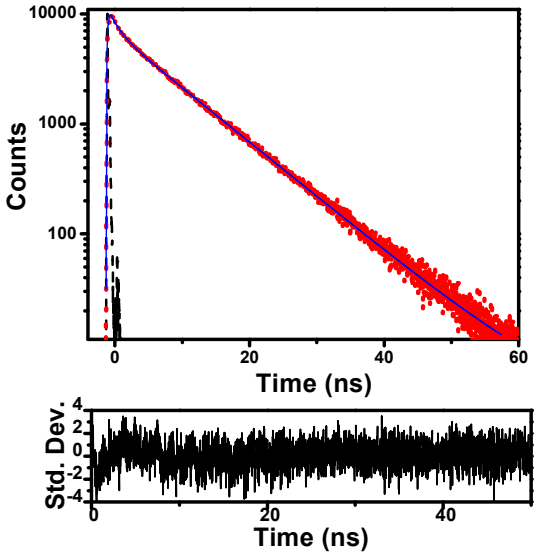

Figure 3.6. Fluorescence decay profiles (λ_{exc} = 439 nm) of ellipticine in ethylene glycol at 550 nm. The experimental decay profiles are indicated by the dots and the instrument profile as dash. The solid lines represent the best-fit to the decay curves. The residuals are indicated below for the respective decay profiles.

In TFE, where only the long wavelength emission is observed, the decay profile is best represented by a biexponential decay function with the characteristic decay times of 3.6 and 7.6 ns (Fig. 3.7.) and no rise component is observed.

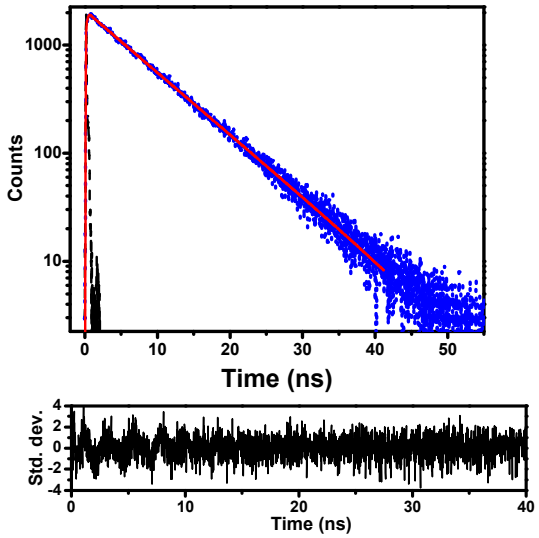

Figure 3.7. Fluorescence decay profiles (λ_{exc} = 405 nm) of ellipticine in TFE at 520 nm. The experimental decay profile is indicated by the dots and the instrument profile as dash. The solid lines represent the best-fit to the decay curves. The residuals for the fit to the decay profile are indicated below.

3.4. Spectral and temporal studies in mixed solvents

3.4.1. Addition of methanol

In order to understand the origin of the second fluorescence band of ellipticine observed only in some alcohols and the nature of interaction responsible for the formation of this species, the study has been extended to mixed solvents containing controlled amount of protic solvent in a polar aprotic solvent (such as acetonitrile, tetrahydrofuran (THF)). Fig. 3.8. displays characteristic changes of the absorption spectrum of an acetonitrile solution of ellipticine in the presence of various quantities of methanol. As can be seen, addition of methanol leads to small changes in the absorbance value with a red shift of the spectrum, but no isosbestic point is observed. Lack of isosbestic point

is suggestive of the presence of more than two absorbing components in the solution.

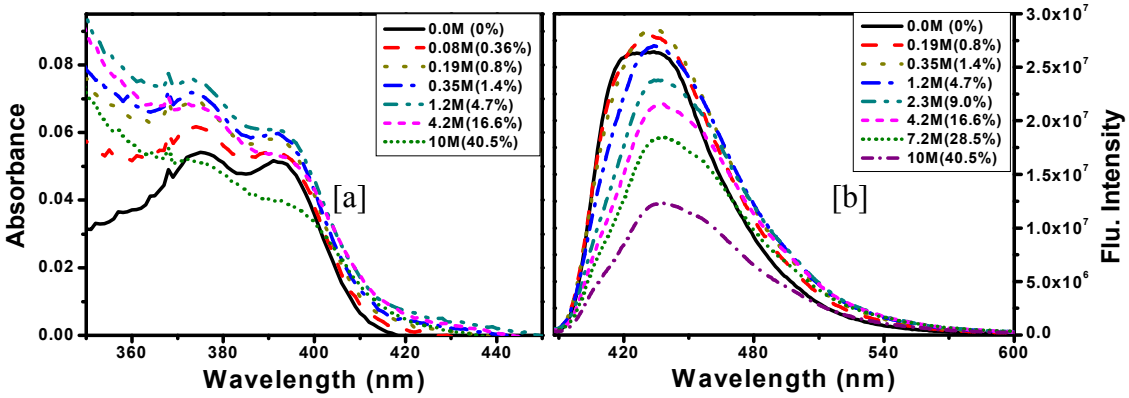

Figure 3.8. Absorption [a] and fluorescence emission [b] (λ_{exc}= 405) spectra of ellipticine in acetonitrile for different concentration of added methanol (0-10 M).

As far as the emission is concerned, a small increase in intensity is observed initially. However, subsequent addition leads to quenching of the short wavelength fluorescence. It is important to note here that neither the second emission band is observed, nor did we observe noticeable increase in the fluorescence intensity in the long wavelength emission region (510-550 nm) even when large quantity (~50 % by volume) of methanol was added. When THF is used in place of acetonitrile, a similar result is observed. The time-resolved fluorescence data in mixed solvents (Table 3.3.) did not show any rise component associated with the long wavelength emission component.

Table 3.3. Time-resolved fluorescence data of ellipticine (λ_{exc} = 405 nm) in THF monitored at 420 and 520 nm with various quantities of methanol.

	Decay parameters/ τ_i (ns) [a_i]		
% addition	**at 420 nm**	**at 520 nm**	**χ^2 (420, 520 nm)**
0%	21.0	21.3	1.1, 1.14
1.2%	21.2	21.6 [0.89], 2.2 [0.10]	1.06, 1.08
6%	21.5 [0.89], 2.2 [0.10]	21.7 [0.86], 2.2 [0.13]	1.01, 1.01
10%	21.0 [0.88], 1.9 [0.11]	21.2 [0.84], 2.0 [0.16]	1.06, 1.04
15%	21.2 [0.84], 1.9 [0.15]	21.1 [0.81], 2.0 [0.18]	1.05, 0.98
24%	20.8 [0.79], 1.8 [0.20]	20.8 [0.75], 2.2 [0.24]	1.02, 1.05
32%	20.0 [0.66], 1.7 [0.33]	20.0 [0.62], 1.8 [0.37]	0.98, 1.02
42%	19.8 [0.51], 1.5 [0.48]	19.7 [0.49], 1.7 [0.50]	1.0, 1.06

3.4.2. Addition of EG

Addition of EG to an acetonitrile solution of ellipticine leads to the appearance of a long wavelength absorption band around 420 nm and also, the long wavelength emission band (Fig. 3.9.). No isosbestic point is observed in this case also. The time-resolved fluorescence decay parameters in mixed solvents, which are presented in Table 3.4. are in accordance with expectation. Similar results were obtained on addition of EG to ellipticine dissolved in hexane, toluene, N,N-dimethylformamide, etc.

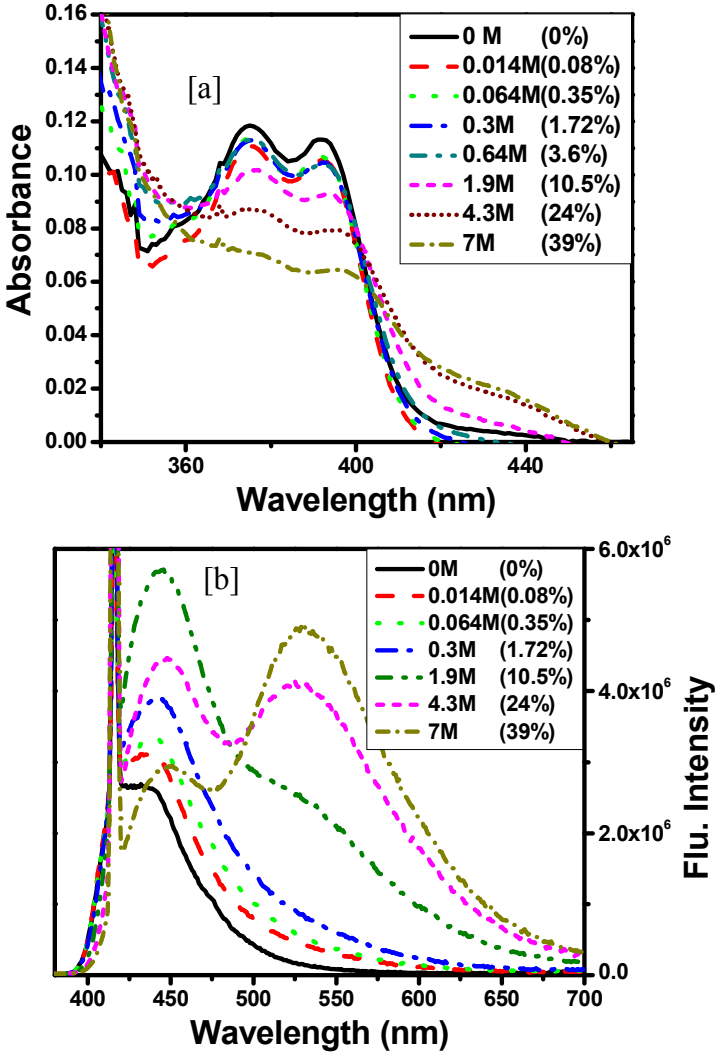

Figure 3.9. Absorption [a] and fluorescence emission [b] (λ_{exc} = 415 nm) spectra of ellipticine in acetonitrile for different concentration of added ethylene glycol (0-7 M).

Table 3.4. Time-resolved fluorescence data of ellipticine (λ_{exc} = 405 nm) in acetonitrile monitored at 440 and 550 nm with various quantities of ethylene glycol (EG).

	Decay parameters/ τ_i (ns) [a_i]		
% addition	**at 440 nm**	**at 550 nm**	**χ^2 (440, 550 nm)**
0%	11.2	11.6	1.06, 1.1
0.08%	11.2	11.7 [0.89], 2.1 [0.10]	1.07, 0.9
0.35%	11.3 [0.87], 1.2 [0.12]	11.2 [0.80], 2.0 [0.19]	1.08, 0.9
0.75%	11.4 [0.84], 1.2 [0.15]	11.2 [0.79], 2.0 [0.20]	1.0, 1.0
1.72%	11.5 [0.80], 1.2 [0.19]	11.3 [0.78], 2.1 [0.21]	1.09, 0.9
3.6%	11.7 [0.74], 1.2 [0.25]	11.2 [0.74], 2.1 [0.25]	1.06, 1.1
10.5%	11.8 [0.67], 1.2 [0.32]	11.5 [0.77], 2.1 [0.23]	1.06, 1.06
24%	11.5 [0.61], 1.3 [0.38]	11.2 [0.83], 1.8 [0.15], 1.3 [-0.01]	1.05, 1.08
39%	11.2 [0.50], 1.3 [0.49]	11.2 [0.58], 1.7 [0.23], 1.2 [-0.18]	1.09, 1.09

3.5. Theoretical calculations

The calculated energies corresponding to the optimized (B3LYP/6-31G*) geometries of the normal and tautomeric forms indicate that in the ground state the normal form of ellipticine is more stable than it's tautomer by ~ 0.927 eV (Fig. 3.10.) in the gas phase. Even though this energy gap between the two forms decreases substantially in acetonitrile and methanol, it still remains much higher than the thermal energy available at room temperature indicating that ellipticine exists in its normal form in the ground state in these solvents as well. The excited state calculations (TD-DFT, B3LYP/6-31G* level), however, show that the first excited singlet state of the tautomer, whose energy is estimated by adding the calculated excitation energy for the lowest energy transition with the ground state energy, is energetically lower than that of the normal form of ellipticine by about 0.324 eV in vacuo. In acetonitrile and methanol, this energy gap is slightly higher

(Fig. 3.10.). Thus the theoretical calculations indicate that the transformation of the normal form to its tautomer is energetically feasible in the excited state. Hence, the long wavelength emission can possibly arise from the tautomer of ellipticine.

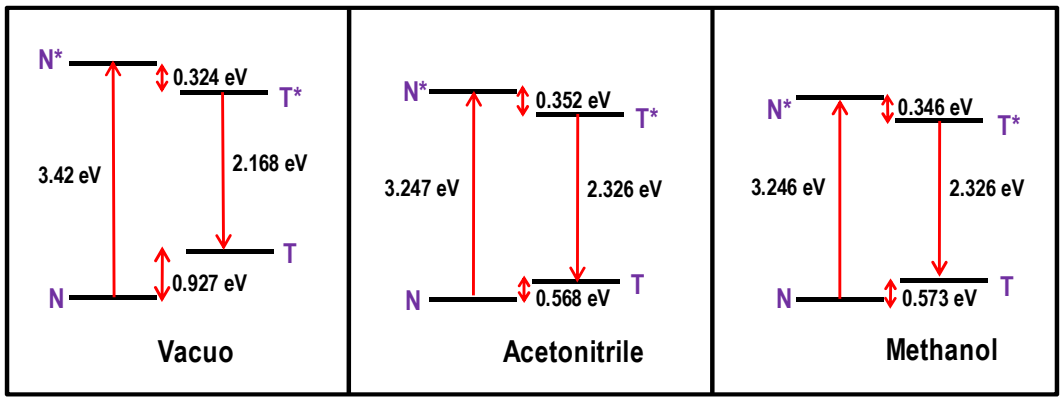

Figure 3.10. Schematic representation of the potential energies of ellipticine for both normal (N) and tautomeric form (T), as obtained by theoretical calculations.

The calculated lowest energy transition for the normal form of ellipticine is found to be 3.247 eV in acetonitrile, which is comparable to the experimental energy (3.166 eV) estimated from the λ_{max}^{abs} value in acetonitrile (Table 3.5.). The molecular orbitals associated with the lowest energy transition are also studied and careful examination of the shapes of the molecular orbitals reveals the nature of the transition. Three different excitations, HOMO-LUMO, (HOMO-1) (LUMO+1) and (HOMO-1)-LUMO contribute to the first excited state of the normal form in vacuum. In all cases, the excitation mainly arises from the HOMO-LUMO transition indicated by the transition coefficients, having π-π* character (Table 3.5.).

Table 3.5. Lowest energy transition (B3LYP/6-31G*), oscillator strength and nature of transition of the normal form of ellipticine in vacuo and in other solvents.

Medium	Transition Energy (eV)		Osc. strength	MOs involved (Tr. Coeff)	Nature
	Theory	Expt.			
Vacuo	3.420		0.0568	HOMO → LUMO (0.64414) HOMO-1 → LUMO+1 (0.12850) HOMO-1 → LUMO (0.12109)	$\pi \rightarrow \pi^*$
ACN	3.247	3.166	0.0661	HOMO → LUMO (0.65799) HOMO-1 → LUMO+1 (-0.10693)	$\pi \rightarrow \pi^*$
MeOH	3.246	3.118	0.0654	HOMO → LUMO (0.65779) HOMO-1 → LUMO+1 (-0.10735)	$\pi \rightarrow \pi^*$

3.6. Discussion

Let us concentrate on the findings in methanol and EG, the two solvents in which dual fluorescence is observed. In all other solvents, where only one emission band is observed, it is not difficult to figure out its origin. As the theoretical calculations suggest that ellipticine exists in its normal form in the ground state, it is evident that in not too acidic protic solvents ($\alpha \leq 0.83$),[39,40] the normal form and its various hydrogen bonded forms are present in the ground state. In highly acidic solvents such as in TFE and HFP, whose α values are greater than 1.5,[39,40] the basic pyridine nitrogen of the molecule is expected to be protonated and hence, ellipticine is present in its protonated form in the ground state.

Among all the alcohols, dual emission is observed only in neat methanol and EG, whose α values (0.98 and 0.90, respectively) are in between these two group of protic solvents. As the long wavelength absorption and emission bands are related to the hydrogen bond donating ability of the solvent, it is quite

reasonable to assume that these bands arise from the protonated form of ellipticine, as Miskolczy et al. suggested.[32] However, this picture presents the following difficulties.

(i) Even though methanol has a higher hydrogen bond donating ability compared to EG,[39,40] the long wavelength absorption band (λ_{max} ~ 424 nm) is observed in EG and in mixed solvents containing EG, but not in methanol. (ii) A higher intensity of the long wavelength emission relative to the short wavelength emission (I_{LW}/I_{SW}) is also not expected for the same reason. (iii) If solvent acidity is the only parameter responsible for the formation of the long wavelength emission band, one would have expected this emission in methanol containing mixed solvents as well. However, the absence of this band in acetonitrile-methanol mixture suggests that other factors also contribute to this emission. (iv) A biexponential fluorescence decay behavior of the short wavelength emission band with the kind of decay parameters observed cannot be explained if the excited state reaction leads to the formation of the protonated form of ellipticine. This is because if ellipticine undergoes protonation in the excited state and the two species are in equilibrium, one would expect biexponential fluorescence time profile for both the species with two identical lifetimes. On the other hand, if the two species are not in equilibrium, one would expect single exponential decay for ellipticine and biexponential decay (with one lifetime component same as that observed for ellipticine) for the protonated species. However, as can be seen, the experimental decay parameters (Table 3.2.) do not correspond to either of these two possible scenarios.

In order to understand the nature of the excited state reaction in methanol and to determine the kinetics of the reaction, we begin by considering the presence of the normal form of ellipticine and its hydrogen bonded forms, which are represented as N in the following schemes, in the ground state. When excited, these species give rise to the short wavelength emission and undergo reaction to form another species (S*), which is responsible for the long wavelength emission. S* can be the protonated form of ellipticine, or its tautomer (Chart 3.1.).[43] If N* is in equilibrium with S*, as shown in Scheme 3.1, then the time dependence of the two species is given by eqn. (1) and (2), which imply that both the species would exhibit a biexponential fluorescence time profile with the two decay times associated with N * and S* are identical. However, the kinetic data (Table 3.2.) for the present system is not consistent with this scheme.

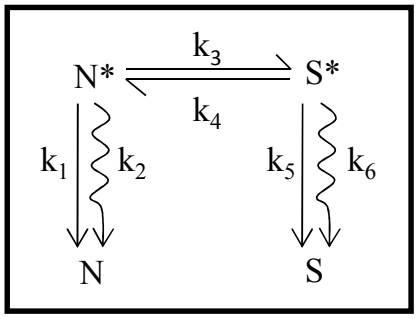

Scheme 3.1.

$$[N^*] = \frac{[N^*]_0}{\lambda_2 - \lambda_1}\left[(\lambda_2 - X)e^{-\lambda_1 t} + (X - \lambda_1)e^{-\lambda_2 t}\right] \qquad (1)$$

$$[S^*] = \frac{k_3\,[N^*]_0}{\lambda_2 - \lambda_1}\left[e^{-\lambda_1 t} - e^{-\lambda_2 t}\right] \qquad (2)$$

Where, $X = k_1 + k_2 + k_3$, $Y = k_4 + k_5 + k_6$

$$\lambda_1 = \frac{1}{2}\left\{(X+Y) - [(X-Y)^2 + 4k_3k_4]^{\frac{1}{2}}\right\}$$

$$\lambda_2 = \frac{1}{2}\left\{(X+Y) + [(X-Y)^2 + 4k_3k_4]^{\frac{1}{2}}\right\}$$

However, if the equilibrium is not established in the excited-state and the formation of S* from N* is represented by Scheme 3.2, then the time-dependence of N* and S* is given by eqs 3 and 4. In this case, N* should show a single exponential decay and S* should exhibit a rise time identical with the decay time of N* and a decay time that is characteristics of the lifetime of S* under the experimental condition.

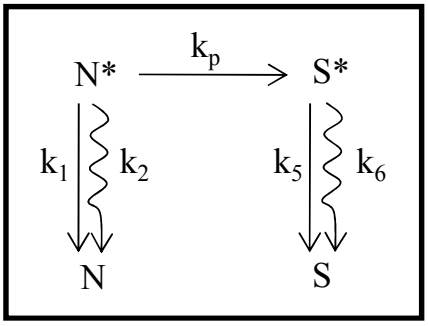

Scheme 3.2.

Where, $k_N = k_1 + k_2$ $k_s = k_5 + k_6$

$$[N^*] = [N^*]_0\, e^{-(k_N+k_p)t} \quad (3)$$

$$[S^*] = \left(\frac{[N^*]_0\, k_p}{k_N+k_p-k_T}\right)\left[e^{-k_T t} - e^{-(k_N+k_p)t}\right] \quad (4)$$

The kinetic data presented in Table 3.2, is however, not consistent with this mechanism as well. An inspection of the decay characteristics reveals that while the 1.1 – 2.2 ns lifetime component is connected with the excited state reaction (as it is associated with both N* and S*), the 3.4 – 3.6 ns decay component of N*, whose origin needs to be found, is not connected with the excited state reaction.

Marks et al. studied the photophysical behavior of pyridocarbazole derivatives, and observed dual emission of dipyrido[2,3-a:3′,2′-i]carbazole (DPC) and 1H-pyrrolo[3,2-h]quinoline (PQ) in alcoholic solvents.[44] The short wavelength fluorescence emission was attributed to the normal solute-solvent complex and long wavelength band was ascribed to the tautomeric form of the cyclic solute-solvent complex.[44] The long wavelength emission displayed a rise component that matched with one of the decay components of the first emission. The decay characteristics of the two emission bands indicated solvent mediated excited state intermolecular proton transfer from a cyclic solute-solvent complex. Interestingly, the presence of another species, which does not undergo excited state proton transfer, was found and the same was attributed to the "blocked" solute-solvent complex.[44] In fact, long distance solvent mediated excited state intramolecular proton transfer has been proposed also for other amphoteric molecule such as 7-hydroxyquinoline in methanol.[36-38]

Taking into consideration the above literature, the kinetic data of ellipticine can be explained by suitably modifying Scheme 3.2. and proposing two different types of hydrogen bonded ellipticine molecules. The first set of solvated molecules of ellipticine, which does not undergo excited state reaction, is

responsible for the long-lived (3.4 – 3.6 ns) component of N*. The 'blocked' solvated species, shown in Chart 3.1, is one of these species. The other set of solvated species, which can form the "cyclic" hydrogen-bonded species (Chart 3.1.) during the excited state lifetime of ellipticine and facilitate the excited state reaction across the hydrogen bonded chain, contributes to the short lifetime component of N*. Essentially, the excited state reaction involves two steps; (i) solvent reorganization around ellipticine to form the "cyclic" solvated species, and (ii) rapid proton transfer (relay) along the chain. The rate constant of the excited state reaction, estimated from the rise time associated with S* emission (8×10^8 s^{-1} and 4.2×10^8 s^{-1} in EG and methanol, respectively), obviously represents the kinetics of the slowest of the two steps, which is clearly the formation of the "cyclic" complex. The very fact that only one particular type of solvated N* (of the two types present) undergoes the excited state reaction, as indicated by the time resolved study, implies that S* is the tautomer of ellipticine. Had the excited state process been a bimolecular reaction between ellipticine and solvent molecules, it would not have been possible to think of two different types of ellipticine of which only one undergoes protonation.

The excited state reaction mechanism proposed here is not only consistent with the theoretical calculations, but can also account for the observations, which cannot be interpreted in terms of proton transfer from the solvent. For example, a higher I_{LW}/I_{SW} in EG compared to methanol can be explained as follows. The pyrrole hydrogen atom is far off (~7 Å) from the pyridine nitrogen atoms. This implies that at least three molecules of methanol are needed to form the cyclic solute-solvent complex through which this proton can be transferred. However, in

the case of EG, only two molecules are sufficient. A higher I_{LW}/I_{SW} in EG compared to methanol is a reflection of the relative ease of formation of the cyclic solute-solvent complex involving two molecules rather with three molecules. This also explains why the rate constant of the excited state reaction is higher in EG compared to methanol despite better hydrogen bond donating ability of the latter.

Both spectral and time-resolved data has shown that the excited state reaction of ellipticine does not occur in mixed solvents (methanol+acetnitrile/THF). This is another observation that cannot be explained in terms of excited state protonation of the molecule. As cyclic solute-solvent complex formation involving three methanol molecules is prevented by a large number of nonalcoholic solvent molecules present in the medium, one can account for this observation easily with the help of this new mechanism.

3.7. Conclusion

The origin of dual fluorescence of ellipticine as observed in some alcoholic solvents is reinvestigated. The steady state and time-resolved experiments presented here provide the first direct evidence of the excited state reaction in ellipticine and the rate constant of this process in neat methanol and ethylene glycol. Contrary to the earlier studies, which suggested the dual emission of ellipticine in methanol to originate from the photoexcited normal and protonated forms of the molecule with the latter produced as a result of proton transfer from the solvent, the present results seem to indicate that the excited state reaction involves solvent reorganization around ellipticine to form the “cyclic” solvated species followed by rapid proton transfer (relay) along the chain and the two emission bands arise from the normal and tautomeric forms of ellipticine. The

measured rate constant of the reaction perhaps represents the kinetics of the formation of the “cyclic” complex, which is the slowest of the two-step process. The ease of formation of cyclic complex involving two molecules of EG compared to that requiring three molecules of methanol explains why the excited state reaction is faster in EG compared to methanol even though the hydrogen bond donating ability of the latter is more than the former. The time-resolved experiments also reveal the existence of a second set of hydrogen bonded ellipticine molecules, which do not contribute to the excited-state proton-transfer process.

Reference and Notes:

(1) Garbett, N. C.; Graves, D. E. *Curr. Med. Chem.* **2004**, *4*, 149.

(2) Smith, A. F.; Horning, E. C.; Goodwin, S. *J. Am. Chem. Soc.* **1959**, *81*, 1903.

(3) Le Pecq, J.-B.; Xuong, N.-D.; Gosse, C.; Paoletti, C. *Proc. Natl. Acad. Sci. U.S.A.* **1974**, *71*, 5078.

(4) Ohashi, M.; Oki, T. *Exp. Opin. Ther. Pat.* **1996**, *6*, 1285.

(5) R.B.Woodward.; Iacobucci., G. A.; Hochstein., F. A. *J. Am. Chem. Soc.* **1959**, *81*, 4434.

(6) Ellies, D.; Rosenberg, W. Ellipticine compounds for treating obesity In *PCT Int. Appl.*, **2010**; Vol. WO 2010107704; pp 1.

(7) Hallard, M.; Pontiggia, P.; Mathe, G. *Biomed & Pharmacother* **1996**, *50*, 510.

(8) Clarysse, A.; Brugarolas, A.; Siegenthaler, P.; Abele, R.; Cavalli, F.; De Jager, R.; Renard, G.; Rozencweig, M.; Hansen, H. H. *Eur. J. Cancer Clin. Oncol.* **1984**, *20*, 243.

(9) Dodion, P.; Rozencweig, M.; Nicaise, C.; Piccart, M.; Cumps, E.; Crespeigne, N.; Kisner, D.; Kenis, Y. *Eur. J. Cancer Clin. Oncol.* **1982**, *18*, 519.

(10) Gouyette, A.; Huertas, D.; Droz, J.-P.; Rouesse, J.; Amiel, J.-L. *Eur. J. Cancer Clin. Oncol.* **1982**, *18*, 1285.

(11) Paoletti, C.; Le Pecq, J. B.; Dat-Xuong, N.; Juret, P.; Garnier, H.; Amiel, J.-L.; Rouesse, J. *Recent Res. Cancer Res.* **1980**, *40*, 107.

(12) Liu, J.; Xiao, Y.; Allen, C. *J. Pharm. Sci.* **2004**, *93*, 132.

(13) Searle, F.; Gac-Breton, S.; Keane, R.; Dimitrijevic, S.; Brocchini, S.; Sauville, E. A.; Duncan, R. *Bioconjugate Chem.* **2001**, *12*, 711.

(14) Trubetskoy, V. S.; Torchilin, V. P. *Adv. Drug Delivery Rev.* **1995**, *16*, 311.

(15) Czerwinski, G.; Tarasova, N. I.; Michejda, C. *J. Proc. Natl. Acad. Sci. U.S.A.* **1998**, *95*, 11520.

(16) Moody, T. W.; Czerwinski, G.; Tarasova, N. I.; Moody, D. L.; Michejda, C. *J. Regul. Pept.* **2004**, *123*, 187.

(17) Moody, T. W.; Czerwinski, G.; Tarasova, N. I.; Michejda, C. *J. Life Sci.* **2002**, *71*, 1005.

(18) Sbai, M.; Lyazidi, S. A.; Lerner, D. A.; del Castillo, B.; Martin, M. A. *Anal. Chim. Acta* **1995**, *303*, 47.

(19) Schwaller, M. A.; Allard, B.; Sureau, F.; Moreau, F. *J. Phys. Chem.* **1994**, *98*, 4209.

(20) Řeha, D.; Kabeláč, M.; Ryjáček, F.; Šponer, J. E.; Elstner, M.; Suhai, S.; Hobza, P. *J. Am. Chem. Soc.* **2002**, *124*, 3366.

(21) Froelich-Ammon, S. J.; Patchan, M. W.; Osheroff, N.; Thompson, R. B. *J. Biol. Chem.* **1995**, *270*, 14998.

(22) El Hage Chahine, J. M.; Bertigny, J.-P.; Schwaller, M.-A. *J. Chem. Soc., Perkin Trans. 2* **1989**, 629.

(23) Auclair, C. *Arch. Biochem. Biophys.* **1987**, *259*, 1.

(24) Bailly, C.; Ohuigin, C.; Rivalle, C.; Bisagni, E.; Waring, M. *J. Nucleic Acids Res.* **1990**, *18*, 6283.

(25) Behravan, G.; Leijon, M.; Selhlstedt, U.; Vallberg, H.; Bergamn, J.; Gräslund, A. *Biopolymers* **1994**, *34*, 599.

(26) Canals, A.; Purciolas, M.; Aymami, J.; Coll, M. *Acta Crystallographica* **2005**, *61*, 1009.

(27) Dodin, G.; Schwaller, M. A.; Aubard, J.; Paoletti, C. *Eur. J. Biochem.* **1988**, *176*, 371.

(28) Elcock, A. H.; Rodger, A.; Richards, W. G. *Biopolymers* **1996**, *39*, 309.

(29) Jain, S. C.; Bhandary, K. K.; Sobell, H. M. *J. Mol. Biol.* **1979**, *135*, 813.

(30) Kohn, K. W.; Waring, M. J.; Glaubiger, D.; Friedman, A. *Cancer Res* **1975**, *35*, 71.

(31) Fung, S. Y.; Duhamel, J.; Chen, P. *J. Phys. Chem. A* **2006**, *110*, 11446.

(32) Miskolczy, Z.; Biczo´k, L.; Jablonkai, I. *Chem. Phys. Lett.* **2006**, *427*, 76.

(33) Sbai, M.; Ait Lyazidi, S.; Lerner, D. A.; del Castillo, B.; Martin, M. A. *J. Pharm. Biomed. Anal.* **1996**, *14*, 959.

(34) Cabo, J. L.; Faria, H. B.; Portuga, S. G. M.; Silva, M. A. A.; Brinn, I. M. *Photochem. Photobiol* **1999**, *69*, 664.

(35) *In fact, one obtains this picture from the spectral data of ellipticine in methanol, as presented in Table 1 of ref 32, indicating the formation of a new species in the ground state.*

(36) Itoh, M.; Adachi, T.; Tokumura, K. *J. Am. Chem. Soc.* **1984**, *106*, 850.

(37) Bhattacharya, B.; Samanta, A. *J. Phys. Chem. B* **2008**, *112*, 10101.

(38) Kang, B.; Ko, K. C.; Park, S.-Y.; Jang, D.-J.; Lee, J. Y. *Phys. Chem. Chem. Phys* **2011**, *13*, 6332.

(39) Reichardt, C. *Chem. Rev.* **1994**, *94*, 2319.

(40) Reichardt, C. In *Solvents and Solvent Effects in Organic Chemistry*; WILEY-VCH **2004**; pp 433.

(41) Diverdi, L. A.; Topp, M. R. *J. Phys. Chem.* **1984**, *88*, 3447.

(42) Mataga, N.; Tsuno, S. *Bull. Chem. Soc. Jpn.* **1957**, *30*, 368.

(43) *We take note of the argument used by Miskolczy et al. (ref 32) in support of their mechanism. However, we are left with no choice but to reconsider an alternative mechanism to account for the new results presented in this work. At this moment, we have no idea how to explain the dual fluorescence of 6-methylellipticine (ref 32) using our mechanism. This is an issue that needs to be looked into.*

(44) Marks, D.; Zhang, H.; Borowicz, P.; Waluk, J.; Glasbeek, M. *J. Phys. Chem. A* **2000**, *104*, 7167.

Chapter 4

Excited State Proton Transfer Kinetics of Ellipticine and Excited State Acidity Constant

Steady state absorption, emission and time-resolved fluorescence behavior of ellipticine have been studied in aqueous media over a wide pH range. Time-resolved fluorescence measurements have been carried out in aqueous alkaline media to monitor the excited state protonation kinetics of ellipticine which is possible by increased basicity of the pyridine nitrogen in the excited state. The individual rate constants are evaluated from the excited state kinetics based on which, the excited state protonation equilibrium constant (pK_a^*) of ellipticine is calculated. The pK_a^* value calculated from relatively simpler and popularly used Förster cycle showed considerable deviation from that calculated from the kinetic method. Weller method, which is based on steady state fluorescence intensity measurements, was also attempted for the estimation of pK_a^*. However, apart from the observation of the variation of fluorescence intensity due to a change in the ground state concentration of the species, no clear inflection point due to the excited state equilibrium could be observed.

4.1. Introduction

Ellipticine was identified as an antineoplastic and anti-HIV drug in the early sixties.[1-10] Anti-cancer activity of ellipticine results mainly from its function as a DNA intercalator due to its ability in π-π stacking, hydrogen bonding and several other non-covalent interactions with the DNA base pairs and phosphate groups.[11-13] Ellipticine, with a π-excessive carbazole and π-deficient pyridine ring,

has both the functional groups for acid-base chemistry and consequently two pK_a values corresponding to the equilibria depicted in Scheme 4.1. in the ground and excited singlet state are of matter of interest.[14-16] According to the literature, the pK_a value of 7.4 for ellipticine is due to the transformation from cationic to neutral form (Scheme 4.1.).[11,13] Hence, it is expected that at physiological pH (~ 7.4) both cationic and neutral forms will be present. Under this circumstance, where both prototropic forms are present, much stronger binding of cationic form with DNA perturbs the equilibrium between neutral and cationic forms. The environment of DNA is quite basic due to the negatively charged phosphate backbone. This causes the enhancement of the pK_a value to 9.1 for ellipticine bound to calf thymus DNA as revealed through confocal laser microspectrofluorimetry studies.[13] Interaction of ellipticine with different biological macromolecules and organelles can also affect the protonation equilibrium due to existence of specific local pH inside the cell.[17,18]

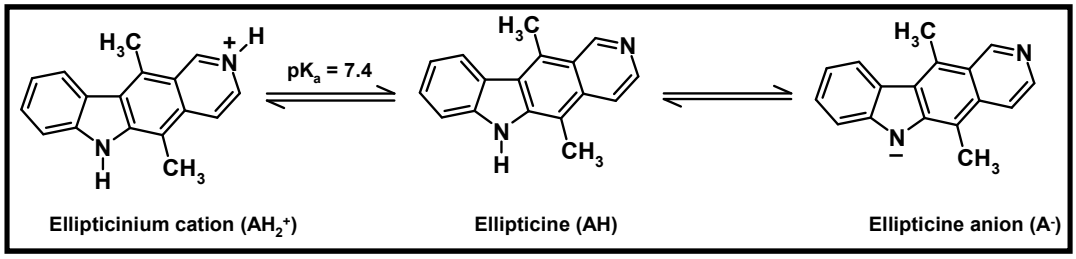

Scheme 4.1.

pH plays an important role in drug design and delivery. The change of pH in extra and intracellular environment in tumor cell is used as a tool for targeted delivery of drug molecules.[11] In some cases, drug binds strongly with the cancer cell because of acidic pH in the extracellular tumor environment compared to that

in normal cell.[19] Depending upon the pH, some drug molecules hydrolyse and produce two structurally different forms. For instance, hydrolysis of camptothecin produces the 'ring opened' carboxylate form from its lactone form at physiological pH.[20] As only the active lactone form (stable at pH < 5.5) can bind to DNA, a local acidic pH environment is needed for the binding where the concentration of its nonactive carboxylate form is very less. So it is inferred that the pH is a key factor in anti-cancer drug chemistry. Exploring the drug's photophysical properties in acidic/basic environment is thus very important and here fluorescence emission can be used as a spectroscopic tool to understand the local environment.

In a patent article, Eren et al. have shown that ellipticine, a DNA intercalating drug can also function as photosensitizer in photodynamic therapy (PDT) and exhibit the properties of an anti-cancer agent.[21,22] The mode of action of any photodynamic therapeutic drug is the accumulation of the drug in the malignant cell, absorption of appropriate wavelength of light and production of reactive singlet oxygen. The above mentioned process involves the singlet and triplet state photophysics of the photosensitizing drug and hence, to get an insight into the mechanism of PDT, the ground and excited state properties of the photosensitizer need to be studied, thoroughly.

Excited state properties of molecule are different from their ground state properties mainly due to different electronic distributions. The ground state protonation equilibrium constant of ellipticine (pK_a = 7.4), which has a key role in DNA binding, is also expected to change markedly in the excited state.[14] Though it is already studied that the ground state protonation equilibrium of ellipticine is

shifted when it is bound to CT-DNA,[13] the effect of binding on the excited state equilibrium constant is yet to be explored.

Though it is known that excited state equilibrium constant calculated by Förster cycle rarely gives the actual pK_a^* value due to several assumptions involved in this method,[23] there are examples,[24,25] including ellipticine,[26] where this method is used to calculate the pK_a^* value to analyze the excited state properties of the respective molecules. This can lead to wrong interpretations of excited state behavior of the molecules. Knowledge of exact value for pK_a^* is crucial for PDT drugs like ellipticine whose anti-cancer activities are mostly related to the excited state characteristics.

It is with this intention the present work has been taken up, where absorption, steady state and time-resolved fluorescence experiments of ellipticine have been carried out in aqueous solutions over a wide pH range. Though there is a possibility of excited state deprotonation, the stronger basicity of pyridinic nitrogen leads only to the excited state protonation of ellipticine. The kinetics in strong basic solution reveals the establishment of excited state protonation equilibrium of ellipticine, based on which, the excited state protonation equilibrium constant of ellipticine is calculated. The value obtained by this method is then compared with that calculated using Förster cycle. Weller method yielded a value which is similar to the ground state protonation constant of ellipticine.

4.2. Absorption and steady state fluorescence behavior

The absorption and emission behavior of ellipticine in various organic solvents is discussed in Chapter 3. Here, the absorption and fluorescence emission properties of ellipticine are studied in aqueous medium of pH ranging from 0 to 14 and even upto H_ 14.8.[27]

Absorption spectrum of ellipticinie at pH 4.2 is presented in Figure 4.1. (i). According to the literature, ellipticinium cation is the dominant species in acidic pH having a characteristic absorption band above 420 nm.[28-30] A hypsochromic shift of the absorption spectrum corresponding to the transformation of the cation to the neutral ellipticine in alkaline solutions (pH = 10.2) is observed (Figure 4.1. (ii)). However, ellipticine anion, which is characterized by absorption band at longer wavelength region,[16,31] is not observed in strong alkaline solution upto H_ 14.2 (Fig. 4.2).

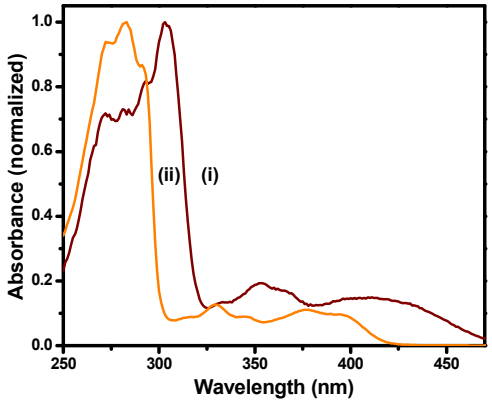

Figure 4.1. Absorption spectra of ellipticine at pH 4.2 (i) and 10.2 (ii).

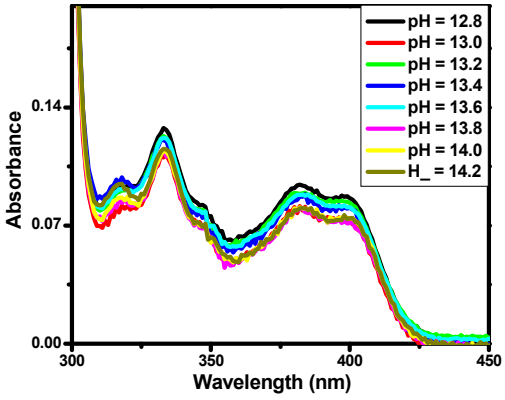

Figure 4.2. Absorption spectra of ellipticine at highly alkaline medium.

In acidic aqueous solution (pH 4.2), a single fluorescence band due to the ellipticinium cation having maximum at 540 nm (Figure 4.3 (i)) is observed. However, dual emission is observed over a wide neutral to alkaline pH range of pH 7.5-10.5 (Figure 4.3 (ii) to (vi)). The shorter wavelength band is assigned to the neutral ellipticine based on literature and its similarity with the emission of ellipticine in acetonitrile, and the longer wavelength emission band is attributed to ellipticinium cation (Figure 4.3).[28,29,32]

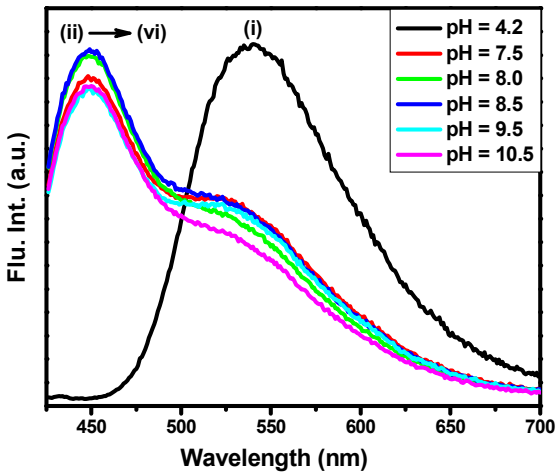

Figure 4.3. Fluorescence emission spectra of aqueous solution of ellipticine at different pH values [λ_{ex} = 416 nm].

A close look of Figure 4.3 reveals that as the pH changes from 7.5 to 8.5, there is a slight increase in the fluorescence intensity of the neutral form but almost no change of fluorescence intensity of the cationic form. This is quite unexpected if the fluorescence intensity is governed only by the ground state protonation equilibrium with a pK_a of 7.4. This observation therefore suggests an excited state protonation of the initially excited neutral ellipticine leading to the formation of

the cation in the excited state. Though at higher pH, the concentration of H_3O^+ ions is insufficient to explain this rapid protonation, neutral ellipticine is expected to abstract protons from water to form the cation.[33] Comparing with structurally related molecule norharman, we infer that another species that can contribute to the long wavelength emission is the excited state anion.[14,33] An excited state pK_a of 7.7 for the transformation from neutral norharman to the anion is calculated by Förster cycle using the ground state absorption maxima of neutral and anionic form.[14,33] However, according to the literature on other β-carboline molecules, the pyridine ring nitrogen in the excited state is a much stronger base than the OH^- ion present in the medium.[16,33,34] So the formation of the cation, from the excited neutral form, by abstracting a proton from water is more favorable process than formation of an anion by losing the pyrrolic hydrogen. Thus in the present case, formation of excited state ellipticinium cation from excited neutral ellipticine is much more feasible. The minimum variation of fluorescence intensity of the neutral ellipticine, from pH 7.5 to 10.5, supports the above explanation as a huge change in the fluorescence intensity of the neutral form would otherwise be expected with varying pH if OH^- ions were involved in the loss of pyrrolic hydrogen in the excited state mechanism.

In strong basic solutions (from pH 12.8 to H_ 14.2), though absorption spectra remain unchanged (Figure 4.2), there is a decrease in total emission from both neutral and cationic forms (Figure 4.4). The shape of the excitation spectra recorded by monitoring emission at 420 and 580 nm however, remain unchanged(Figure 4.5.). This behavior clearly indicates that the long wavelength

emission of ellipticinium cation in highly basic solution is due to the excited state reaction.

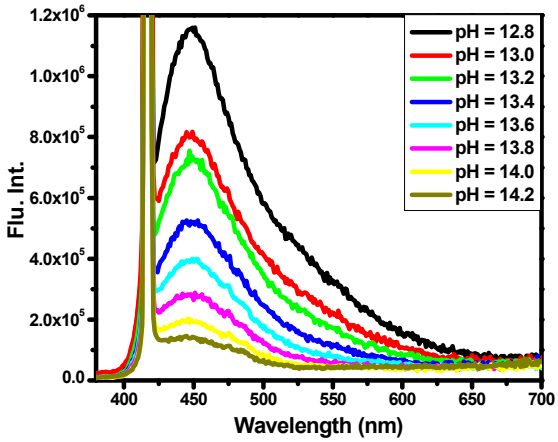

Figure 4.4. Fluorescence emission spectra (λ_{exc} = 416 nm, isosbestic point) of ellipticine at different pH values.

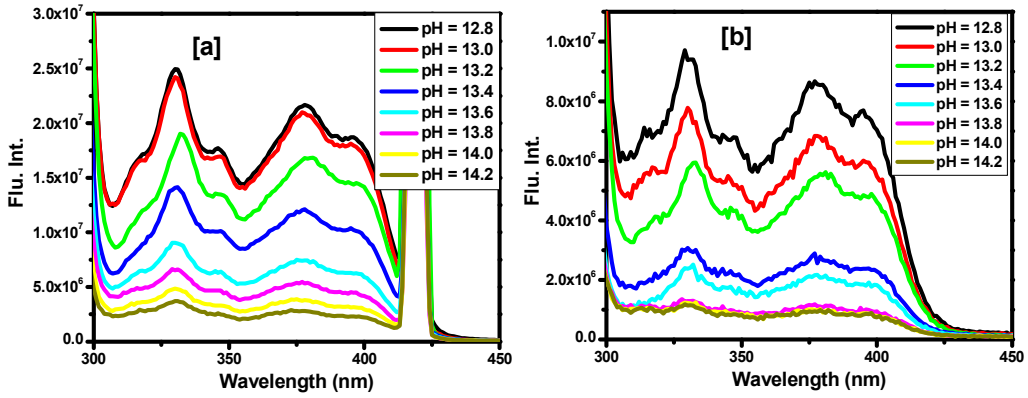

Figure 4.5. Fluorescence excitation spectra of ellipticine at different pH values. The monitoring emission wavelengths are 420 nm [a] and 580 nm [b].

The change of ground state ratio of ellipticinium cation to neutral ellipticine with varying pH is monitored through fluorescence excitation spectra as the absorption spectra of poorly water soluble ellipticine (< 10^{-6}) do not provide much information at longer wavelengths.[26,28,32] The excitation spectra reveal the isosbestic point at 416 nm, which clearly indicates the ground state prototropic equilibrium between the neutral and cationic forms of ellipticine (Figure 4.6). Thus aqueous solutions of ellipticine at various pH are excited at 416 nm in all cases.

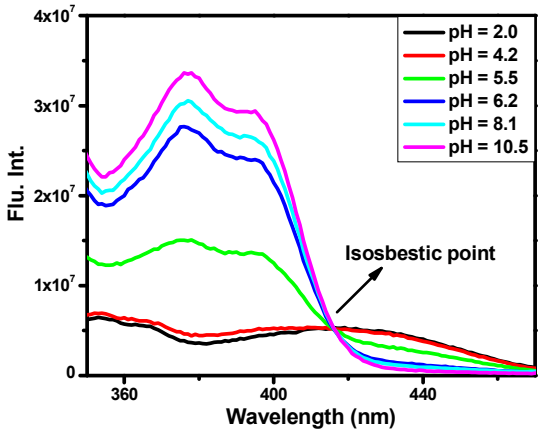

Figure 4.6. Fluorescence excitation spectra of ellipticine at different pH. The monitoring wavelength is 480 nm.

4.3. Time-resolved fluorescence studies at specific pH range

Fluorescence decays of ellipticine in basic aqueous media (from pH 13 to H_ 14.2) are measured at two different wavelengths (430 and 570 nm) corresponding to neutral and cationic form respectively. The results of fluorescence decay measurements are summarized in Table 4.1 which show that the lifetime components present in both the wavelengths are quite similar.

Representative decay profiles at pH 13.2 monitored at two wavelengths along with the biexponenial fits to the emission profiles are shown in Figure 4.7. The time-resolved florescence emission profiles at both the wavelengths and at different pH values are well fitted to biexponential functions and the rates become faster as the pH of the medium gradually increases (Table 4.1.). The short-lifetime component monitored at 430 nm matches well with the initial rise time observed at 570 nm and confirms the formation of ellipticinium cation through excited state reaction in the monitored pH range. The long-lifetime component observed at the decay profile measured at 430 nm suggests the backward reaction leading to re-population the excited state neutral form.

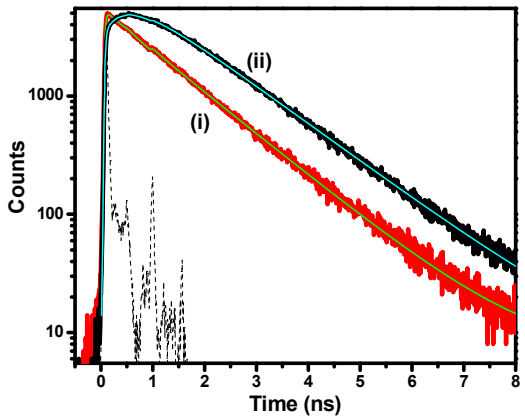

Figure 4.7 Fluorescence decay profiles (λ_{exc}= 405 nm) of aqueous solution of ellipticine (pH = 13.2) at 430 (i) and 570 nm (ii). The instrument response function (prompt) is shown as dashed line.

Table 4.1. Fluorescence decay parameters of ellipticine (λ_{exc} = 405 nm) at different pH values monitored at 430 and 570 nm.

	Decay parameters τ_i (ns) [a_i]		
pH	**At 430 nm**	**At 570 nm**	χ^2
13.0	0.59 [0.65], 1.71[0.35]	0.57[-0.46], 1.88[0.54]	1.2, 1.0
13.2	0.32[0.80], 1.24[0.20]	0.42 [-0.47],1.38 [0.53]	1.2, 1.1
13.4	0.24 [0.75], 0.87 [0.25]	0.27 [-0.43], 0.93[0.57]	1.1, 1.0
13.6	0.19 [0.71], 0.61 [0.29]	0.24 [-0.37], 0.68[0.63]	1.2, 1.1
13.8	0.097 [0.75],0.52[0.25]	0.093 [-0.30],0.54[0.70]	1.2, 1.0
14.0	0.053 [0.74], 0.3 [0.26]	0.059 [-0.35], 0.38[0.65]	1.2, 1.1
14.2	0.051 [0.80], 0.23 [0.20]	0.057 [-0.31], 0.28 [0.69]	1.0, 1.2

To follow the kinetics of the excited state reaction we particularly concentrated on the highly alkaline pH (from pH 13 to H_ 14.2) range where neutral ellipticine is the only species present in the ground state. On photoexcitation, neutral ellipticine, represented as AH, can undergo excited state protonation reaction to produce cationic form of ellipticine (AH_2^{+*}) or deprotonation to produce ellipticine anion (A^{-*}) as presented in Scheme 4.2. Following Scheme 4.2, ($k_3' + k_4'$), ($k_3'' + k_4''$) and ($k_3 + k_4$) are the radiative and non-radiative rate constants for the neutral, anionic and cationic forms of ellipticine respectively. From Scheme 4.2, AH^* is in equilibrium with AH_2^{+*} having k_{H_2O} ($k_{H_2O} = k_2[H_2O]$) and k_1 as the excited state forward and backward rate constants and on the other hand, k_{OH^-} and k_6 are the forward and backward rate constant for the transformation of AH^* to A^{-*} in the excited state.

As already mentioned in the previous section, on electronic excitation the pyridine ring nitrogen becomes a stronger base[33,34] and the excited state reaction of neutral ellipticine producing ellipticinium cation by abstracting a proton from water is expected to be the dominant process rather than the excited state anion formation through deprotonation of pyrrole hydrogen by OH^- ions present in the medium. Thus in the present scheme (Scheme 4.2) the excited state kinetics are mainly governed by the protonation equilibrium and deprotonation of excited neutral ellipticine can be neglected.

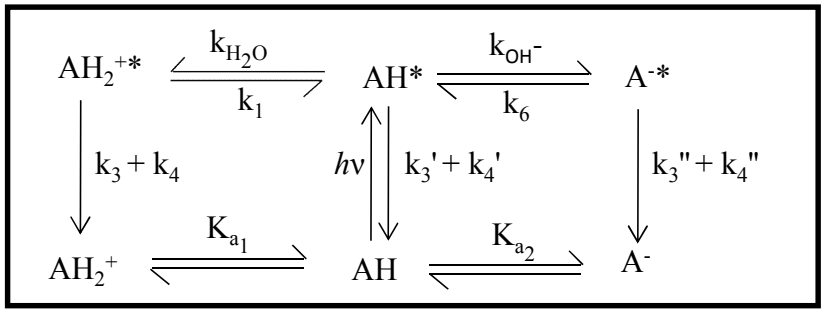

Scheme 4.2.

Following Scheme 4.2, the time dependence of the cationic and neutral forms is given by equation 1 and 2.

$$-d[AH_2^{+*}] / dt = (k_1 + k_3 + k_4)\,[AH_2^{+*}] - k_{H_2O}\,[AH^*] \quad (1)$$

$$-d[AH^*] / dt = (k_{H_2O} + k_3' + k_4')\,[AH^*] - k_1[AH_2^{+*}] \quad (2)$$

By using the boundary conditions at t = 0, $[AH_2^{+*}] = 0$ and $[AH^*] = [AH^*]_0$, the concentration of excited state ellipticine and ellipticinium cation with time can be obtained (eqn. 3 and 4).

$$[AH^*](t) = \frac{[AH^*]_0}{\lambda_1 - \lambda_2} [(x - \lambda_2) \exp(-\lambda_1 t) + (\lambda_1 - x) \exp(-\lambda_2 t)] \quad (3)$$

$$[AH_2^{+*}](t) = \frac{k_2[H_2O][AH^*]_0}{\lambda_1 - \lambda_2} [\exp(-\lambda_2 t) - \exp(-\lambda_1 t)] \quad (4)$$

Where $X = k_3' + k_4' + k_{H_2O}$, $Y = k_3 + k_4 + k_1$,

And $\lambda_1, \lambda_2 = \tau_1^{-1}, \tau_2^{-1}$

$$= \frac{1}{2}\{(X + Y) \pm [(Y - X)^2 + 4k_1 k_{H_2O}]^{1/2}\} \quad (5)$$

4.4. Estimation of excited state pK_a

4.4.1. Kinetic method

The kinetic data from the time-resolved fluorescence experiments can be exploited to estimate the excited state prototropic equilibrium constant. Based on the data from the previous section the individual rate constants can be evaluated to calculate the excited state pK_a.

At pH = 4, k_{H_2O} $[AH^*] = 0$ and $[AH^*]$ is very small so, $k_1 << k_3 + k_4$ and eqn. 1 becomes,

$$[AH_2^{+*}] = [AH_2^{+*}]_0 \exp[(k_3 + k_4)t] \quad (6)$$

Comparing eqn. 6 with the experimental data obtained after analyzing the decay profile at pH = 4, the radiative and non-radiative decay constant ($k_3 + k_4$) of ellipticinium cation is found to be 1.64×10^8 s^{-1}.

Combining the values of λ_1 and λ_2 from eqn. 5,

$\lambda_1 + \lambda_2 = X + Y = k_3' + k_4' + k_{H_2O} + Y$ (7)

Assuming $[H_2O] \approx [OH^-]$ at pH 13 to H_ 14.2 range, $k_2[H_2O](k_{H_2O}) \approx k_2[HO^-]$ (k_{OH}), a value of 1.86×10^{10} M^{-1} s^{-1} for k_2 is obtained from the slope of the plot of $(\lambda_1 + \lambda_2)$ against $[OH^-]$ (Figure 4.8).

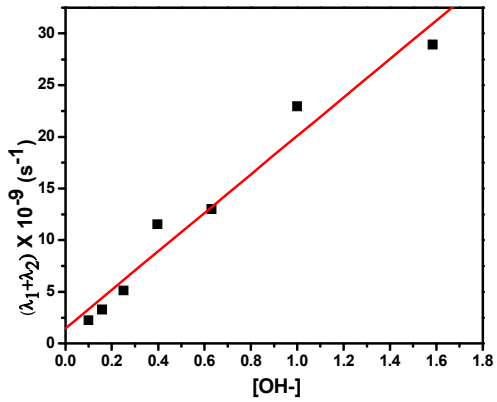

Figure 4.8. A plot of $(\lambda_1 + \lambda_2)$ against $[OH^-]$, following eqn. 7.

Again from eqn. 5, multiplying λ_1 and λ_2 to get,

$\lambda_1\lambda_2 = XY - k_1 k_{OH}$ (8)

After substituting the value of X and Y in eqn. 8

$\lambda_1\lambda_2 = (k_3' + k_4')Y + (k_3 + k_4) k_2[OH^-]$ (9)

Combining eqn. 7 and 9 gives

$\lambda_1 + \lambda_2 = k_3 + k_4 + [1 - (k_3 + k_4)/(k_3' + k_4')]Y + \frac{\lambda_1 \lambda_2}{k_3' + k_4'}$ (10)

According to eqn. 10 a plot of $\lambda_1 + \lambda_2$ versus $\lambda_1\lambda_2$ gives the value of radiative and nonradiative decay $(k_3' + k_4')$ of ellipticine, which is found to be 3.7×10^9 s^{-1} (Figure 4.9.).

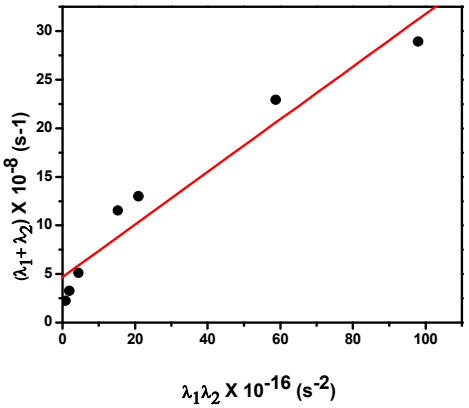

Figure 4.9. A plot of $(\lambda_1 + \lambda_2)$ against $\lambda_1\lambda_2$, following eqn. 10.

Again a plot of $\lambda_1\lambda_2$ against $[OH^-]$ (eqn. 9) gives a straight line (Figure 4.10).

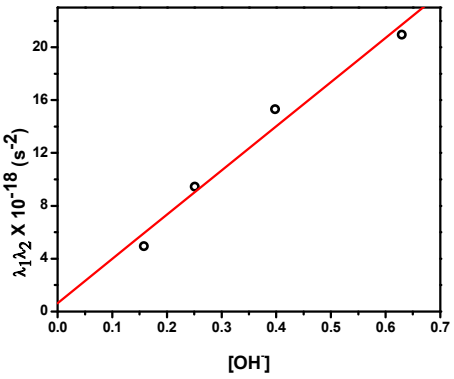

Figure 4.10. A plot of $\lambda_1\lambda_2$ against $[OH^-]$, following eqn. 9.

From the intercepts of Figures 4.8 and 4.10, the value of k_1 was evaluated as 1.11 X 10^9 s^{-1}. All the rate constants are tabulated in Table 4.2. The excited state pK_a value was then calculated using

$$\log (k_1 / k_2) = pK_a^* + \log K_w \qquad (11)$$

Thus, from the kinetic data of the time-resolved fluorescence experiments the estimated pK_a^* value is 12.7

Table 4.3. Rate constants of ellipticine and ellipticinium cation derived from fluorescence decay parameters.

Rate constants	
$k_3 + k_4$	1.64 x 10^8 s^{-1}
$k_3' + k_4'$	3.7 X 10^9 s^{-1}
k_1	1.11 X 10^9 s^{-1}
k_2	18.6 X 10^9 M^{-1} s^{-1}

4.4.2. Förster Cycle

Excited state pK_a for the protonation equilibrium of ellipticine is calculated using Förster cycle described elaborately in section 1.2.1. of Chapter 1.[35]

$$pK^* - pK = \frac{N_a hc}{2.303RT} \quad (\bar{\nu}_{AH} - \bar{\nu}_{AH_2{}^*}) \qquad (12)$$

In this method, energy difference between the ground and excited states of neutral and cationic forms is used for the estimation of excited state pK_a. The energy difference is measured through 0-0 transition energy, which is taken as the intersection point of the absorption and emission spectra. The 0-0 energy for neutral ellipticine at 411 nm and for the cation at 468 nm leads to the excited state pK_a value of 13.5. This value is somewhat higher than that estimated from the time-resolved fluorescence studies ($pK_a^* = 12.7$). This difference can be explained considering some of the limitation of the Förster cycle.

4.4.3. Weller Method

Weller method[36-38] described in section 1.2.2. of Chapter 1 is also attempted for the calculation of the excited state pK_a. According to this method the excited state pK_a is determined from the pH dependence of the fluorescence intensities.

$$\Phi/\Phi_0 = 1/ (1+ R \times 10^{pH}) \quad (13)$$

Where $R = k_1\tau_0 K_w / (1 + k_{-1} \tau_0')$

Equation 13 suggests a plot of relative fluorescence quantum yield vs pH to yield a sigmoidal curve, from which pK_a^* will be obtained at the inflection point.

In the present case relative fluorescence intensities of ellipticine and ellipticinium cation are plotted over a large pH range (Figure 4.11.). The inflection point at pH ~ 6.6 reflects the variation of the concentration of ground state species and thus corresponds to the pK_a value. However, at pH > 11, we could not observe substantial variation of fluorescence intensities to allow determination of pK_a^* by this method.

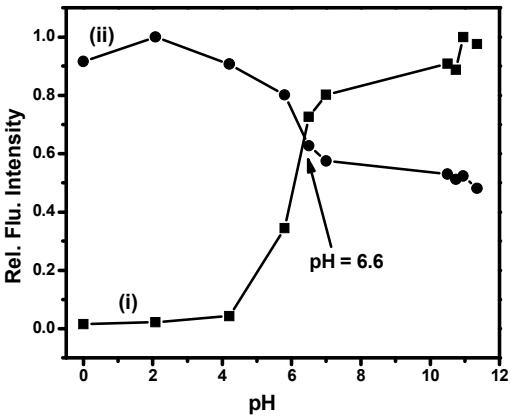

Figure 4.11. Plot of relative fluorescence intensity against pH of the solution for ellipticine (i) and ellipticinium cation (ii).

4.5. Conclusion

Spectral properties of ellipticine in aqueous solutions over a large pH range are investigated by steady state and time-resolved fluorescence techniques. The studies presented here provide the first and most direct evidence of excited state reaction of ellipticine in basic aqueous media. Kinetics of the excited state reaction established the prototropic equilibrium of ellipticine. The pK_a^* value of 12.7 is obtained from the individual rate constants involved in the excited state proton transfer process of ellipticine. The pK_a^* value is calculated by applying Förster cycle. However this value is slightly higher than that obtained using kinetic method. Weller method was also attempted for the estimation of pK_a^*. However, the inflection point could only be attributed to the ground state pK_a.

Reference

(1) Smith, A. F.; Horning, E. C.; Goodwin, S. *J. Am. Chem. Soc.* **1959**, *81*, 1903.

(2) Masood, F.; Chen, P.; Yasin, T.; Hasan, F.; Ahmad, B.; Hameed, A. *J. Mater. Sci. - Mater. Med.* **2013**, *in press*.

(3) Garbett, N. C.; Graves, D. E. *Curr. Med. Chem.* **2004**, *4*, 149.

(4) Le Pecq, J.-B.; Xuong, N.-D.; Gosse, C.; Paoletti, C. *Proc. Natl. Acad. Sci. U.S.A.* **1974**, *71*, 5078.

(5) R.B.Woodward.; Iacobucci., G. A.; Hochstein., F. A. *J. Am. Chem. Soc.* **1959**, *81*, 4434.

(6) Ohashi, M.; Oki, T. *Exp. Opin. Ther. Pat.* **1996**, *6*, 1285.

(7) Clarysse, A.; Brugarolas, A.; Siegenthaler, P.; Abele, R.; Cavalli, F.; De Jager, R.; Renard, G.; Rozencweig, M.; Hansen, H. H. *Eur. J. Cancer Clin. Oncol.* **1984**, *20*, 243.

(8) Dodion, P.; Rozencweig, M.; Nicaise, C.; Piccart, M.; Cumps, E.; Crespeigne, N.; Kisner, D.; Kenis, Y. *Eur. J. Cancer Clin. Oncol.* **1982**, *18*, 519.

(9) Gouyette, A.; Huertas, D.; Droz, J.-P.; Rouesse, J.; Amiel, J.-L. *Eur. J. Cancer Clin. Oncol.* **1982**, *18*, 1285.

(10) Paoletti, C.; Le Pecq, J. B.; Dat-Xuong, N.; Juret, P.; Garnier, H.; Amiel, J.-L.; Rouesse, J. *Recent Res. Cancer Res.* **1980**, *40*, 107.

(11) Dodin, G.; Schwaller, M. A.; Aubard, J.; Paoletti, C. *Eur. J. Biochem.* **1988**, *176*, 371.

(12) Řeha, D.; Kabeláč, M.; Ryjáček, F.; Šponer, J. E.; Elstner, M.; Suhai, S.; Hobza, P. *J. Am. Chem. Soc.* **2002**, *124*, 3366.

(13) Sureau, F.; Moreau, F.; Millot, J.-M.; Manfait, M.; Allard, B.; Aubard, J.; Schwaller, M.-A. *Biophysical Journal* **1993**, *65*, 1767.

(14) Draxler, S.; Lippitsch, M. E. *J. Phys. Chem.* **1993**, *97*, 11493.

(15) Dias, A.; Varela, A. P.; Miguel, M. G.; Macanita, A. L.; Becker, R. S. *J. Phys. Chem.* **1992**, *96*, 10296.

(16) Wolfbeis, O. S.; Fürlinger, E.; Wintersteiger, R. *Monatsh. Chem.* **1982**, *113*, 509.

(17) Sbai, M.; Lyazidi, S. A.; Lerner, D. A.; del Castillo, B.; Martin, M. A. *Anal. Chim. Acta* **1995**, *303*, 47.

(18) Schwaller, M. A.; Allard, B.; Sureau, F.; Moreau, F. *J. Phys. Chem.* **1994**, *98*, 4209.

(19) Adams, D. J.; Dewhirst, M. W.; Flowers, J. L.; Gamcsik, M. P.; Colvin, O. M.; Manikumar, G.; Wani, M. C.; Wall, M. E. *Cancer Chemother. Pharmacol.* **2000**, *46*, 263.

(20) Kruszewski, S.; Kruszewska, D. M. *Acta Physica Polonica A* **2010**, *118*, 99.

(21) Eren, D.; Yechezkel, T.; Salitra, Y.; Uses, T. Preparation of RGD-containing peptidomimetics and their pharmaceutical compositions useful for diagnosis of tumors and photodynamic therapy. In *PCT Int. Appl.*, **2010**; Vol. WO2010046900.

(22) Torchilin, P. V.; Lukyanov, N. A.; Gao, Z. Micelle drug delivery system containing a phospholipid-PEG component. In *PCT Int. Appl.*, **2004**; Vol. WO 2004098569.

(23) Samanta, A.; Chattopadhyay, N.; Nath, D.; Kundu, T.; Chowdhury, M. *Chem. Phys. Lett.* **1985**, *121*, 507.

(24) Wierzchowski, J.; Sepioł, J.; Sulikowski, D.; Kierdaszuk, B.; Shugar, D. *J. Photochem. Photobiol. A: Chem.* **2006**, *179*, 276.

(25) Kumar, S.; Jain, S. K.; Sharma, N.; Rastogi, R. C. *Spectrochim. Acta. Part A* **2001**, *57*, 299.

(26) Thakur, R.; Das, A.; Chakraborty, A. *Chem. Phys. Lett.* **2013**, *563*, 37.

(27) Yagil, G. *J. Phys. Chem.* **1967**, *71*, 1034.

(28) Kohn, K. W.; Waring, M. J.; Glaubiger, D.; Friedman, A. *Cancer Res.* **1975**, *35*, 71.

(29) Fung, S. Y.; Duhamel, J.; Chen, P. *J. Phys. Chem. A* **2006**, *110*, 11446.

(30) Banerjee, S.; Pabbathi, A.; Sekhar, M. C.; Samanta, A. *J. Phys. Chem. A* **2011**, *115*, 9217.

(31) Vert, F. T.; Sanchez, I. Z.; Torrent, A. O. *J. Photochem.* **1983**, *23*, 355.

(32) Sbai, M.; Ait Lyazidi, S.; Lerner, D. A.; del Castillo, B.; Martin, M. A. *J. Pharm. Biomed. Anal.* **1996**, *14*, 959.

(33) Sakurovs, R.; Ghiggino, K. P. *J. Photochem.* **1982**, *18*, 1.

(34) Deumié, M.; Viallet, P. *J. Photochem.* **1979**, *10*, 365.

(35) Förster, T. *Z. Elektrochem* **1950**, *54*, 551.

(36) Weller, A. *Z. Elektrochem.* **1952**, *56*, 662.

(37) Weller, A. *Z. Elektrochem.* **1956**, *60*, 1144.

(38) Weller, A. *Prog. React. Kinetics* **1961**, *1*, 189.

Chapter 5

Steady State and Time-Resolved Fluorescence Behavior of 4-Aminophthalimide in Aqueous Media: A Reinvestigation of the Role of Solvent and Isotope Effect

In this chapter the fluorescence behavior of 4-aminopthalimide (AP) and its imide-H protected derivative (N-BuAP) has been reinvestigated in aqueous media to address some of the points raised in a recent paper (J. Phys. Chem. B 2013, 117, 2160 – 2168). The results show that solvent assisted keto-enol transformation does not contribute to the observed steady state and time-resolved emission behavior of AP in aqueous media. Instead, the results reveal that the fluorescence of AP in aqueous media arises from two distinct hydrogen bonded species. The deuterium isotope effect on the fluorescence quantum yield and lifetime of AP, earlier thought to be a reflection of the excited state proton transfer process, is now explained considering the difference between the influence of deuterated and undeuterated solvents on the rate of non-radiative processes and also the ground state exchange of the proton with the solvent.

5.1. Introduction

Photophysics of 4-aminophthalimide (AP) has been studied extensively in the past and in recent years and due to its attractive fluorescence properties (high fluorescence quantum yield, long fluorescence lifetime and sensitivity of these properties to the surrounding environment), the molecule is being used routinely as a fluorescence probe for studies in solvation dynamics, estimating the polarity

of unknown media and probing the organized environments of complex chemical and biological systems.[1-36] It is generally accepted that photoexcitation of AP leads to enhanced separation of charge and the molecule emits from an intramolecular charge transfer (ICT) state, whose energy is governed by the polarity of the medium and also by the hydrogen bonding interaction with the solvent.[3,8,10] The fluorescence quantum yield and lifetime of AP are also strongly dependent on the medium.[3,8,10] In contrast to its behavior in aprotic media, where AP is strongly fluorescent, it emits weakly and possesses a short fluorescence lifetime in protic solvents. Even though solute-solvent hydrogen bonding interaction was considered to be responsible for large Stokes shift of the fluorescence maximum, low fluorescence yield and short fluorescence lifetime of the molecule in protic media, an alternative explanation in terms of solvent-assisted intramolecular proton transfer (Scheme 5.1.) was also proposed, according to which the emission of AP originates from its enol form in protic media.[7,13,16] Even though no kinetic evidence in support of this transformation was provided, a higher fluorescence lifetime and quantum yield of AP in D_2O compared to H_2O was considered to be consistent with this mechanism.[13]

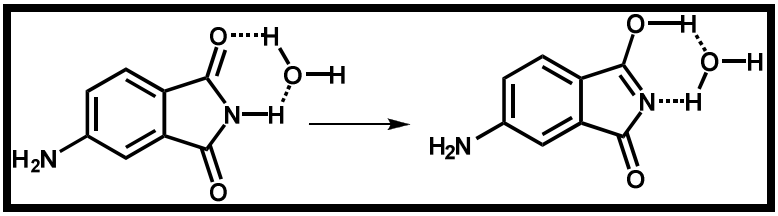

Scheme 5.1.

However, even though subsequent studies have brought into light the drawback of this mechanism,[14] solvent mediated excited state keto-enol transformation of the system is reinvoked recently to account for the excitation wavelength dependence of the emission spectrum, and a progressive blue shift of the emission maximum of AP with time in aqueous media.[22] A bi-exponential fluorescence decay behavior and time-dependent shift of the fluorescence spectrum in aqueous media have been argued as direct kinetic evidence of the excited state reaction of AP in aqueous media.[22] As the excitation wavelength dependence of steady state fluorescence spectrum of AP reported in this paper,[22] could not be reproduced by us,[23] we had to comment that the mechanism cannot be taken seriously. However, the kinetic data presented by Durantini et al. in support of the excited state reaction[22] required careful consideration as a bi-exponential decay behavior and time-dependent shift of the emission spectrum is not expected in the absence of an excited state reaction. Moreover, even though a dynamic Stokes shift of the fluorescence spectrum due to excited state reaction is common, a progressive shift towards higher energy is very unusual, if not unprecedented. It is also puzzling why the spectral shift is not continuous but it is observed only between 2 and 4 ns.[22] In order to investigate these important points and establish once again beyond any reasonable doubt that excited state proton transfer reaction does not influence the photophysics of AP in aqueous media, we have studied and compared the steady state and time-resolved fluorescence behavior of AP and its derivative N-butyl-4-aminophthalimide (N-BuAP, Chart 5.1.), where the imide hydrogen atom is replaced by an n-butyl group.

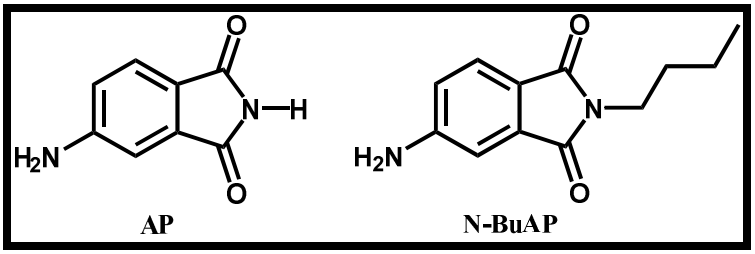

Chart 5.1.

5.2. Spectral studies in neat and mixed solvents

Figure 5.1. compares the steady state fluorescence spectra (λ_{ex} = 370 nm) of AP and N-BuAP in aprotic (acetonitrile, ACN) and protic (water) solvents. It is interesting to note that the large (~100 nm, Table 5.1.) difference in the λ_{max}^{em} values of AP in the two solvents, which led to the postulation of the emission originating from the enol form of the molecule produced as a result of excited state water-assisted transfer of the imide proton (Scheme 5.1.), is also observable in the case of N-BuAP, which lacks the imide proton and hence, cannot emit from its enol form. The strikingly similar fluorescence spectra of the two systems thus clearly rule out the possibility of the enol form of AP as the emitting species in protic solvents such as in water.

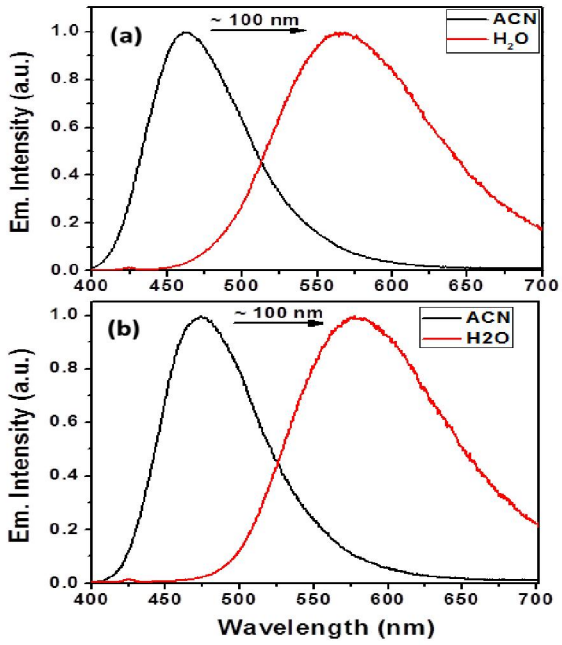

Figure 5.1. Steady state emission spectra of (a) AP and (b) N-BuAP (λ_{ex} = 370 nm).

Table 5.1. Comparison of some of the fluorescence parameters of AP and N-BuAP.

Solvent	λ_{max}^{em} / *nm*		$(I_{AP}/I_{N\text{-}BuAP})^a$	Φ_f (AP)
	AP	N-BuAP		
ACN	460	472	1.2	0.63[b]
H_2O	565	577	1.5	0.022[b]

[a]I_{AP} and $I_{N\text{-}BuAP}$ are integrated area under the fluorescence spectra of AP and N-BuAP, respectively, recorded under identical experimental conditions. [b]ref. 18.

One can argue against the excited state solvent-mediated proton transfer mechanism from another angle. There is no second opinion that in aprotic solvent acetonitrile AP emits (λ_{max} = 460 nm) from its normal (keto) form. Hence, if the emission of AP in aqueous media (λ_{max} = 565 nm) indeed originates from its enol form, then on gradual addition of water to an acetonitrile solution of AP a progressive increase of the fluorescence intensity of the 565 nm band at the expense of the ~460 nm emission is expected. Considering low fluorescence quantum yield of AP in water (compared to acetonitrile), one expects that the decrease in intensity at 460 nm to be more pronounced than the increase in intensity at 565 nm. However, the spectral behavior of AP and N-BuAP presented in Fig. 5.2. shows a gradual shift of the emission spectrum towards a longer wavelength instead of the expected trend thus disproving the excited state proton transfer reaction of AP. Absorption spectra of AP and N-BuAP on gradual addition of water to an acetonitrile solution is also presented in Fig. 5.3. Moreover, a very similar time-resolved fluorescence response (Figure 5.4.) of AP and N-BuAP, the latter lacking the imide hydrogen essential for the formation of the enol form of the molecule, further reinforces our conclusion.

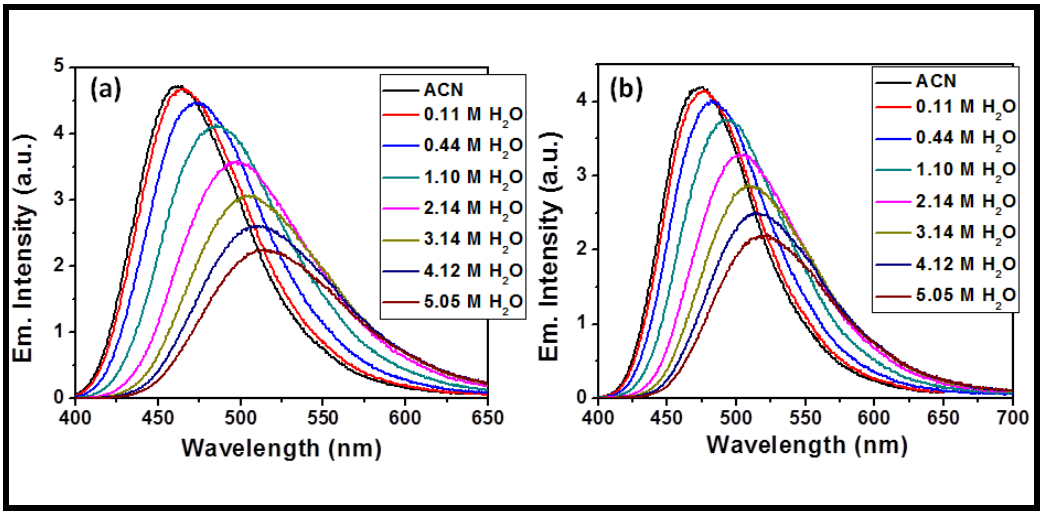

Figure 5.2. Steady state emission spectra of (a) AP and (b) N-BuAP in acetonitrile-water mixture (λ_{ex} = 370 nm).

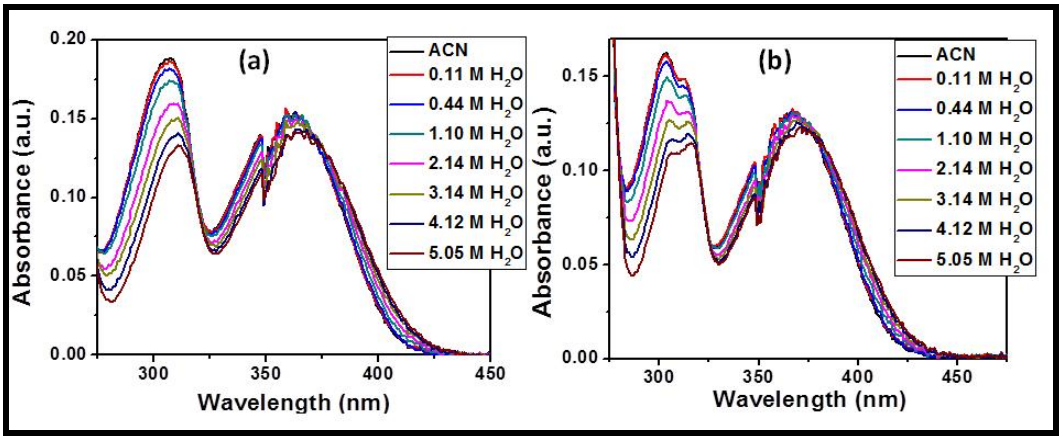

Figure 5.3. Absorption spectra of (a) AP and (b) N-BuAP in acetonitril-water mixture.

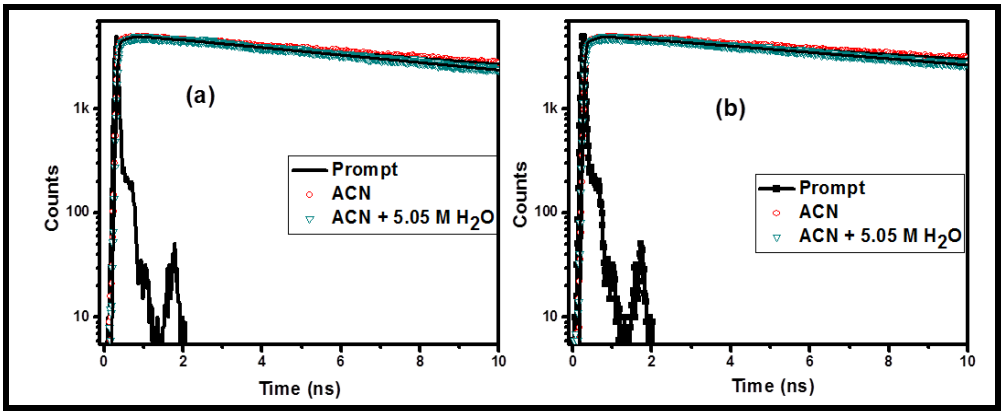

Figure 5.4. Fluorescence decay profiles of (a) AP and (b) N-BuAP monitor in acetonitril-water mixture at 575 nm. Solid lines represent single-exponential fit to decay profiles (λ_{ex} = 375 nm).

5.3. Isotope effect

As stated in the Introduction, a significantly higher fluorescence quantum yield (φ_f) and lifetime (τ_f) of AP in D_2O when compared with that in H_2O was thought to be consistent with solvent-mediated transfer of the imide hydrogen to the carbonyl oxygen.[16,22] However, as the results presented above clearly rule out the possibility of an excited state proton transfer process contributing to the fluorescence response of AP, it is necessary to reexamine the isotope effect carefully and determine its origin. For this purpose, we first find out whether N-BuAP, which lacks the imide hydrogen, also exhibits deuterium isotope effect or not. It is interesting to note that like AP, the Φ_f and τ_f of N-BuAP are also found higher in D_2O by a factor of 2.0 and 4.5, respectively. We also observed a 2.9-fold increase of Φ_f and τ_f for both AP and N-BuAP in CD_3OD compared to CH_3OH. As the isotope effect is real, but is clearly not due to proton transfer process, its origin lies elsewhere.

Deuterium isotope effect of the solvent on φ_f and τ_f implies merely a change in the rate of radiationless relaxation processes of the system on isotopic substitution.[37] This change expected to be most pronounced when solvent proton participates in the excited state proton transfer reaction, which serves as one of the nonradiative decay channels.[38] However, the proton exchange process need not be the only radiationless process. It is well known that solvent often plays a crucial role in influencing the nonradiative relaxation (intersystem crossing and internal conversion) rates by directly interacting with the solute.[39] A strong interaction of the electronic motion of the fluorescent system with the nuclear motion of the solvent provides a mechanism for the conversion of electronic energy of the system into the vibrational energy of the solvent and can thus results in radiationless interconversion[40,41] leading to a change in the Φ_f and τ_f values. In such situation, isotopic substitution in the solvent can influence the coupling between the electronic motions of the solute and vibrational motion of the solvent and thus can contribute to the isotope effect.

In the present case, one needs to consider an additional factor. While the excited state proton transfer reaction contributing to the emission behavior of these systems is completely ruled out, it does not necessarily mean that no proton of the fluorescent system is exchanged with the solvent (H_2O or D_2O) in the ground state. Both AP and N-BuAP possess amino protons, which are sufficiently acidic (due to the inductive influence of the carbonyl group) to be exchanged with the H or D atoms of the solvents in the ground state. Evidence of this kind of exchange process is often obtained from ^{1}H-NMR measurements, where the signals due to the acidic protons are seldom observed. One must note however

that as these rates are much slower compared to the radiative/nonradiative rates of the systems by several orders of magnitude, and that they play no noticeable role in the fluorescence behavior of the systems. However, under this kind of situation, in deuterated solvents, one is essentially dealing not only with the original molecule, but is also dealing with partially deuterium-exchanged molecule. If the fluorescence efficiency of a system and its deuterated analog are different due to different rates of the nonradiative relaxation process (which is quite likely),[37,42] deuterium isotope effect, can also arise due to this factor. Hence, in our opinion the isotope effect exhibited by AP and N-BuAP arises from one or both the factors described above.

5.4. Wavelength dependent fluorescence decay and time-resolved emission spectrum

We now reinvestigate carefully the time-resolved fluorescence behavior of the two systems and find out whether it is suggestive of an excited state reaction. Considering the fact that the emission peak of the two systems in aqueous media is observed at around 565 nm, we have measured first the fluorescence decay profiles at this wavelength. These fluorescence intensity vs time profiles of the two systems, which are shown in Fig. 5.5, can be fitted satisfactorily to a single exponential decay function yielding lifetimes of around 1.10 ns, which is consistent with literature.[13,18]

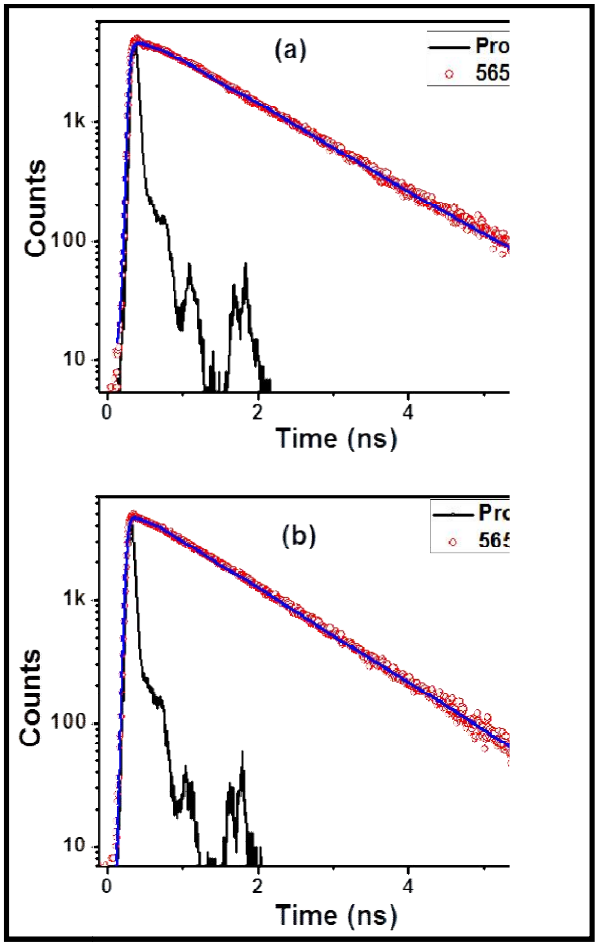

Figure 5.5. Fluorescence decay profiles of (a) AP and (b) N-BuAP monitored at 565 nm in water. Solid lines represent single exponential fit to decay profiles (λ_{ex} = 375 nm).

Considering the recent report[22] of time-dependent shift of the fluorescence spectrum we thought it pertinent to examine the time-resolved fluorescence response of the systems in more details. As it is possible to construct the time resolved emission spectra (TRES) of a system by measuring its fluorescence

decay profiles at several wavelengths covering the entire emission spectra, we measured the fluorescence decay profiles of the two systems at different wavelengths and the results, which are presented in Fig. 5.6, are quite revealing.

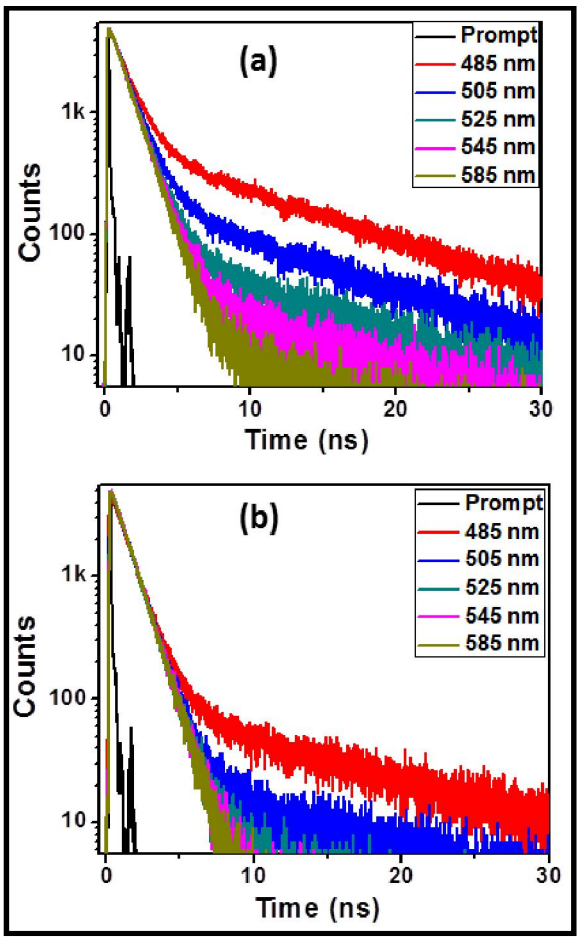

Figure 5.6. Wavelength dependent fluorescence decay profiles of (a) AP and (b) N-BuAP in water (λ_{ex} = 375 nm).

As can be seen, contrary to the decay profiles measured at the peak maxima or at higher wavelengths, which are mainly characterized by a single exponential decay function, those measured at shorter wavelengths are clearly biexponential, consisting along with the short lifetime component of a ~1.1 ns (major) and a long ~10.0 ns (minor) component as well. As the monitoring wavelength is increased the contribution of the long component diminishes gradually and as the emission peak position is reached, the long component vanishes almost completely and one obtains a single exponential decay with a lifetime around 1.1 ns, which is commonly taken as the fluorescence lifetime of AP in aqueous media. We shall return to discuss about the origin of the two specific lifetime components in the next section. However, having observed the two lifetime components and their variation with the monitoring wavelength, the blue shift of the TRES, as reported recently,[22] became quite clear to us. The TRES recorded at early times consisted primarily of the short component and those recorded beyond 3 ns did not have any contribution from the short component, thus making it clear why the blue shift was observed in the 3 – 4 ns time range.

5.5. Possible origin of the two lifetime components

While the dependence of the fluorescence decay profiles on the monitoring wavelength (as observed by us) explains the blue shift of TRES (as observed by Durantini et al),[22] one does not expect decay profiles of this kind in the case of an excited state reaction. The fact that the time-resolved behavior, depicted in Fig. 5.7, is strikingly similar for AP and N-BuAP suggests immediately that the emission of AP in aqueous media does not originate from the enol form. The nature of the decay profiles is indicative of the presence of two

separate emitting species that are not related through an excited state reaction. Had the two species been related through an excited state reaction, one would have observed a rise component in the fluorescence time profiles monitored at longer wavelengths. It is also understood why the TRES do not shift much with time and it is only during 2-4 ns the shift is observed.

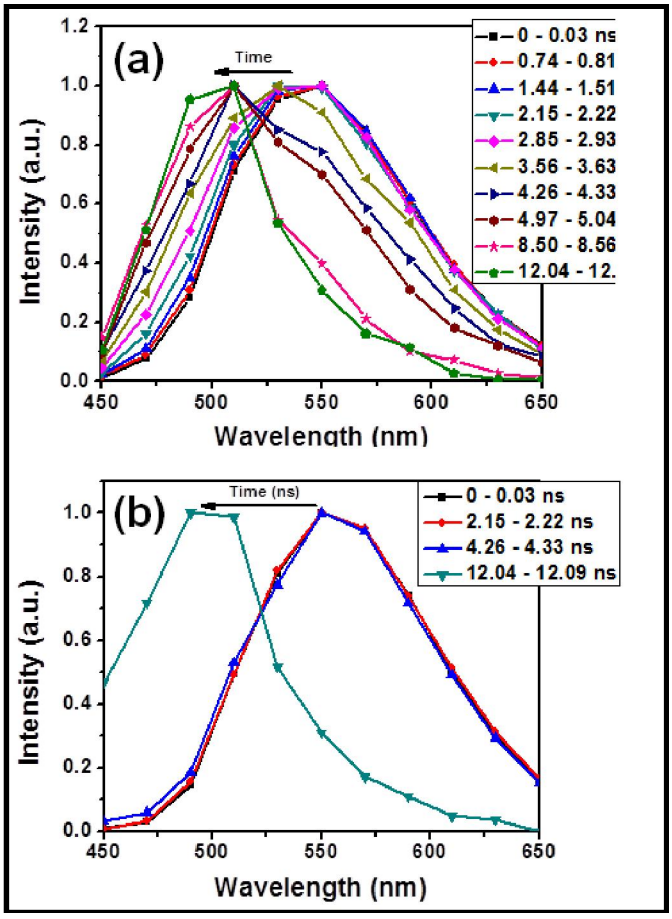

Figure 5.7. Time-resolved emission spectra of (a) AP and (b) N-BuAP in water (λ_{ex} = 375 nm).

Here we attempt to find out possible origin of the two lifetime components in water. The fluorescence quantum yield and lifetime of AP in polar media depend on the hydrogen bond donating/accepting ability of the solvents.[18] These values are low in polar protic solvents and is minimum in water.[11,13,18] The low values in polar protic solvents are believed to be due to stabilization of the emitting state of the system arising from strong hydrogen bonding interaction of AP with the solvent and consequent increase in the nonradiative rate of the emitting state. Two different kinds of hydrogen bonding interaction (Scheme 5.2.) are documented in the literature.[18] The most common being hydrogen bond formation between the carbonyl oxygen of AP and hydrogen bond donating protic solvents such as hexafluoroisopropanol, trifluoroethanol, which leads to a red shift of the emission maximum and decrease in fluorescence quantum yield and lifetime values.[18] Another hydrogen bonding interaction that is possible between the amino hydrogen of AP and hydrogen bond accepting solvents such as DMSO, leads to an increase in fluorescence quantum yield and lifetime.[18] The solvents such as alcohols and water, which can serve both as H-bond donor and acceptor,[43] can therefore interact with AP through both kinds of hydrogen bond formation (Scheme 5.2.). As the hydrogen bonding interaction with the amino moiety leads to a blue shift and that with the carbonyl moiety results in a red shift of the emission spectrum, when one monitors at wavelengths corresponding to the blue side of the spectrum, the molecules hydrogen-bonded at the amino end (and are characterized by long lifetime) contribute more to the fluorescence. On the other hand, as one moves towards the longer wavelength the contribution due

to hydrogen bonded species with the carbonyl moiety dominates and one observes only the species with short lifetime.

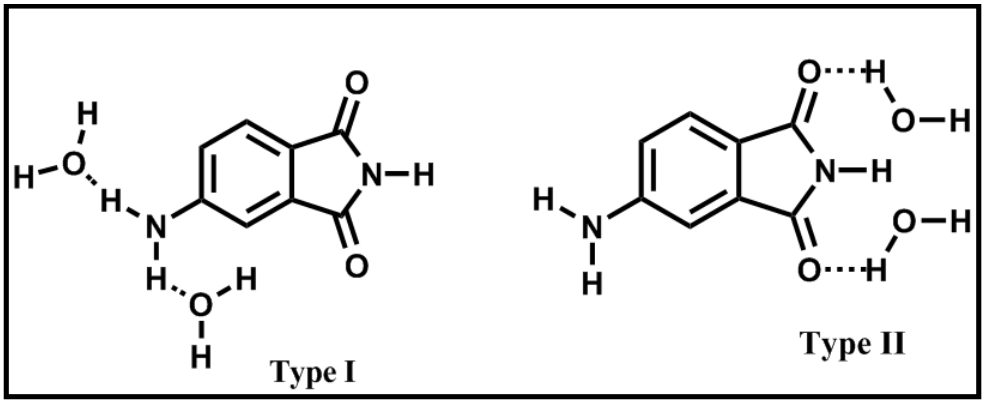

Scheme 5.2.

5.6. Conclusion

We have convincingly established in this paper that solvent-mediated excited state proton transfer reaction does not contribute to the fluorescence behavior of AP and its derivatives. We have also shown that the time-dependent blue shift of the fluorescence spectrum of AP in aqueous media, which is recently presented as evidence in support of the water-mediated excited state keto-enol transformation of the molecule, arises simply because of the presence of two different types of hydrogen bonded species of AP having distinctly different fluorescence lifetimes in the aqueous media. The isotope effect on the fluorescence properties of AP and its derivative is explained in terms of the difference of the influence of two isotopes on the nonradiative rates of the systems. It is suggested that ground state exchange of the amino hydrogen of the systems with the solvent can also contribute to the isotope effect.

Reference

(1) Ware, W. R.; Lee, S. K.; Brant, G. J.; Chow, P. P. *J. Chem. Phys.* **1971**, *54*, 4729.

(2) Suppan, P. *J. Chem. Soc. Faraday Trans. 1* **1987**, *83*, 495.

(3) Noukakis, D.; Suppan, P. *J. Lumin.* **1991**, *47*, 285−295.

(4) Soujanya, T.; Krishna, T. S. R.; Samanta, A. *J. Photochem. Photobioi. A: Chem.* **1992**, *66*, 185.

(5) Soujanya, T.; Krishna, T. S. R.; Samanta, A. *J. Phys. Chem.* **1992**, *96*, 8544.

(6) Saroja, G.; Samanta, A. *Chem. Phys. Lett.* **1995**, *246*, 506.

(7) Harju, T. O.; Huizer, A. H.; Varma, C. A. G. O. *Chem. Phys.* **1995**, *200*, 215.

(8) Soujanya, T.; Fessenden, R. W.; Samanta, A. *J. Phys. Chem.* **1996**, *100*, 3507.

(9) Yuan, D.; Brown, R. G. *J. Phys. Chem. A* **1997**, *101*, 3461.

(10) Saroja, G.; Soujanya, T.; Ramachandram, B.; Samanta, A. *J. Fluoresc.* **1998**, *8*, 405.

(11) Saroja, G.; Samanta, A. *J. Chem. Soc., Faraday Trans.* **1996**, *92*, 2697.

(12) Laitinen, E.; Salonen, K.; Harju, T. *J. Chem. Phys.* **1996**, *104*, 6138.

(13) Das, S.; Datta, A.; Bhattacharyya, K. *J. Phys. Chem. A* **1997**, *101*, 3299.

(14) Saroja, G.; Samanta, A. *J. Chem. Soc., Faraday Trans.* **1998**, *94*, 3141.

(15) Saroja, G.; Ramachandram, B.; Saha, S.; Samanta, A. *J. Phys. Chem. B* **1999**, *103*, 2906.

(16) Datta, A.; Das, S.; Mandal, D.; Pal, S. K.; Bhattacharyya, K. *Langmuir* **1997**, *13*, 6922.

(17) Wetzler, D. E.; Chesta, C.; Fernandez-Prini, R.; Aramendıa, P. F. *J. Phys. Chem. A* **2002**, *106*, 2390.

(18) Krystkowiak, E.; Dobek, K.; Maciejewski, A. *J. Photochem. & Photobio. A: Chem.* **2006**, *184*, 250.

(19) Dobek, K. *Photochem. Photobiol. Sci.* **2008**, *7*, 361.

(20) Dobek, K.; Karolczak, J.; Komar, D. *J. Phys. Chem. A* **2012**, *116*, 6655−6663.

(21) Maciejewski, A.; Krystkowiak, E.; Koput, J.; Dobek, K. *ChemPhysChem* **2011**, *12*, 322

(22) Durantini, A. M.; Falcone, R. D.; Anunziata, J. D.; Silber, J. J.; Abuin, E. B.; Lissi, E. A.; Correa, N. M. *J. Phys. Chem. B* **2013**, *117*, 2160−2168.

(23) Khara, D. C.; Samanta, A. *J. Phys. Chem. B* **2013**, *117*, 5387.

(24) Durantini, A. M.; Falcone, R. D.; Anunziata, J. D.; Silber, J. J.; Abuin, E. B.; Lissi, E. A.; Correa, N. M. *J. Phys. Chem. B* **2013**, *117*, 5389−5391.

(25) Durantini, A. M.; Falcone, R. D.; Anunziata, J. D.; Silber, J. J.; Abuin, E. B.; Lissi, E. A.; Correa, N. M. *J. Phys. Chem. B* **2013**, *117*, 5392−5392.

(26) Karmakar, R.; Samanta, A. *J. Am. Chem. Soc.* **2001**, *123*, 3809.

(27) Maciejewski, A.; Kubicki, J.; Dobek, K. *J. Phys. Chem. B* **2003**, *107*, 13986.

(28) Mukherjee, S.; Sahu, K.; Roy, D.; Mondal, S. K.; Bhattacharyya, K. *Chem. Phys. Lett.* **2004**, *384*, 128.

(29) Maciejewski, A.; Kubicki, J.; Dobek, K. *J. Phys. Chem. B* **2005**, *109*, 9422.

(30) Mondal, S. K.; Roy, D.; Sahu, K.; Sen, P.; Karmakar, R.; Bhattacharyya, K. *J. Photochem. Photobiol., A: Chem.* **2005**, *173*, 334.

(31) Samanta, A. *J. Phys. Chem. B* **2006**, *110*, 13704.

(32) Maciejewski, A.; Kubicki, J.; Dobek, K. *J. Colloid. Interface. Sci.* **2006**, *295*, 255−263.

(33) Wang, R.; Hao, C.; Li, P.; Wel, N.-N.; Chen, J.; Qiu, J. *J. Comput. Chem.* **2010**, *31*, 2157.

(34) Samanta, A. *J. Phys. Chem. Lett.* **2010**, *1*, 1557.

(35) Khara, D. C.; Kumar, J. P.; Mondal, N.; Samanta, A. *J. Phys. Chem. B* **2013**, *117*, 5156.

(36) Chapman, C. F.; Fee, R. S.; Maroncelli, M. *J. Phys. Chem.* **1995**, *99*, 4811.

(37) Dresner, J.; Prochorow, J.; Sobolewski, A. *Chem. Phys. Lett.* **1978**, *54*, 292

(38) Mirbach, M. J.; Mirbach, M. F.; Cherry, W. R.; Turro, N. J.; Engel, P. *Chem. Phys. Lett.* **1978**, *53*, 266.

(39) Lakowicz, J. R. *Principles of Fluorescence Spectroscopy*, Third Edition ed.; Springer Science Business Media: New York, **2006**.

(40) Forster, T.; Rokos, K. *Chem. Phys. Lett.* **1967**, *1*, 279.
(41) Robinson, G. W.; Frosch, R. P. *J. Chem. Phys.* **1962**, *37*, 1962
(42) Muller, P.-A.; Hogemann, C.; Allonas, X.; Jacques, P.; Vauthey, E. *Chem. Phys. Lett.* **2000**, *326*, 321.
(43) Kamlet, M. J.; Abboud, J.-L. M.; Abraham, M. H.; Taft, R. W. *J. Org. Chem.* **1983**, *48*, 2877.

Chapter 6

Laser Flash Photolysis Study on 9-Phenylxanthenium Tetrafluoroborate: Identification of New Features Attributed to the Triplet State of the System

This chapter deals with laser flash photolysis studies on a highly fluorescent and stable salt of 9-phenylxanthenium cation in neutral environment. A new transient absorption band of this extensively studied system that most probably remained buried under the fluorescence envelope and hitherto undetected has been identified and attributed to the triplet state of the system. The newly identified triplet–triplet absorption band of 9-phenylxanthenium cation, which is insensitive to oxygen and appears in the visible region, is well-separated from the absorption bands of 9-phenylxanthenyl radical or 9-phenylxanthenol triplet and hence, interference from these species has been avoided.

6.1. Introduction

The carbocation intermediates are of considerable interest in physical and organic chemistry.[1-6] 9-Phenylxanthenium cation (**PX+**) is a highly fluorescent and fairly stable species, whose photophysical properties have received noticeable attention.[7-13] **PX+** can be generated from 9-phenylxanthenol (**PX**) in acidic environment ($\mathbf{pK_{R+}}$ = 1.0 ± 0.5 for **PX** in water) (Scheme 6.1.) [8,14,15] or by photoexcitation of **PX** in polar (hydroxylic) solvent, where it undergoes adiabatic dehydroxylation in the excited state surface.[9,10,15]

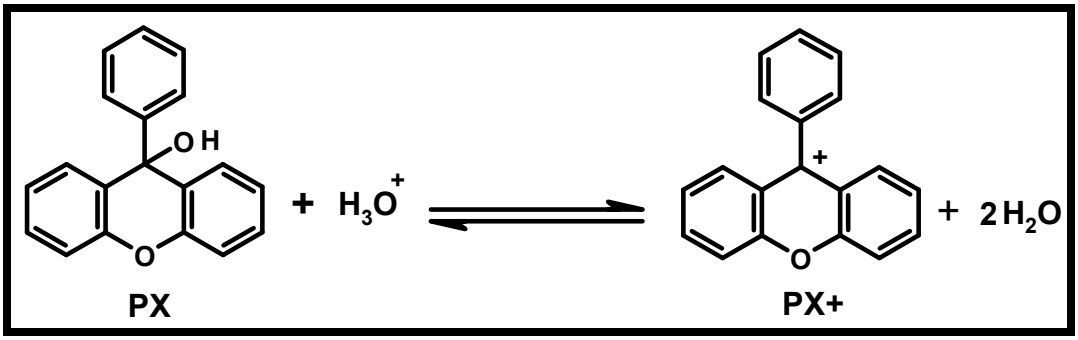

Scheme 6.1.

Wan et al. have shown that in the pH range of 3-12 water acts as a catalyst in this photoinduced reaction and the quantum yield of formation of **PX**+ is 0.4 in 1:1 acetonitrile/water.[8,15] However, the catalytic activity of water was not quantitative due to efficient quenching of the singlet excited states of both **PX** and **PX**+ by water and the ground state interaction between **PX** and water. **PX**+ can also be obtained as a stable species in other acidic environment such as in nafion flims and zeolite matrices.[10] The driving force of adiabatic dehydroxylation of **PX** is its enhanced basicity in the excited state and strong conjugation of the oxygen lone pair to the aromatic system. Although **PX**+ is less reactive in the ground state, considerable increase of its electrophilicity is observed in the singlet excited state.[5] The reactivity of **PX**+ in the first excited singlet state toward a series of alcohols, amines and ethers has been measured by monitoring the strong fluorescence of the system.[11,16] The fluorescence quenching rate constants have been found to lie between 10^7 and 10^{10} M^{-1} s^{-1}. [5,11,16] As an electron deficient system, photoexcited **PX**+ undergoes electron transfer reaction with a wide variety of aromatic donor molecules producing 9-phenylxanthenyl radical.[10,13]

The rate constants of photoinduced electron transfer reactions, which have also been measured by monitoring the quenching of fluorescence, are close to the diffusion limited values. However, the yield of net electron transfer (Φ_{et}) process is found to be very small (≤ 0.02) due to efficient back electron transfer reaction between the products of the photoinduced electron transfer reactions, i.e., 9-phenylxanthenyl radical and radical cation of the corresponding reactant. Even though the singlet excited state of **PX+** has been studied extensively by monitoring the fluorescence of the system, barring a couple of papers by Johnston and Wong,[17,18] there is hardly any literature dealing with the triplet state of this system. In these papers, the authors have characterized the triplet-triplet absorption spectra of **PX+** by generating this species from **PX** in the presence of varied concentrations (1-10 mM) of trifluoroacetic acid.[17,18] They found that the triplet-triplet absorption due to **PX+** shows maximum at < 300 nm and is characterized by a lifetime of several microseconds. The exact lifetime depends on the concentration of **PX** in the medium (which can be varied by adjusting the concentration of the added acid) as **PX+** triplet undergoes electron transfer reaction with **PX** and produces 9-phenylxanthenyl radical, which can be characterized by the 340 nm band in the transient absorption spectrum.[17,18] This triplet state of **PX+** can also undergo electron transfer reaction with several arene molecules.[18] The lack of studies involving the triplet state of **PX+** can partly be attributed to strong fluorescence quantum yield of the species, which is reported to be 0.8 in 2,2,2-trifluoroethanol,[18] a value much higher than 0.42 reported by Minto and Das (in acetonitrile containing 8% H_2SO_4).[8] A high fluorescence quantum yield of the system not only implies a low yield of the triplet, but the fact

that the intense and broad fluorescence covers a large portion of the visible region makes observation of transient absorption due to triplet, if any, in this region a difficult exercise indeed. Minto and Das further pointed out that in addition to high fluorescence yield of **PX+**, rapid electron transfer between the parent alcohol and singlet excited state of **PX+** is responsible for the absence of triplet **PX+**.[8] Herein, we attempt to probe the triplet state of **PX+** by following a different strategy. Unlike the earlier studies, which were performed on *in situ* generated **PX+** (from **PX**) in acidic environments, we have investigated here the triplet excited state of **PX+** in nonaqueous medium and in neutral condition by preparing a stable borate salt of the cation.

6.2. Absorption and emission behavior

The absorption spectrum of yellow coloured acetonitrile solution of 9-phenylxanthenium tetrafluoroborate is shown in Fig. 6.1. The spectrum consists of a broad band with maximum ~ 445 nm ($\varepsilon_{max}/ 10^3$ M^{-1} cm^{-1} = 4.7) and relatively sharp and intense peaks at ~ 372 nm (31.9) and 259 nm (44.4). These spectral features are consistent with the literature data.[7-11,14,19] The emission spectrum of the system is characterized by a broad structureless band between 470 and 700 nm, with maximum around 540 nm. This emission behavior is also very similar to that of an acetonitrile solution of **PX** acidified with 8-10% H_2SO_4 or with 6.5 M TFA, as reported earlier.[7-11,14,19] The measurement of the emission decay profile and its analysis reveal that in acetonitrile the salt exhibits a single exponential decay with lifetime of 29 ns, a value which is comparable to the literature value of **PX+**.[7,8,10]

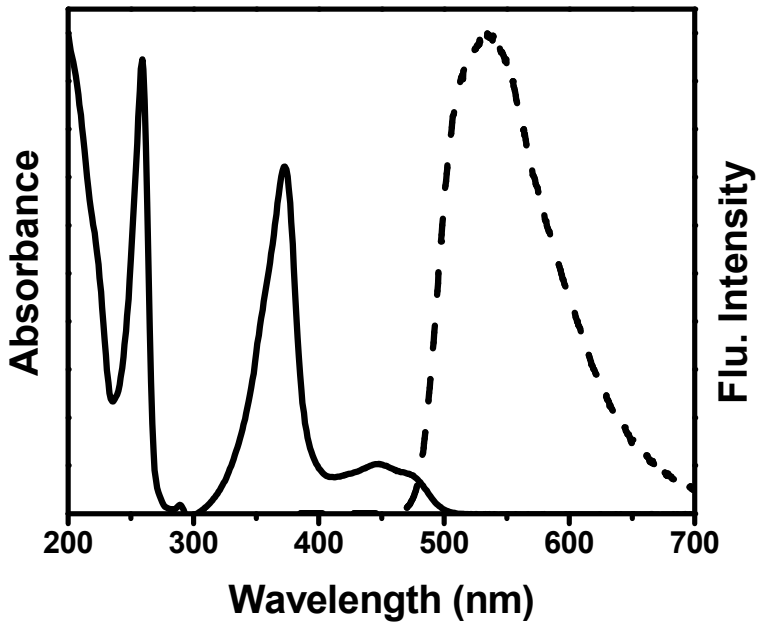

Figure 6.1. UV-vis absorption (solid line) and steady state fluorescence spectra (dashed line) of 9-phenylxanthenium tetrafluoroborate in acetonitrile (not scaled). λ_{exc} 450 nm, for fluorescence measurements.

6.3. Transient behavior

The transient absorption spectra of 9-phenylxanthenium tetrafluoroborate at early times (Fig. 6.2.) consist primarily of a negative signal in the wavelength range of 400 - 700 nm. An inspection of the steady state absorption and emission spectra of **PX+** suggests that strong negative signal in the 470 – 700 nm range is due to its fluorescence and relatively small negative signal between 400 and 470 nm is due to the ground state bleaching. The decay profile measured at 530 nm, and is shown as an insert to Fig. 6.2 (a), yielded a lifetime of 29 ns, which is the same as the fluorescence lifetime obtained from the single photon counting measurements.[8,10] Interestingly, when the same wavelength region is probed at a

later time (when the fluorescence has decayed completely), one can observe an absorption band (480 – 600 nm) which is centered around 510 nm (Fig. 6.2 (b)). We were really surprised how a strongly absorbing species like this one could be missed by others, particularly when taken into consideration the large number of investigations made on **PX**+.[7-13,15,20]

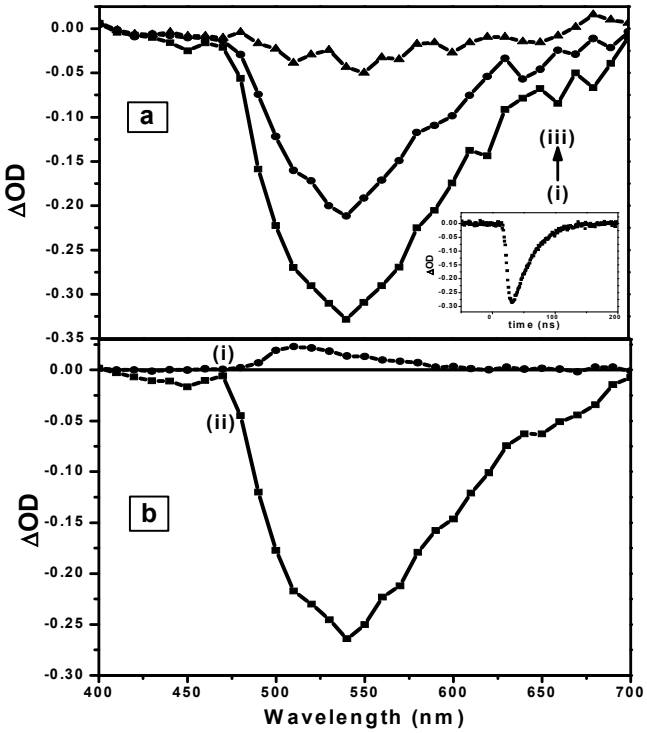

Figure 6.2. (a) Transient absorption spectra of 9-phenylxanthenium tetrafluoroborate in acetonitrile, recorded at t = 0 (i), 20 ns (ii) and 60 ns (iii) after 355 -nm laser pulse excitation. The inset shows the decay profile of the 530 nm emission band. (b) Transient absorption spectra at 8 ns (i) and at 100 ns (ii) following the 355 -nm laser pulse excitation of 9-phenylxanthenium tetrafluoroborate in acetonitrile.

We carried out several control experiments to establish that this transient species is indeed a real one and not due to any impurities in the salt or in the solvents used in the experiments. Moreover, we generated **PX+** from an acetonitrile solution of **PX** by adding trifluoroacetic acid (the way earlier studies were conducted) and confirmed that the transient absorption behavior of the resulting solution is also very similar to that observed with the salt solution.[7,9-11,13,20] We soon figured out that this band was probably overlooked or missed due to the strong fluorescence emission that dominates in this region, particularly in the early time scale. This transient, as depicted in Fig. 6.3., survives for a reasonably long time. The lifetime of the species is estimated to be ~ 2.1 μs under the experimental conditions.

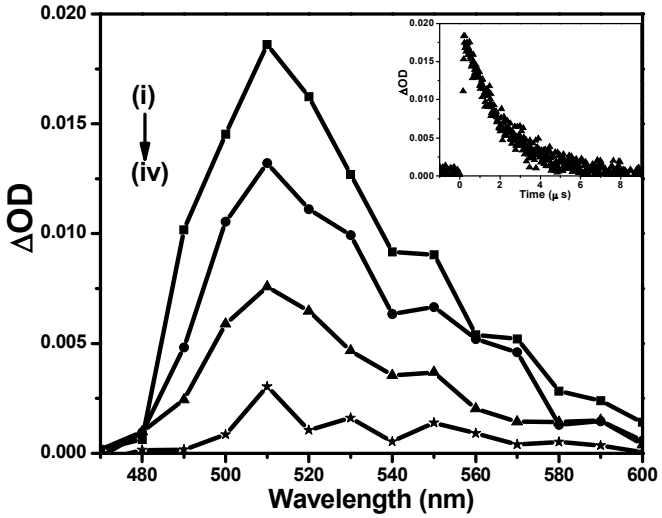

Figure 6.3. Transient absorption spectra of 9-phenylxanthenium tetrafluoroborate in acetonitrile recorded at t = 0 (i), 0.65 μs (ii), 1.7 μs (iii), 5.2 μs (iv) after 355 -nm laser pulse excitation. The inset shows the decay profile at 510 nm for the triplet-triplet absorption.

6.4. Nature of the transient species

This transient species responsible for this new absorption band can be 9-phenylxanthenyl radical, triplet state of **PX** or triplet state of **PX+**. The first two possibilities can be ruled out based on literature. Minto and Das reported that the 9-phenylxanthenyl radical absorbs around 345 nm and is a fairly long-lived species (~ 150 μs in air saturated n-heptane) and the triplet of **PX** exhibits an absorption maximum at ~ 440 nm with a lifetime of $\tau_T \leq 0.3$ μs in acetonitrile.[8] As the new transient absorption is neither due to 9-phenylxanthenyl radical nor is it due to the triplet of **PX**, it must be attributed to the triplet of **PX+**. This assignment is confirmed by expanding the wavelength range of the transient absorption spectrum (Fig. 6.4.) and by observing another band ~ 300 nm, which is previously characterized as a triplet-triplet absorption band of **PX+**[17,18] and whose decay behavior is almost identical with that of the newly observed 510 nm band (inset of Fig. 6.4). The triplet nature of the transient is further confirmed by studying the effect of ethyl iodide (a heavy atom containing molecule) on the transient absorption band and on the fluorescence behavior of the molecule. It is found that addition of ethyl iodide leads to significant reduction of the fluorescence lifetime of **PX+** and quenching of the lifetime of the transient species along with a decrease of the ΔOD value. The former is clearly a reflection of the enhancement of $S_1 - T_1$ intersystem crossing rate and the latter is indicative of the enhancement of the decay of the T_1 state.

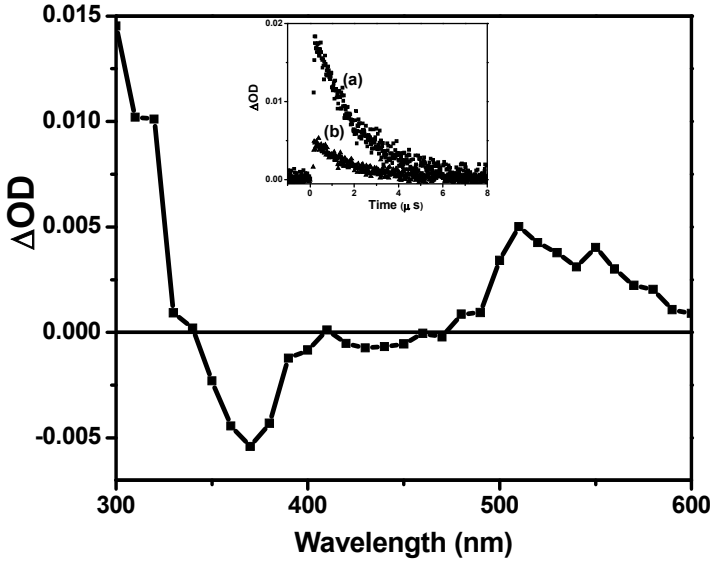

Figure 6.4. Transient absorption spectrum of 9-phenylxanthenium tetrafluoroborate in acetonitrile recorded 1 μs after 355 nm laser pulse excitation. The inset shows the comparison between the decay profiles at 300 nm (a) and 510 nm (b).

6.5. Effect of oxygen

Even though the fluorescence lifetime of **PX+** is quite long, it is quite insensitive to molecular oxygen.[8,10] The oxygen quenching rate constant ($k_q < 5 \times 10^8$ M^{-1} s^{-1}) is much smaller than those observed for the singlet state of other hydrocarbons (typically of the order of 10^{10} M^{-1} s^{-1}).[8] The transient species contributing to the new absorption ~ 510 nm, which we attribute to the triplet state of **PX+**, is also reluctant to interact with oxygen (Fig. 6.5.). On purging oxygen gas, the lifetime of the triplet state reduces from 2.1 μs to 1.8 μs. The rate constant (k_T) of quenching of the triplet state by molecular oxygen, estimated by using the relation, $k_T = 1/\tau_T [O_2]$,[21] where τ_T is the lifetime of the species undergoing triplet-triplet absorption equilibrated with air and $[O_2]$ is the

concentration of oxygen in solution, is found to be 1.8 X 10^8 $M^{-1}s^{-1}$ in acetonitrile (assuming $[O_2]$ ~3 mM under air saturation).[22] This behavior, i.e., oxygen quenching rate constant of **PX+** triplet to be smaller than the observed diffusion controlled values (~ 10^{10} M^{-1} s^{-1}), is in accordance with the literature.[22] Even though the triplet state energy of molecular oxygen is much lower than that of **PX+** (48 kcal/mol),[17] the energy transfer between the two is not favoured as the process requires formation of a charge transfer complex in which the electron deficient species, **PX+** has to serve as an electron donor.[11]

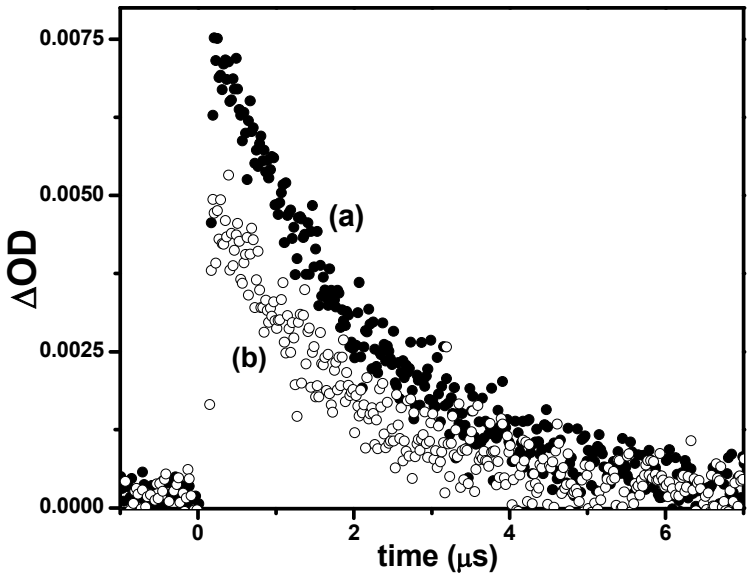

Figure 6.5. The triplet absorption decay profiles at 520 nm of (a) deoxygenated by purging argon gas and (τ_T = 2.05 μs), (b) oxygen saturated solution (τ_T = 1.81 μs) of 9-phenylxanthenium tetrafluoroborate in acetinitrile.

6.6. Triplet-triplet energy transfer

One of the methods of characterization of the triplet state of a species and determination of the triplet state parameters such as the extinction coefficient (ε_T) and quantum yield (Φ_T) is by triplet-triplet energy transfer process, in which the energy is transferred from the excited triplet state of the donor molecule to the triplet state of the acceptor. In order to characterize the newly observed band, we attempted sensitization of the triplet state of **PX+** using several donor molecules with high triplet energies. Among the sensitizers chosen, benzophenone and thioxanthone were expected to be quite appropriate for their high triplet energies,[23-25] but we encountered problems due to trace quantity of moisture induced generation of **PX** (*vide* Scheme 6.1.) during the addition of the sensitizer presumably because we avoided using any acid and preferred working with an acetonitrile solution of the 9-phenylxanthenium tetrafluoroborate salt. As, a solution of **PX** in 25% H_2SO_4 consists entirely of the cation,[16] we attempted sensitization of **PX+** triplet in acidic environment as well. However, in acidic environment, as commonly used high-energy sensitizers like benzophenone or thioxanthone, formed ketyl radicals from their triplet state, triplet sensitization of **PX+** was no longer possible. To circumvent this problem, we tried the arenes as sensitizers as these are not so much affected in acidic environment. However, high energy arenes such as naphthalene cannot be excited at 355 nm (excitation wavelength) and for other low energy arenes even though it was possible to adjust the concentration of the species to ensure that the donor to absorb 80-90% light, we could not avoid a situation in which direct excitation of **PX+** was completely avoided. Secondly, these arenes are electron rich compounds, which undergo

facile electron transfer reaction with electron deficient **PX**+.[9,10] Hence, this excited state reaction between arenes and **PX**+ competes with the triplet-triplet energy transfer process. Thus sensitizers like phenanthrene, triphenylene, coronene, fluoranthene, which possess high triplet energy, did not serve as donor in the triplet-triplet energy transfer process. We are searching for a suitable sensitizer for the triplet of **PX**+.

6.7. Conclusion

This laser flash photolysis study on 9-phenylxanthenium tetrafluoroborate in neutral medium reveals a new feature that is attributed to the somewhat elusive triplet state of **PX**+. The newly identified triplet-triplet absorption band of **PX**+, which is insensitive to oxygen and appears in the visible region, is well separated from the absorption bands of 9-phenylxanthenyl radical or **PX** triplet and hence, interference from these species is avoided. The finding is thus expected to be helpful in the exploration of the triplet state properties and a better understanding of the photochemistry of **PX**+.

References

(1) Azarani, A.; Berinstain, A. B.; Johnston, L. J.; Kazanis, S. *J. Photochem. Photobiol. A: Chem* **1991**, *57*, 175.

(2) Bartl, J.; Steenken, S.; Mayr, H.; McClelland, R. A. *J. Am. Chem. Soc* **1990**, *112*, 6918.

(3) Johnston, L. J.; Kanigan, T. *J. Am. Chem. Soc* **1990**, *112*, 1271.

(4) McClelland, R. A.; Kanagasabapathy, V. M.; Banait, N. S.; Steenken, S. *J. Am. Chem. Soc* **1991**, *113*, 1009.

(5) Mecklenburg, S. L.; Hilinski, E. F. *J. Am. Chem. Soc* **1989**, *111*, 5471.

(6) Wan, P.; Krogh, E. *J. Am. Chem. Soc* **1989**, *111*, 4887.

(7) Boyd, M. K.; Lai, H. Y.; Yates, K. *J. Am. Chem. Soc.* **1991**, *113*, 7294.

(8) Minto, R. E.; Das, P. K. *J. Am. Chem. Soc* **1989**, *111*, 8858.

(9) Samanta, A.; Gopidas, K. R.; Das, P. K. *Chemical Physics Letters* **1990**, *167*, 165.

(10) Samanta, A.; Gopidas, K. R.; Das, P. K. *J. Phys. Chem.* **1993**, *97*, 1583.

(11) Valentino, M. R.; Boyd, M. K. *J. Org. Chem.* **1993**, *58*, 5826.

(12) Bedlek, J. M.; Valentino, M. R.; Boyd, M. K. *J. Photochem. Photobiol. A: Chem* **1996**, *94*, 7.

(13) Samanta, A.; Gopidas, K. R.; Das, P. K. *Chemical Physics Letters* **1993**, *204*, 269.

(14) Feldman, M. R.; Thame, N. G. *J. Org. Chem.* **1979**, *44*, 1863.

(15) Wan, P.; Yates, K.; Boyd, M. K. *J. Org. Chem.* **1985**, *50*, 2881.

(16) McClelland, R. A.; Banait, N.; Steenken, S. *J. Am. Chem. Soc.* **1989**, *111*, 2929.

(17) Johnston, L. J.; Wong, D. F. *Can. J. Chem.* **1992**, *70*, 280.

(18) Johnston, L. J.; Wong, D. F. *J. Phys. Chem.* **1993**, *97*, 1589.

(19) Berger, R. M.; Weir, D. *Chemical Physics Letters* **1990**, *169*, 213.

(20) Samanta, A.; Bhattacharyya, K.; Das, P. K.; Kamat, P. V.; Weir, D.; Hug, G. L. *J. Phys. Chem* **1989**, *93*, 3651.

(21) Kruk, N. N.; Nichiporovich, I. N. *Journal of Applied Spectroscopy* **2004**, *71*, 343.

(22) Murov, S. L. *Handbook of Photochemistry*; Marcel Dekker: New York, **1973**.
(23) Lewis, G. N.; Kasha, M. *J. Am. Chem. Soc* **1944**, *66*, 2100.
(24) Wilkinson, F. *J. Phys. Chem* **1962**, *66*, 2569.
(25) Herkstroeter, W. G.; Lamola, A. A.; Hammond, G. S. *J. Am. Chem. Soc* **1964**, *86*, 4537.

Chapter 7

Characterization of the Triplet State of Ellipticine and Solvent Dependent Triplet Energy Transfer Process Monitored by Laser Flash Photolysis

This chapter is focused on the characterization of the triplet excited state of ellipticine in different solvents by using laser flash photolysis technique. The various triplet state parameters (extinction coefficient and quantum yield) of the molecule are estimated by triplet-triplet energy transfer and relative actinometry technique. Interestingly, even though in polar aprotic solvent acetonitrile, the triplet-triplet energy transfer from thioxanthone to ellipticine is observed, the process is found to be inefficient in nonpolar methylcyclohexane. This observation is attributed to the dependence of triplet state energy on the solvent polarity, which is confirmed by low-temperature phosphorescence studies. In methylcyclohexane, the triplet-triplet energy transfer process is observed between xanthone (having higher triplet state energy) and ellipticine. Nearly 4-fold decrease in the triplet extinction coefficient and a noticeable increment in the triplet quantum yield of ellipticine are found on changing the solvent from polar acetonitrile to nonpolar methylcyclohexane. Studies in 1,1,1,3,3,3-hexafluoro-2-propanol reveal complete ground state protonation of ellipticine thereby producing transient of ellipticinium cation. However, in 2,2,2-trifluoroethanol, where both neutral and cationic forms are present in the ground state, sensitized triplet absorption spectrum resembles that of neutral ellipticine only.

7.1. Introduction

Ellipticine (5,11-dimethyl-6H-pyrido[4,3-b]carbazole), known to exhibit antitumor and anti-HIV activity,[1] was discovered as a potent anti-cancer drug in early sixties, but its use of this drug was limited.[2-4] High cytotoxicity of ellipticine made the molecule very interesting to the biomedical chemists in the initial years of its discovery. Most of the research work involving ellipticine was about its biological activity, sequence selectivity, metabolism, binding interactions etc.[5-15] Difficulty arises in its in vivo use as the drug is almost insoluble in water. With the help of modern drug delivery systems, the poorly soluble drug can be transferred to the target site by help of polymer based nanoparticles, peptides, micelles and liposomes.[1,16-22] This kind of carriers not only enhanced the therapeutic efficiency of this drugs but also circumvented the toxicity towards the normal cells. Mode of pharmacological action of ellipticine is very complex indicating several mechanisms involving DNA intercalation, inhibition of Topoisomerase II, Inhibition of RNA polymerase I transcription etc.[23,24] Recently, the photophysical studies on this drug have attracted a great deal of attention of many chemists. Photophysical and photodynamic properties of ellipticine have not only been studied in aqueous and conventional organic solvents, the reverse micelles and bile salts are also used.[22,25,26]

Ellipticine, which contains both proton donating and accepting sites, exhibits very interesting fluorescence properties in different solvents. In neutral aqueous medium, ellipticine exists in both neutral and cationic forms (pK_a = 7.4) and shows dual fluorescence. Chen and co-workers have reported photophysical properties of ellipticine in different organic solvents of varying polarity.[25] The

authors have reported solvent dependent absorption and emission spectral changes.[27] Specific hydrogen bonding effect between ellipticine and alcoholic solvents leads to more pronounced shift in emission maxima and longer fluorescence lifetime compared to non-alcoholic solvents. It is also reported that ellipticine exhibits a second fluorescence band in methanol.[25] Even though the dual fluorescence was attributed to two different forms of ellipticine, no attempt was made either to identify the two forms or to clarify the existence of two forms in ground or excited state. In Chapter 3, it is shown that the dual emission of ellipticine in methanol is due to the solvent-assisted excited state intramolecular proton transfer from the pyrrole nitrogen to the pyridine nitrogen.[27]

Understanding the triplet state properties of ellipticine is also very crucial. In a recent patent article ellipticine has been used as a photosensitizing agent in photodynamic therapy (PDT).[28,29] In generally accepted mechanism of PDT, photosensitizing drugs are accumulated in the malignant cells and then irradiated by light of appropriate wavelength and power. The photoexcited drug molecule reaches its triplet state through intersystem crossing and produces highly reactive singlet oxygen through triplet-triplet energy transfer (TET) process. This extremely reactive singlet oxygen destroys the malignant cells. As the triplet state of the photosensitizing drug is involved in the mode of action, a thorough knowledge of the triplet state is absolutely essential. Though some reports provide information on the singlet excited state of ellipticine,[25,27,30] studies involving the triplet state of the molecule can hardly be found in the literature. Görner et al. have thrown some light on the triplet state of ellipticine by monitoring the

quantum yield of singlet oxygen formation and this was the only literature found regarding the triplet state of ellipticine.[31]

In order to obtain details on the triplet state properties of ellipticine the present study is undertaken in which the triplet state of the molecule is characterized through both direct excitation and photosensitization processes. The experiments have been carried out using nanosecond laser flash photolysis technique and the studies are extended to solvents of different polarity. Different photosensitizers have been employed to estimate the triplet state extinction coefficient via triplet-triplet energy transfer process. Triplet quantum yield is determined using relative actinometry method employing benzophenone as the reference actinometer. The triplet state energy levels estimated through phosphorescence studies at low temperature further support the triplet-triplet energy transfer process

7.2. Transient Absorption Spectra

7.2.1. At Shorter Time Scale

In the shorter time scale, a negative signal was observed throughout the transient absorption spectra (300-600 nm) of ellipticine irrespective of the solvent. Representative transient absorption spectra in acetonitrile, recorded at different times in the nanosecond time regime, are shown in Figure 7.1. It is evident that the stimulated emission has major contribution towards the negative signal compared to the ground state bleaching. Polarity and specific hydrogen bonding ability of the solvent usually control the position of the emission band and the same is manifested in the present case of stimulated emission of ellipticine. The

fluorescence bleach recovery time obtained from the transient decay profile also matches with the fluorescence decay time in the respective solvents.

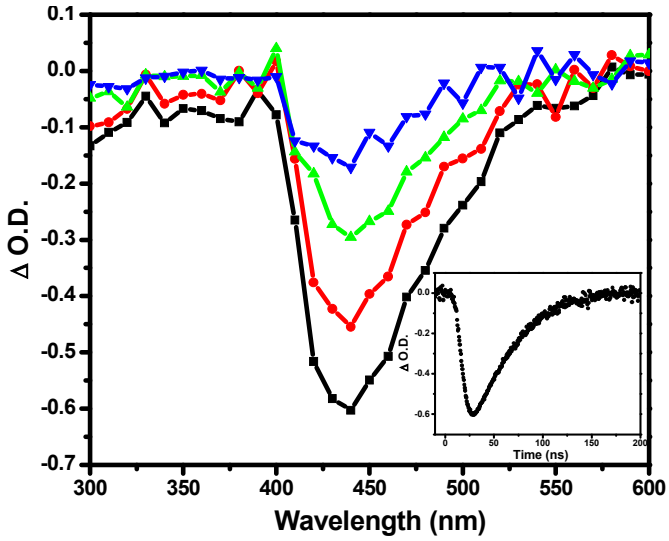

Figure 7.1. Transient absorption spectra of ellipticine in acetonitrile, recorded at t = 0 (i), 18 ns (ii), 30 ns (iii) and 50 ns (iv) after 355 nm laser pulse excitation. The inset shows the emission decay profile at 430 nm.

7.2.2. At Longer Time Scale

Transient absorption spectra at longer time scale of ellipticine mainly consist of two bands in the 300-400 nm and 500-600 nm regions in solvents of different polarity. The absorption decay profiles for two bands are quite similar, having lifetime ~ 10-20 μs, depending upon the solvent. Representative transient absorption spectra of ellipticine in methylcyclohexane, recorded at different times, are shown in Figure 7.2, which indicates a maximum at < 300 nm. As the polarity of the solvent increases, the triplet absorption maximum shifts towards longer wavelength. In polar solvent such as acetonitrile, the red shifted transient

absorption maximum is observed at 310 nm. The peak wavelengths observed in other media are tabulated in Table 7.1. The intensity of the 300-400 nm band is stronger compared to the 500-600 nm band. That both the transient bands are due to triplet-triplet absorption of ellipticine is evident from the facts that (i) purging of O_2 leads to the disappearance or a decrease of intensity of both the bands, (ii) same lifetime of the transient species at both the regions and (iii) triplet sensitization studies, which is discussed in the following sections.

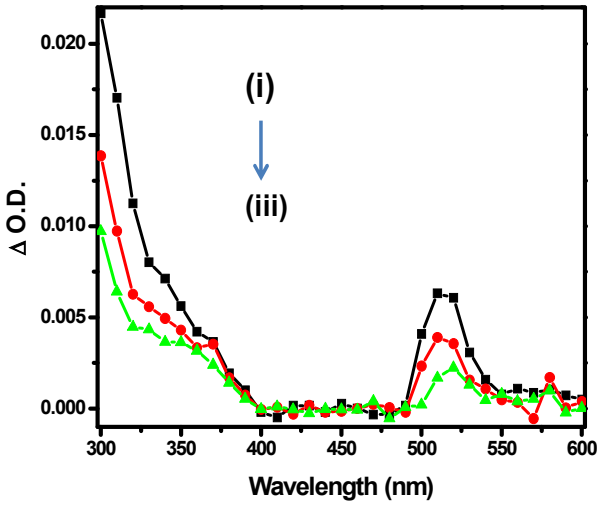

Figure 7.2. Transient absorption spectra of ellipticine in methylcyclohexane, recorded at t = 1.5 μs (i), 6.3 μs (ii) and 14 μs (iii) after 355 nm laser pulse excitation.

Table 7.1. Triplet state parameters of ellipticine in different solvents.

Solvent	E_T^N	λ_{max}^T (nm)	τ_T (μs)	ε_T(M^{-1} cm^{-1})	Φ_T
Methylcyclohexane	~0.006	< 300	10	0.9 X 10^3	0.37
Acetonitrile	0.460	310	15	3.1 X 10^3	0.26
Ethanol	0.654	317	21	4.7 X 10^3	0.15
TFE	0.898	340	40	0.1 X 10^3	
HFP	1.068	520	3		

7.3. Triplet Extinction Coefficient and Quantum Yield

7.3.1. Acetonitrile

Triplet quantum yield was determined by relative actinometry method that required the knowledge of triplet extinction coefficient, which was determined by a triplet-triplet energy transfer process where ellipticine served as the acceptor.

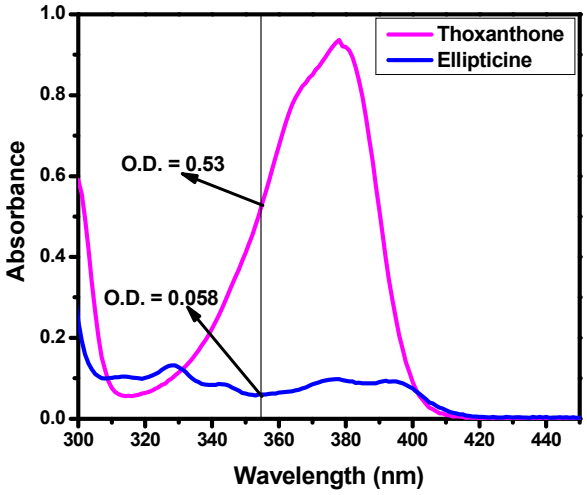

Figure 7.3. Absorption spectra of thioxanthone (1.2 X 10^{-4} M) and ellipticine (2.5 X 10^{-5} M) in acetonitrile.

Thioxanthone was chosen as the donor for its high triplet energy (E_T = 63.2 kcal/mol)[32] and the quenching of thioxanthone was assumed to be entirely dominated by exothermic triplet-triplet energy transfer process. Triplet energy transfer experiments were performed with solutions containing both energy donor and acceptor in a proportion that ensured that maximum of incident light (355 nm) was absorbed by the donor. Figure 7.3. represents the absorption spectra of thioxanthone and ellipticine used in triplet energy transfer process. The end of the pulse absorbance change $(\Delta OD)_o^R$ caused by thioxanthone triplet at 630 nm was compared with the absorbance change $(\Delta OD)_\infty$ of the sample at 360 nm and the triplet absorption decay of thioxanthone after addition of ellipticine was found to match with the rise of ellipticine triplet at 360 nm (Figure 7.4).

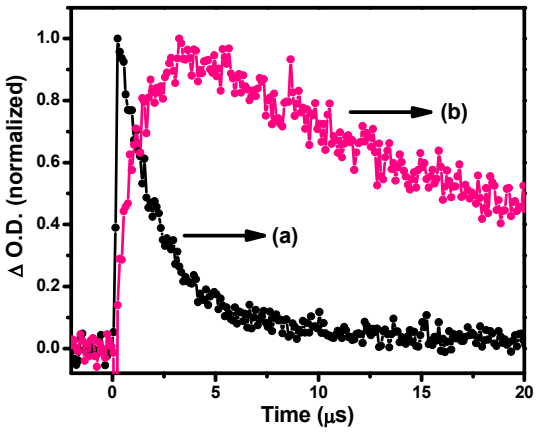

Figure 7.4. The triplet absorption decay profiles of (a) thioxanthone (1.2×10^{-4} M) monitored at 630 nm after addition of acceptor and (b) rise of ellipticine (2.5×10^{-5} M) monitored at 360 nm in acetonitrile after 355 nm laser pulse excitation.

The ε_T values were calculated using the following equation

$$\varepsilon_T - \varepsilon_S = \frac{\varepsilon_T^R (\Delta OD)_\infty k_{obs}}{(\Delta OD)_0^R (k_{obs} - k_0)}$$

where ε_T^R is the extinction coefficient of the thioxanthone triplet–triplet absorption (ε_T^R = 3 X 10^4 M^{-1} cm^{-1} at 630 nm),[32] ε_S is the ground state extinction coefficient of ellipticine (2.77 X 10^3 M^{-1} cm^{-1} at 360 nm)[25] and k_{obs} and k_0 are the rate constants for the decay of thioxanthone triplet in the presence and absence of ellipticine, respectively. The time-resolved absorption spectra of thioxanthone after addition of ellipticine were recorded at different time scales. Figure 7.5 shows, a time-dependent decrease in intensity of the transient absorption of the thioxanthone and a subsequent enhancement in intensity of the ellipticine absorption in the 350-400 nm and 500-565 nm regions. The sensitized transient absorption spectrum of ellipticne, which is presented in Figure 7.6, is found identical to that obtained on direct excitation.

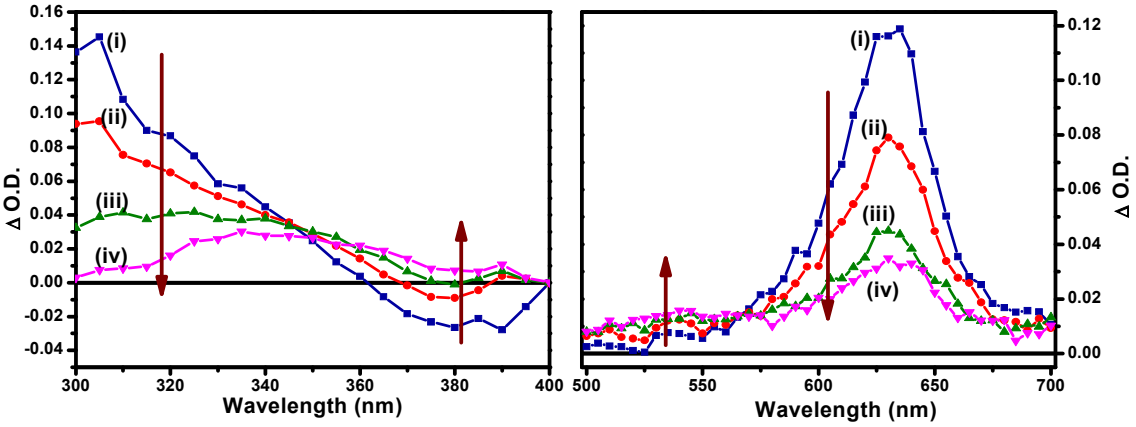

Figure 7.5. The transient absorption spectra obtained by 355 nm laser photolysis of thioxanthone (1.2×10^{-4} M) in the presence of ellipticine (2.5×10^{-5} M) in acetonitrile observed at t = 0 (i), 1.2 μs (ii), 2.8 μs (iii), 3.5 μs (iv).

After determining the triplet extinction coefficient, the triplet quantum yield (Φ_T) was determined by comparative actinometry method using benzophenone as a standard (ε_T^R = 6.2 X 10^3 M^{-1} cm^{-1} at 525 nm, Φ_T^R = 1).[32] Both ellipticine and benzophenone were excited at the same wavelength (355 nm) at which the absorbance values were maintained the same for both. The Φ_T value was calculated using the following equation

$$\Phi_T = \frac{\Phi_T^R (\Delta OD)_0 \varepsilon_T^R}{(\Delta OD)_0^R \varepsilon_T}$$

The end of pulse absorbance change $(\Delta OD)_0$ due to the triplet of ellipticine at λ_{max}^T (310 nm) was compared with $(\Delta OD)_0^R$ due to the benzophenone triplet at

525 nm. The values obtained for triplet extinction coefficient and triplet quantum yield of ellipticine in acetonitrile are tabulated in Table 7.1.

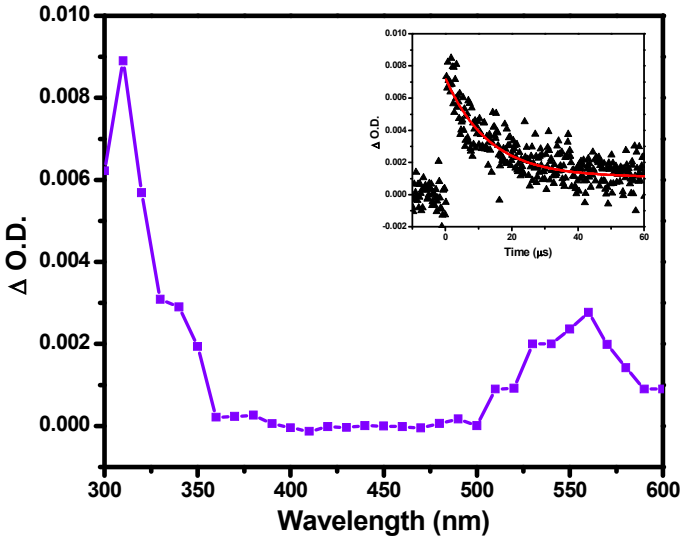

Figure 7.6. Sensitized transient absorption spectrum of ellipticine in acetonitrile obtained upon flash photolysis of thioxanthone in presence of ellipticine. The spectrum was monitored 5 μs following the excitation at 355 nm. The inset shows the decay profile at 310 nm.

7.3.2. Ethanol

Transient absorption spectrum of ellipticine in ethanol was found to be very similar to that in acetonitrile. The absorption peak in ethanol is found to be red-shifted by ~ 7 nm due to higher solvent polarity compared to acetonitrile as well as the hydrogen bonding ability of the alcohol. The estimated values of the molar extinction coefficient and triplet quantum yield in ethanol are tabulated in Table 7.1.

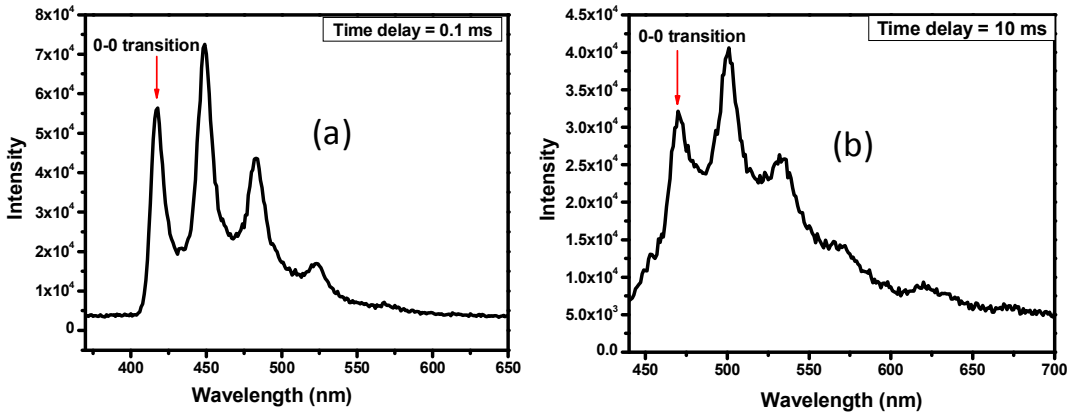

Figure 7.7. Phosphorescence spectra of ellipticine in (a) methylcyclohexane and (b) ethanol at 77 K by excitation at 290 nm.

7.3.3. Methylcyclohexane

Interestingly, in a nonpolar solvent like methylcyclohexane, the absorption due to thioxanthone sensitized triplet state of ellipticine could not be observed. No quenching of thioxanthone triplet in the presence of ellipticine also clearly suggests absence of energy transfer between the two species in methylcyclohexane. To understand this surprising observation, we have estimated the triplet state energies of ellipticine in different solvents from its low temperature phosphorescence spectra. In polar media, the 0-0 transition peak of the phosphorescence spectrum at liquid nitrogen temperature (77 K) provides a triplet state energy of 60.7 kcal/mol for ellipticine. This value is ~ 3 kcal lower than the triplet energy of thioxanthone. In methylcyclohexane glassy matrix at 77 K, the phosphorescence spectrum is found to be blue-shifted compared to polar glassy matrix formed from ethanol (Figure 7.7.). The calculated triplet state energy in methylcyclohexane (68.4 kcal/mol) is higher than the triplet state

energy of thioxanthone (E_T = 63.2 kcal/mol). Thus explains why energy transfer from thioxanthone to ellipticine could not be observed in non-polar media. As thioxanthone triplet is essentially lower than that of ellipticine in methylcyclohexane (Figure 7.8.), we chose xanthone having a higher triplet state energy in methylcyclohexane (E_T = 74.1 kcal/mol)[32] as triplet sensitizer of ellipticine in this solvent. The triplet molar extinction coefficient calculated using the already stated procedure by monitoring the end of the pulse absorbance change $(\Delta OD)_o^R$ due to xanthone triplet at 600 nm and with the absorbance change $(\Delta OD)_\infty$ of the sample at 330 nm. The triplet-triplet absorption decay of xanthone in the presence of ellipticine is found to match with the rise of ellipticine triplet at 330 nm. The triplet quantum yield was calculated by relative actinometry method and the value is tabulated in Table 7.1.

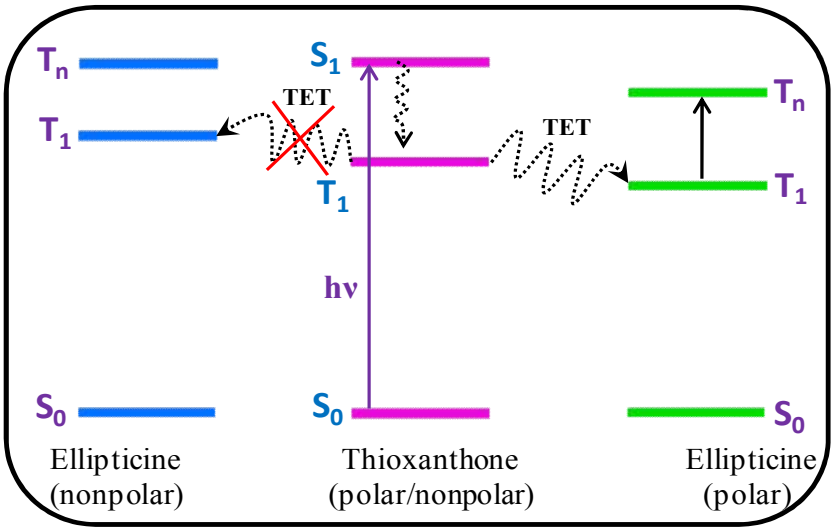

Figure 7.8. Schematic representation of the singlet and triplet state energies of thioxanthone and ellipticine in nonpolar and polar solvents (not scaled).

It is commonly believed that the molar extinction coefficients of the triplet-triplet absorption are independent of solvent polarity.[33] However, there are some cases where this quantity is found to be dependent on the solvent polarity. Our present study reveals that the extinction coefficients for the triplet-triplet absorption of ellipticine are solvent dependent. The decrease in triplet quantum yield in polar media suggests an increased rate of internal conversion processes in those solvents.

7.3.4. 2,2,2-Trifluoroethanol

Although ellipticine is completely protonated in its ground state in 1,1,1,3,3,3-hexafluoro-2-propanol (HFP), in less acidic solvent 2,2,2-trifluoroethanol (TFE) it is not.[27] The fluorescence excitation spectra monitored at the low and high wavelength region of the fluorescence band of ellipticine in TFE confirm the presence of two ground state species (Figure 7.9.).

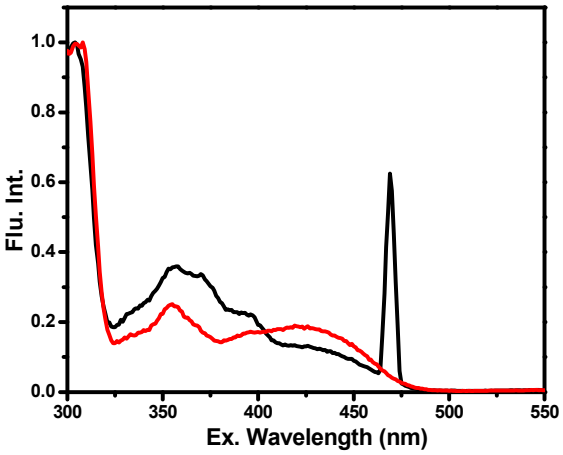

Figure 7.9. Fluorescence excitation spectra of ellipticine in TFE. The monitoring wavelengths were 470 nm (black) and 620 nm (red).

The presence of two different species can also be ascertained by the study of time-resolved fluorescence behavior. Fluorescence decay profile (λ_{exc} = 405 nm) recorded at 470 nm, consisted of two lifetime components 1.8 ns (60.5 %) and 7.5 ns (39.5 %), where as that recorded at 620 nm was best represented by a single exponential function with lifetime of 7.5 ns. Considering the excitation spectra, fluorescence decay profiles and related literature,[27] it is confirmed that in TFE both neutral and protonated forms of ellipticine are present in the ground state. The bleaching due to ground state absorption and stimulated emission are observed in the early times in the transient absorption spectra. But no transient absorption due to the triplet state could be observed in this solvent on direct excitation. Triplet sensitization was attempted for determination of the triplet extinction coefficient and to record the triplet sensitized spectra. Although both thioxanthone and xanthone can serve as a triplet donor, the latter was employed in this study.[32] Despite the formation of xanthone ketyl radical by abstraction of hydrogen atom from the solvent in this solvent, the triplet-triplet absorption due to the donor molecule is found to be well-separated and can be monitored without any difficulty.[34]

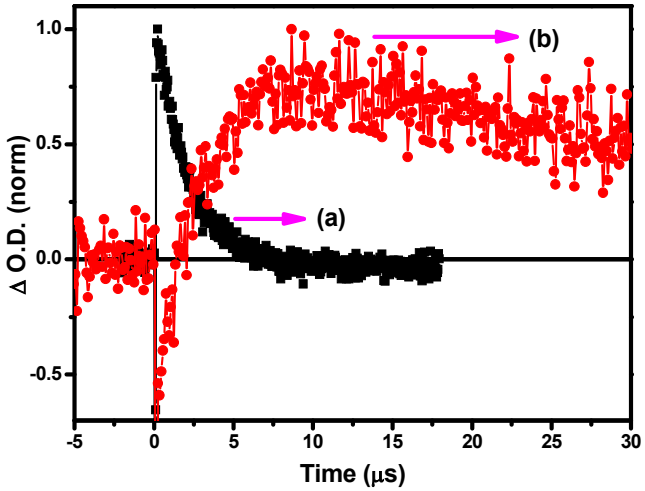

Figure 7.10. The triplet-triplet absorption decay profile of (a) xanthone (2.3×10^{-4} M) monitored at 600 nm after addition of acceptor and (b) rise of ellipticine (2.5×10^{-5} M) monitored at 330 nm in TFE, after 355 nm laser pulse excitation.

Decay time at 600 nm for the triplet state of xanthone was found comparable with the rise time (3 μs) of triplet state of ellipticine on addition of the latter (Figure 7.10.) and triplet extinction coefficient value is tabulated in Table 7.1. Triplet state lifetime of ellipticine in this solvent, produced by sensitization, is longer compared to other solvents. Sensitized time-resolved absorption spectra of ellipticne in TFE, which are recorded at different time intervals (presented in Figure. 7.11.) show a shift in the absorption maximum towards a longer wavelength. Sensitized decay curves are well fitted to single exponential equation and the two bands of the sensitized spectra possess same lifetimes. Although both neutral and protonated form of ellipticne are present in the ground state, the spectral position suggests that the triplet-triplet absorption in this solvent is due to the neutral form of ellipticine. Absence of the triplet state of protonated form in

sensitized spectra can be due to very low extinction coefficient of the triplet-triplet absorption or low intersystem crossing rate in the protonated form of ellipticine.

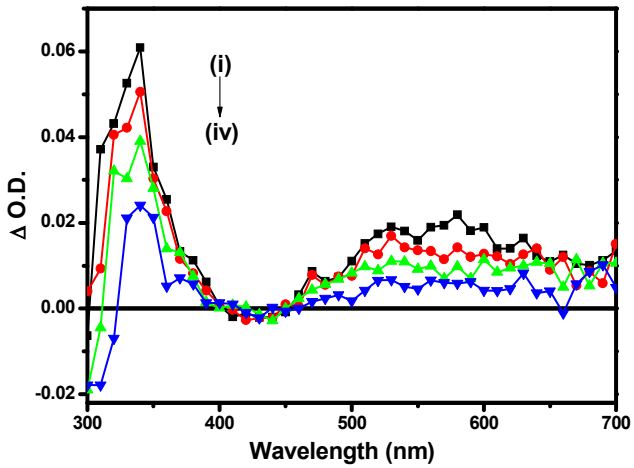

Figure 7.11. Sensitized transient absorption spectrum of ellipticine in TFE obtained upon flash photolysis of thioxanthone in presence of ellipticine. The spectra were monitored at t = 9 μs (i), 15 μs (ii), 25 μs (iii), 35 μs (iv) following the excitation at 355 nm.

7.3.5. 1,1,1,3,3,3-Hexafluoro-2-propanol

The transient absorption spectrum of ellipticine is also recorded in 1,1,1,3,3,3-Hexafluoro-2-propanol (HFP). It is stated in Chapter 3 that in this solvent ellipticine is completely protonated in the ground state and hence, its spectral behavior in singlet state is completely different from that in other polar protic solvents.[27] Transient absorption spectrum of ellipticine in HFP is also found to be different. By direct excitation, no transient band around 300-400 nm and 500-600 nm could be observed in this solvent and instead, a new and very weak band in the 460-600 nm region appeared. In Figure 7.12, the transient absorption

showed maximum at 520 nm and the transient species is found to have a lifetime of 3-4 μs.

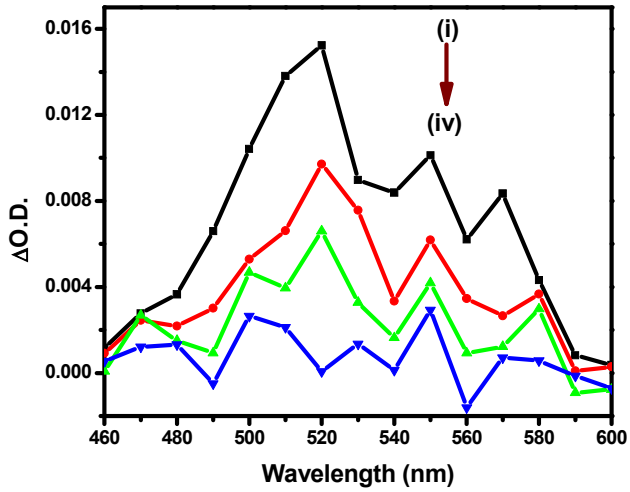

Figure 7.12. The transient absorption spectra of ellipticine in HFP obtained upon 355 nm laser excitation. The spectra were monitored at t = 0 (i), 0.9 μs (ii), 2.7 μs (iii) and 4.8 μs (iv).

7.4. Conclusion

The triplet state of ellipticine is studied in different solvents using laser flash photolysis technique by both direct excitation and triplet sensitization process. Triplet state properties such as molar extinction coefficient of the triplet-triplet absorption and triplet quantum yield are found to be sensitive to the media. The energy of the triplet state is determined from the 0-0 transition in the phosphorescence spectra (77 K) in both polar and nonpolar glassy matix. The triplet state energy were found to vary by as much as 7.7 kcal/mol on changing the solvent which explains the inefficiency of triplet-triplet energy transfer between thioxanthone and ellipticine in nonpolar solvent, methylcyclohexane.

Nearly 4-fold decrease in the triplet extinction coefficient and a noticeable increment in the triplet quantum yield of ellipticine are observed on changing the solvent from polar acetonitrile to nonpolar methylcyclohexane. The latter indicated an enhancement of the internal conversion process in polar solvents. No transient absorption could be observed in TFE, where both neutral and protonated forms are present in the ground state, on direct excitation. Triplet sensitization by xanthone however produces transient which resembles the triplet state of the neutral form. On the other hand, in HFP, where ellipticine is completely protonated in the ground state, transient absorption due to transition between the triplet states of ellipticinium cation could be observed.

Reference

(1) Masood, F.; Chen, P.; Yasin, T.; Hasan, F.; Ahmad, B.; Hameed, A. *J. Mater. Sci. - Mater. Med.* **2013**, *in press*.

(2) Clarysse, A.; Brugarolas, A.; Siegenthaler, P.; Abele, R.; Cavalli, F.; De Jager, R.; Renard, G.; Rozencweig, M.; Hansen, H. H. *Eur. J. Cancer Clin. Oncol.* **1984**, *20*, 243.

(3) Dodion, P.; Rozencweig, M.; Nicaise, C.; Piccart, M.; Cumps, E.; Crespeigne, N.; Kisner, D.; Kenis, Y. *Eur. J. Cancer Clin. Oncol.* **1982**, *18*, 519.

(4) Gouyette, A.; Huertas, D.; Droz, J.-P.; Rouesse, J.; Amiel, J.-L. *Eur. J. Cancer Clin. Oncol.* **1982**, *18*, 1285.

(5) Auclair, C. *Arch. Biochem. Biophys.* **1987**, *259*, 1.

(6) Bailly, C.; Ohuigin, C.; Rivalle, C.; Bisagni, E.; Waring, M. *J. Nucleic Acids Res.* **1990**, *18*, 6283.

(7) Behravan, G.; Leijon, M.; Selhlstedt, U.; Vallberg, H.; Bergamn, J.; Gra¨slund, A. *Biopolymers* **1994**, *34*, 599.

(8) Canals, A.; Purciolas, M.; Aymami, J.; Coll, M. *Acta Crystallographica* **2005**, *61*, 1009.

(9) Dodin, G.; Schwaller, M. A.; Aubard, J.; Paoletti, C. *Eur. J. Biochem.* **1988**, *176*, 371.

(10) El Hage Chahine, J. M.; Bertigny, J.-P.; Schwaller, M.-A. *J. Chem. Soc., Perkin Trans. 2* **1989**, 629.

(11) Elcock, A. H.; Rodger, A.; Richards, W. G. *Biopolymers* **1996**, *39*, 309.

(12) Froelich-Ammon, S. J.; Patchan, M. W.; Osheroff, N.; Thompson, R. B. *J. Biol. Chem.* **1995**, *270*, 14998.

(13) Jain, S. C.; Bhandary, K. K.; Sobell, H. M. *J. Mol. Biol.* **1979**, *135*, 813.

(14) Kohn, K. W.; Waring, M. J.; Glaubiger, D.; Friedman, A. *Cancer Res.* **1975**, *35*, 71.

(15) Řeha, D.; Kabeláč, M.; Ryjáček, F.; Šponer, J. E.; Elstner, M.; Suhai, S.; Hobza, P. *J. Am. Chem. Soc.* **2002**, *124*, 3366.

(16) Trubetskoy, S. V.; Torchilin, P. V. *Adv. Drug Delivery Rev.* **1995**, *16*, 311.

(17) Searle, F.; Gac-Breton, S.; Keane, R.; Dimitrijevic, S.; Brocchini; Brocchini, S.; Sauville, A. E.; Duncan, R. *Bioconjugate Chem.* **2001**, *12*, 711.

(18) Moody, W. T.; Czerwinski, G.; Tarasova, I. N.; Michejda, C. *J. Life Sci.* **2002**, *71*, 1005.

(19) Liu, J.; Xiao, Y.; Allen, C. *J. Pharm. Sci.* **2004**, *93*, 132.

(20) Czerwinski, G.; Tarasova, I. N.; Michejda, C. *J. Proc. Natl. Acad. Sci. U.S.A* **1998**, *95*, 11520.

(21) Moody, W. T.; Czerwinski, G.; Tarasova, I. N.; Moody, L. D.; Michejda, C. *J. Regul. Pept.* **2004**, *123*, 187.

(22) Thakur, R.; Das, A.; Chakraborty, A. *Physical Chemistry Chemical Physics* **2012**, *14*, 15369.

(23) Andrews, W. J.; Panova, T.; Normand, C.; Gadal, O.; Tikhonova, I. G.; Panov, K. I. *Journal of Biological Chemistry* **2013**, *288*, 4567.

(24) Baviskar, A. T.; Madaan, C.; Preet, R.; Mohapatra, P.; Jain, V.; Agarwal, A.; Guchhait, S. K.; Kundu, C. N.; Banerjee, U. C.; Bharatam, P. V. *Journal of Medicinal Chemistry* **2011**, *54*, 5013.

(25) Fung, S. Y.; Duhamel, J.; Chen, P. *J. Phys. Chem. A* **2006**, *110*, 11446.

(26) Thakur, R.; Das, A.; Chakraborty, A. *Chem. Phys. Lett.* **2013**, *563*, 37.

(27) Banerjee, S.; Pabbathi, A.; Sekhar, M. C.; Samanta, A. *J. Phys. Chem. A* **2011**, *115*, 9217.

(28) Eren, D.; Yechezkel, T.; Salitra, Y.; Uses, T. Preparation of RGD-containing peptidomimetics and their pharmaceutical compositions useful for diagnosis of tumors and photodynamic therapy. In *PCT Int. Appl.*, **2010**; Vol. WO2010046900.

(29) Torchilin, P. V.; Lukyanov, N. A.; Gao, Z. Micelle drug delivery system containing a phospholipid-PEG component. In *PCT Int. Appl.*, **2004**; Vol. WO 2004098569.

(30) Miskolczy, Z.; Biczók, L.; Jablonkai, I. *Chem. Phys. Lett.* **2006**, *427*, 76.

(31) Görner, H.; Miskolczy, Z.; Megyesi, M.; Bicźok, L. *Photochem. Photobiol.* **2011**, *87*, 1967.

(32) Murov, S. L.; Carmichael, I.; Hug, G. L. *Handbook of Photochemistry*, Second Edition ed.; Marcel Dekker: New York, **1993**.

(33) Bhattacharya, B.; Samanta, A. *Chem. Phys. Lett.* **2007**, *442*, 316.

(34) Garner, A.; Wilkinson, F. *J. Chem. Soc., Faraday Trans. 2* **1976**, *72*, 1010.

Chapter 8

Concluding Remarks

This chapter summarizes the results of this thesis. The scope of further studies based on the present findings has also been outlined.

8.1. Overview

The present thesis is devoted to the study of effect of hydrogen bond donating and accepting ability of a solvent on the excited state proton transfer kinetics, effect of pH on the protonation equilibrium and proton transfer kinetics and characterization of the triplet states of molecular systems of interest. We have chosen molecules with either π-deficient or both π-excessive and π-deficient functional groups. Specifically, ellipticine, 4-aminophthalimide and 9-phenylxanthenium tetrafluoroborate (PX+) have been studied.

While ellipticine and 4-aminophthalimide are obtained from commercial sources, PX+ and N-butyl-4-aminophthalimide (N-BuAP) are synthesized and purified for this study.

Photophysical studies have been carried out using UV-visible absorption, steady state and time-resolved fluorescence and phosphorescence and laser flash photolysis techniques. Theoretical calculations based on density functional methods have also been performed in some cases for a better understanding of the experimental results.

The origin of dual fluorescence of ellipticine, observed in some alcoholic solvents, is investigated in Chapter 3. Steady state and time-resolved fluorescence studies provide a direct evidence of the excited state reaction of ellipticine. Contrary to the earlier studies, which suggested the dual emission of ellipticine in methanol to originate from the photoexcited normal and protonated forms of the molecule, the latter produced as a result of proton transfer from the solvent, the present results seem to indicate that the excited state reaction involves solvent reorganization around ellipticine to form a "cyclic" solvated species followed by rapid proton transfer (relay) along the chain. Thus two emission bands arise from the normal and tautomeric forms of ellipticine. The measured rate constant of the reaction represents the kinetics of the formation of "cyclic" complex, which is the slowest of the two-step process. The ease of formation of the cyclic complex involving two molecules of ethylene glycol compared to those requiring three molecules of methanol explains why the excited state reaction is faster in ethylene glycol compared to methanol even though the hydrogen bond donating ability of the latter is better than the former. The time-resolved experiments also reveal the existence of a second set of hydrogen bonded ellipticine molecules, which do not contribute to the excited state proton transfer process. Theoretical calculations based on density functional methods have also been carried out the results of which support the experimental findings.

Spectral properties of ellipticine in aqueous solutions over a wide pH range have been studied by steady state and time-resolved fluorescence techniques in Chapter 4. In basic media, excited state protonation of ellipticine thus producing ellipticinium cation is observed. Kinetics of the excited state

process is investigated and excited state acidity constant (pK_a^*) is estimated from the measured individual rate constants involved in the excited state proton transfer process. The pK_a^* value is also calculated by applying Förster cycle. However, the value obtained by this method is found to be slightly higher than that obtained from the kinetic method. The observation highlights the importance of the kinetic method in the evaluation of the excited state behavior of the anti-cancer drug. Weller method is also attempted for the calculation of pK_a^*. However, the inflection point observed is only due to the variation of the concentration of the species in the ground state.

The fluorescence behavior of 4-aminopthalimide (AP) and its imide-H protected derivative (N-BuAP) has been reinvestigated in aqueous media in Chapter 5. It is convincingly established in this study that solvent-mediated excited state proton transfer reaction does not contribute to the fluorescence behavior of AP and its derivatives. The time-dependent blue shift of the fluorescence spectrum of AP in aqueous media, which is recently presented as evidence in support of the water-mediated excited state keto-enol transformation of the molecule, is shown to be simply because of the presence of two different types of hydrogen bonded species of AP having distinctly different fluorescence lifetimes in the aqueous media. The isotope effect on the fluorescence properties of AP and its derivative is explained in terms of the difference of the influence of two isotopes on the nonradiative rates of the systems. It is suggested that ground state exchange of the amino hydrogen of the systems with the solvent may also contribute to the isotope effect.

Chapter 6 deals with laser flash photolysis studies on a highly fluorescent and stable salt of 9-phenylxanthenium cation in neutral environment. A new transient absorption band of this extensively studied system that most probably remained buried under the fluorescence envelope and hitherto undetected is identified and attributed to the triplet state of the system. The newly identified triplet–triplet absorption band of 9-phenylxanthenium cation, which is insensitive to oxygen and appears in the visible region, is well-separated from the absorption bands of 9-phenylxanthenyl radical or 9-phenylxanthenol triplet and hence, the observation opens up an opportunity for the study of the elusive triplet state of this species.

Chapter 7 is focused on the characterization of the triplet excited state of ellipticine in different solvents by using laser flash photolysis technique. The various triplet state parameters (extinction coefficient and quantum yield) of the molecule are estimated by triplet-triplet energy transfer and relative actinometry technique. Interestingly, even though in polar aprotic solvent acetonitrile, the triplet-triplet energy transfer from thioxanthone to ellipticine is observed, the process is found to be inefficient in nonpolar methylcyclohexane. This observation is attributed to the dependence of triplet state energy on the solvent polarity, confirmed by low-temperature phosphorescence studies. Nearly 4-fold decrease in the triplet extinction coefficient and a noticeable increase of the triplet quantum yield of ellipticine are observed on changing the solvent from acetonitrile to methylcyclohexane. In trifluoroethanol, where both neutral and protonated forms of ellipticine are present in the ground state, no transient species could observed on direct excitation. The use of a sensitizer (xanthone) however

produces a transient species, which resembles the triplet state of the neutral form. In hexafluoropropanol, the triplet-triplet absorption due to ellipticinium cation is observed.

8.2. Future scope and challenges

Ellipticine, a plant alkaloid, is long known to scientists for its anti-cancer activity by intercalating into DNA, inhibiting Topoisomerase II and as a photosensitiser in photodynamic therapy (PDT). Photophysics of this potent anticancer drug deserves detailed attention as the action of a PDT drug is heavily dependent on its excited state properties. Considering the lack of such studies in literature (the main focus so far has been mainly on the DNA and/or protein binding interactions of the drug and biological activity), a detailed analysis of excited state of ellipticine and the role of surrounding media in the regulation of the excited state properties command immense attention. In this context we have studied and understood the solvent mediated excited state proton transfer process of ellipticine, which gives rise to dual fluorescence in some specific alcoholic solvents. However, solvent mediated proton transfer in the presence of small amounts of polar solvents in non-polar media still remains completely unexplored and our work might serve as a template for such studies in the future. Study of ellipticine in non-polar media with different amount of polar solvent is important as biological environments consists of non-polar and polar (containing different amounts of biological water) constituents which might affect the ground and excited states of the drug.

Ellipticine contains both acidic and basic functional groups and it has a ground state pK_a of 7.4. Both neutral and cationic forms of the drug are present at

biological pH of which the cationic form mainly intercalates into double-stranded DNA. Though it is reported that the ground state protonation equilibrium of ellipticine is shifted when it is bound to CT-DNA, the effect of binding on the excited state equilibrium constant is yet to be explored. Our study on the excited state protonation kinetics of ellipticine in aqueous media might help understanding the fate of excited state protonation equilibrium when ellipticine is bound to DNA and other biological entities.

PDT drugs usually damage DNA by generating highly reactive singlet oxygen through energy transfer from its triplet state. Characterization of the triplet state of a photosensitiser like ellipticine is thus very important from this point of view. The triplet state properties of ellipticine such as triplet extinction coefficient and triplet quantum yield explored by us are found to be sensitive to the surrounding media. The fate of the triplet state of the drug in different biological media, especially when intercalated into double-stranded DNA still remains to be explored carefully and our results could serve well as a standard for such a venture. Knowledge of the triplet state could be vital when undertaking such a study and holds a lot of promise.

Ellipticine, like many other intercalating cancer drugs or dyes, may or may not undergo photoinduced electron transfer with the DNA bases and this remains largely unexplored. Interaction of anti-cancer drug ellipticine and DNA bases can be studied using electrochemical and spectroscopic methods.

Although photophysics of 4-aminophthalimide (AP) has been studied extensively in the past and in recent years, there are still some ambiguities

regarding its behavior specifically in aqueous media. Additional studies on AP and its derivatives in aqueous media and in mixed solvents are necessary for a clear understanding of the excited state behavior of AP.

Our laser flash photolysis study on 9-phenylxanthenium cation reveals a new transient absorption band due to triplet-triplet transition that perhaps remained buried under the fluorescence envelope and left undetected. With this finding, the triplet state properties and reactivity of this cationic species can be reinvestigated.